



HAL
open science

Prise en compte de l'effet des déviations géométriques du produit durant son cycle de vie

Dinh Son Nguyen

► **To cite this version:**

Dinh Son Nguyen. Prise en compte de l'effet des déviations géométriques du produit durant son cycle de vie. Sciences de l'ingénieur [physics]. Institut National Polytechnique de Grenoble - INPG, 2010. Français. NNT: . tel-00561475

HAL Id: tel-00561475

<https://theses.hal.science/tel-00561475>

Submitted on 1 Feb 2011

HAL is a multi-disciplinary open access archive for the deposit and dissemination of scientific research documents, whether they are published or not. The documents may come from teaching and research institutions in France or abroad, or from public or private research centers.

L'archive ouverte pluridisciplinaire **HAL**, est destinée au dépôt et à la diffusion de documents scientifiques de niveau recherche, publiés ou non, émanant des établissements d'enseignement et de recherche français ou étrangers, des laboratoires publics ou privés.

Abstract

TODAY, requirements of customers concerning product they would like to purchase, such as quality, reliability, robustness, innovativeness and cost are more and more tight and high. Thus, product designer must ensure that the designed product meets fully the requirements of customers and users as well. In other words, satisfaction of these plays an important role in the context of design product-process.

The research work presented in my thesis is a complete answer for management of geometrical variations throughout the product life cycle. In fact, the geometrical deviation model introduced in my thesis allows to model geometrical deviations generated from the manufacturing to assembly stage of the product life cycle. Monte-Carlo simulation method is then used to generate an image of the real manufactured product. As a result, the geometrical deviations are integrated into simulation of product performance in order to establish the relationship between the performance and the parameters of geometrical deviations or variation sources. An image of the real performance of the manufactured product is generated by using the result of geometrical deviations simulation. From the result of performance simulation, the parameters of variation sources influencing the product performance are identified and classified according to their impact level. The variance of the product performance variation is established by two different approaches based on the relation between the performance and the parameters of geometrical deviations or variation sources. Finally, the robust design solution can be found by minimization of the variance of the product performance variation.

Keywords: Life-cycle Engineering, Geometrical Deviation Model, Performance simulation, Manufacturing simulation, Geometrical variability management.

Résumé

AUJOURD'HUI, les exigences des clients concernant le produit qu'ils achètent, exigence telles que la qualité, la fiabilité, la robustesse, l'innovation et le coût sont de plus en plus élevées. Le concepteur du produit doit s'assurer que le produit conçu satisfait aux exigences des clients et des utilisateurs. En d'autres mots, la satisfaction de ceux-ci joue un rôle important dans la conception du produit et du process.

Le travail de recherche présenté dans ce mémoire de thèse est une réponse complète pour la gestion des variations géométriques durant le cycle de vie du produit. Le modèle de déviations géométriques du produit exposé dans ce mémoire permet de modéliser les déviations géométriques générées de l'étape de fabrication à l'étape d'assemblage de son cycle de vie. La méthode de simulation Monte-Carlo est utilisée pour générer une image des produits fabriqués. A partir de ces résultats, les déviations géométriques sont intégrées dans la simulation de performance du produit afin d'établir la relation entre la performance et les paramètres des sources de variation. Une image de la performance réelle du produit fabriqué est générée par l'utilisation des résultats de la simulation des déviations géométriques. A partir des résultats de la simulation de performance, les paramètres des sources de variation influençant la performance du produit sont identifiés et classifiés par rapport au leur niveau d'impact. La variance de la variation de la performance est établie par deux approches différentes s'appuyant sur la relation entre la performance et les paramètres. Finalement, la solution de robuste de conception peut-être déterminée par minimisation de la variance de la performance du produit.

Mots clés : Cycle de vie du produit, Modèle des déviations géométriques, Simulation de performance, Simulation de fabrication, Gestion de variabilité géométrique.

Remerciement

Le travail présenté dans ce mémoire de thèse a été réalisé au sein de l'équipe CPP du Laboratoire G-SCOP, dirigée par le Professeur Daniel BRISSAUD et Frédéric VIGNAT. C'est grâce à eux, à leurs remarques, conseils et à leur soutien que j'ai pu débiter dans le monde de la recherche dans d'excellentes conditions. Je les en remercie grandement.

Je remercie vivement les Pr. Jean-Yves DANTAN et Pr. Luc LAPERRIERE, pour m'avoir accordé de leur temps afin d'évaluer mes travaux de thèse en tant que rapporteurs. Je remercie également les membres du jury de thèse: Pr. Serge SAMPER en tant que président du jury, et Pr. Cung LE en tant que examinateur, de m'avoir fait l'honneur de leur présence : leurs remarques et questions, très enrichissantes, me motivent à poursuivre mon travail de recherche.

Je remercie également mes amis à Grenoble pour m'avoir encouragé et soutenu dans les moments difficiles.

Je remercie enfin ma famille et plus particulièrement mes parents pour m'avoir toujours encouragé à prolonger mes études, et m'avoir transmis une envie de découvertes.

Contents

- 1 INTRODUCTION** **10**

- 2 STATE OF ART AND SCIENTIFIC QUESTIONS** **15**
 - 2.1 Manufacturing Stage 15
 - 2.1.1 State Space Approach 16
 - 2.1.1.1 Zhou et al. (2003) 17
 - 2.1.1.2 Huang et al. (2003) 19
 - 2.1.1.3 Other researches 22
 - 2.1.2 Small Displacement Torsor Approach 25
 - 2.1.2.1 Villeneuve et al. (2001) 26
 - 2.1.2.2 Vignat et al. (2005) 28
 - 2.1.2.3 Tichadou et al. (2005) 28
 - 2.2 Assembly Stage 29
 - 2.2.1 State Transition Model Approach 30
 - 2.2.1.1 Mantripragada and Whitney (1999) 30
 - 2.2.2 Stream of Variation Model Approach 32
 - 2.2.2.1 Jin and Shi (1999) 32
 - 2.2.2.2 Camelio et al. (2003) 34
 - 2.2.2.3 Huang et al. (2007) 35
 - 2.2.3 Small Displacement Torsor Approach 36
 - 2.2.3.1 Ballot et al. (1997, 2000) and Thiebaut (2001) 36
 - 2.3 Robust Design Methodology 38
 - 2.3.1 Chen et al. (1996) 39
 - 2.3.2 Vlahinos et al. (2003) 41
 - 2.3.3 Gu et al. (2004) 42
 - 2.3.4 Other Researches 43
 - 2.4 Conclusion and Scientific Questions 44

TABLE OF CONTENTS

3	GDM FOR PRODUCT LIFE CYCLE ENGINEERING	47
3.1	Small Displacement Torsors	47
3.1.1	Definition	48
3.1.2	Torsor Transformations	50
3.1.3	Surface Deviation Torsor	52
3.1.4	Link Deviation Torsor	53
3.1.5	Part Deviation Torsor	54
3.2	Geometrical Deviation Model	55
3.2.1	Model of Manufactured Part	56
3.2.2	Model of Assembled Part	60
3.3	Geometrical Deviation Simulation	63
3.3.1	Monte-Carlo Simulation	63
3.4	A Case Study	69
3.4.1	A Centrifugal Pump	69
3.4.1.1	CAD model of the centrifugal pump	69
3.4.1.2	MMP of the centrifugal pump	70
3.4.1.3	MAP of the centrifugal pump	75
3.4.1.4	Geometrical deviation simulation for the centrifugal pump	80
3.5	Conclusion	83
4	INTEGRATION OF GDS INTO SIMULATION OF PRODUCT PERFORMANCE	84
4.1	Method Description	85
4.1.1	Mathematical Analysis Approach	85
4.1.2	Design of Experiment Approach	91
4.1.2.1	From nominal model to deviated one in a CAD software	91
4.1.2.1.1	Nominal model	91
4.1.2.1.2	Deviated model	92
4.1.2.2	Regression model	95
4.1.2.3	Factorial design	96
4.1.2.4	Taguchi design	98
4.1.2.5	Random design	101

TABLE OF CONTENTS

4.2	Case Studies	103
4.2.1	A centrifugal pump	103
4.2.1.1	Factorial design	104
4.2.1.2	Taguchi design	106
4.2.2	A Spring System	107
4.2.2.1	Mathematical analysis approach	110
4.2.2.2	Factorial design	111
4.2.2.3	Taguchi design	112
4.2.2.4	Random design	113
4.2.2.5	Comparison	114
4.3	Conclusion	116
5	INFLUENCE FACTOR ANALYSIS AND ROBUST DESIGN METHODOLOGY	118
5.1	Influence Factor Analysis	118
5.1.1	Mathematical Approach	119
5.1.1.1	Global sensitivity analysis	119
5.1.1.1.1	Sobol' global sensitivity indices	120
5.1.1.1.2	Classification of design factors	121
5.1.2	Data Mining Approach	122
5.1.2.1	Covariance and correlation	122
5.1.2.1.1	Covariance	123
5.1.2.1.2	Correlation	124
5.1.2.2	Influence index approach	124
5.1.2.2.1	Data processing	125
5.1.2.2.2	Definition of influence index	126
5.1.3	Case Study	127
5.1.3.1	A centrifugal pump	127
5.1.3.1.1	Global sensitivity analysis	127
5.1.3.1.2	Covariance and Correlation Analysis	129
5.1.3.1.3	Influence Index Analysis	130
5.1.3.1.4	Conclusion	133

TABLE OF CONTENTS

5.2 Robust Design within Product Life Cycle	134
5.2.1 Mathematical approach	134
5.2.2 Data Mining Approach	136
5.2.3 A Case Study	137
5.2.3.1 A centrifugal pump	137
5.2.3.1.1 Mathematical approach	137
5.2.3.1.2 Data mining approach	139
5.3 Conclusion	141
6 CONCLUSION AND PERSPECTIVE	142

List of Figures

1.1	The overview of method	13
1.2	The nominal model of the centrifugal pump	14
2.1	Illustration of feature representation [ZHS03]	17
2.2	Diagram of a multistage machining process [ZHS03]	18
2.3	Composition of overall feature deviation [ZHS03]	19
2.4	Error propagation in MMPs [HSY03]	20
2.5	Coordinate systems[HSY03]	21
2.6	Error propagation [HSY03]	21
2.7	Equivalent fixture error [WHK05]	23
2.8	Steps of the derivation of variation propagation model [LZC07]	24
2.9	SDT of a machining operation (set-up 10) [VLL01]	27
2.10	SDT of a part-holder (set-up 10) [VLL01]	28
2.11	Charts of three set-ups [TLH05]	29
2.12	Multi-station assembly modeling methodology [CHC03]	35
2.13	An assembly process with N stations [HLKC07]	35
2.14	A comparison of two types of robust design [CATM96]	39
2.15	Workflow for Robust Optimization [VKDS03]	41
3.1	Displacement of a rigid body	48
3.2	Torsor transformations – Local to Global	51
3.3	Deviation torsor of a plane [NVV09]	53
3.4	Deviation of associated part and nominal part	56

TABLE OF CONTENTS

3.5	Assembly process and MAP generation	61
3.6	The algorithm diagram of the Monte-Carlo simulation	64
3.7	Random sample numbers	66
3.8	Floating cylindrical contact	66
3.9	Slipping planar contact	68
3.10	The parts of designed centrifugal pump	70
3.11	Model of manufactured shaft of the pump	70
3.12	Assembly process of the pump	76
3.13	Assembly graph of the pump	78
3.14	The gap between the casing and the impeller of the pump	79
3.15	Monte-Carlo simulation results	82
4.1	Cross section of the impeller passage	87
4.2	Distribution of deviation flowrate of the pump	90
4.3	CSG operations [Wik10]	92
4.4	Deviated model of a plane	93
4.5	Deviated model of a part in PTC ProEngineer	94
4.6	Performance simulation of the product with geometrical deviations	98
4.7	Performance simulation with Taguchi design	100
4.8	The algorithm diagram of random design method	101
4.9	The selected factors of the pump	103
4.10	Response surfaces of the flowrate	106
4.11	Distribution of the flowrate of one million pumps by factorial design	107
4.12	Distribution of the flowrate of one million pumps by Taguchi design	110
4.13	The parts of the spring system	110
4.14	The distribution of frequency by mathematical analysis approach	111
4.15	The distribution of frequency by factorial design	112
4.16	The distribution of frequency by Taguchi design	113
4.17	The distribution of frequency by random design	114

LIST OF FIGURES

4.18 The distribution of frequency error 115

5.1 The overview of the covariance and correlation approach 123

5.2 The overview of the influence index approach 125

5.3 Global sensitivity indices of design parameters 129

5.4 Pareto charts of covariance and correlation 131

5.5 Data filtered by moving average technique 132

5.6 Influence index of manufacturing parameters 132

5.7 Pump flowrate and deviation parameters 137

5.8 Linear and non linear regression 140

6.1 The overview of research works 143

List of Tables

2.1	The geometrical deviation models in manufacturing stage.	45
2.2	The geometrical deviation models in assembly stage	46
3.1	Deviation torsor of elementary surfaces	54
3.2	Link deviation torsors of elementary connections. [Vig05]	55
3.3	Non-penetration conditions and positioning functions of elementary connections	59
3.4	Turning process	72
3.5	Variation range of the input variables	80
4.1	Table of Taguchi design	100
4.2	The value of the selected parameters	104
4.3	The results of the flowrate simulation	105
4.4	List of the geometrical deviation parameters of the pump	108
4.5	The results of the flowrate simulation in CFDesign for Taguchi design	109
4.6	Coefficient comparison among proposed approaches	116
4.7	Summary of the proposed approaches	116

LIST OF TABLES

5.1 The result of global sensitivity analysis 129

5.2 The classification of parameters 130

5.3 The classification of parameters 133

Chapter 1

INTRODUCTION

TODAY, the requirements of customers concerning the product they buy are more and more tight and high. Thus, satisfaction of these such as quality, reliability, robustness, innovativeness and cost plays an important role in the context of global and competitive economy. Due to the development of information technology, computers are becoming a useful and effective tool to support engineering activities in product design and manufacturing. Product designers usually create a numerical model of the product with a CAD software and then use this model to perform engineering simulation. However, the product model created in this environment is a nominal representation of the product and thus does not deal with variations generated along the product life cycle.

In fact, the product must pass through many stages of its life cycle before arriving in the hand of the customer and of the users. Each part making up the product is manufactured from raw material by the manufacturing processes (forging, cutting, grinding, etc.) and geometrical deviations are generated and accumulated over the successive set-up of the multistage manufacturing process. These deviations result from the imperfections of material, tooling and machine. The manufactured parts, with deviations, are then assembled at assembly stage. The deviations of the surfaces of the parts affect the assemblability and are accumulated on the final

product. The product geometry is, therefore, different from the nominal one at the end of the manufacturing and assembly stages and obviously its performances will also vary. Finally, the real product is different from the one we promised to the customer, and it is not obvious that it will satisfy him. The question is then how to manage this performance variability in order to reduce it and at least ensure that it is compatible with the customer satisfaction.

The current product modelling technology cannot deal with these deviations. Most of the simulations to predict the behaviour of the product (kinematics, dynamics, resistance, fluid flow, etc.) and to evaluate its performances are carried out based on the nominal model of the product. The result of designed product performance simulation can be considered as nominal and consequently different from the real one. The risk is then that the designed product does not fully meet the requirements of the customers and users. The main issue for the designer is then: Does the “real” product satisfy the customers’ requirements from the point of view of product performance?. Thus, the management of geometrical variations throughout the product life cycle is an important issue in product-process design and concurrent engineering and requires to consider the following questions:

- How to model the geometrical deviations generated throughout the product life cycle?
- How to manage causes and consequences of these deviations at design stage?
- How to give the feedback about the effects of the geometrical deviations to the various actors of the product life cycle?

The research works for the thesis have been done within G-SCOP laboratory. This thesis contributes to develop a unified model for modelling the geometrical deviations generated and accumulated at manufacturing and assembly stage of the product life cycle. This model is based on the research works developed in the Integrated Design team, including the model of manufactured part (MMP) proposed

by Villeneuve and Vignat [VLL01, VV05a, VV05b, VV07] and the Product Model for Life-Cycle developed by Brissaud and Tichkiewitch [TV97, TB99, TB00, BT01]. The method applied for this research was first to work on case studies and mainly the design of a centrifugal pump. Based on this case study, I proposed and tested methods and tools to model deviation all along the product life cycle, integrate these deviations in product performance simulation and identify key deviation sources. The next step was to generalise the proposed methods and tools to define the global methodology for integration of geometrical deviations from manufacturing and assembly stage in product performance simulation and identification of key deviation sources. I then applied parts of the global method to test example for the purpose of comparison of the obtained results with the theoretical purpose and thus verification of the validity of the proposed tools.

Many researches to model the geometrical deviations generated and accumulated by the manufacturing/assembly processes have been done. They will be presented in chapter 2. However, these models are not consistent with all stages of the product life cycle. Thus the work presented in this thesis focuses on proposing a method that is able to model the geometrical deviations generated throughout the product life cycle and to integrate these into the simulation of the product performance.

The overview of the method is described in figure 1.1. It is separated in two distinct branches. The first one consists in the generation of the geometrical deviation model (GDM) by simulation of manufacturing and assembly stage of the product life cycle. This model is based on the concept of small displacement torsor proposed by Bourdet [Bou87]. It includes the MMP¹ proposed by Vignat et al. [VV07] for modelling the geometrical deviations generated by manufacturing processes and the MAP² based on the GDM for part and mechanism proposed by Ballot et al. [BB97, BB00] and Thiébaud [Thi01]. Then geometrical deviations of a population of products are produced by using the Monte-Carlo simulation method. The gener-

¹Model of Manufactured Part

²Model of Assembled Part

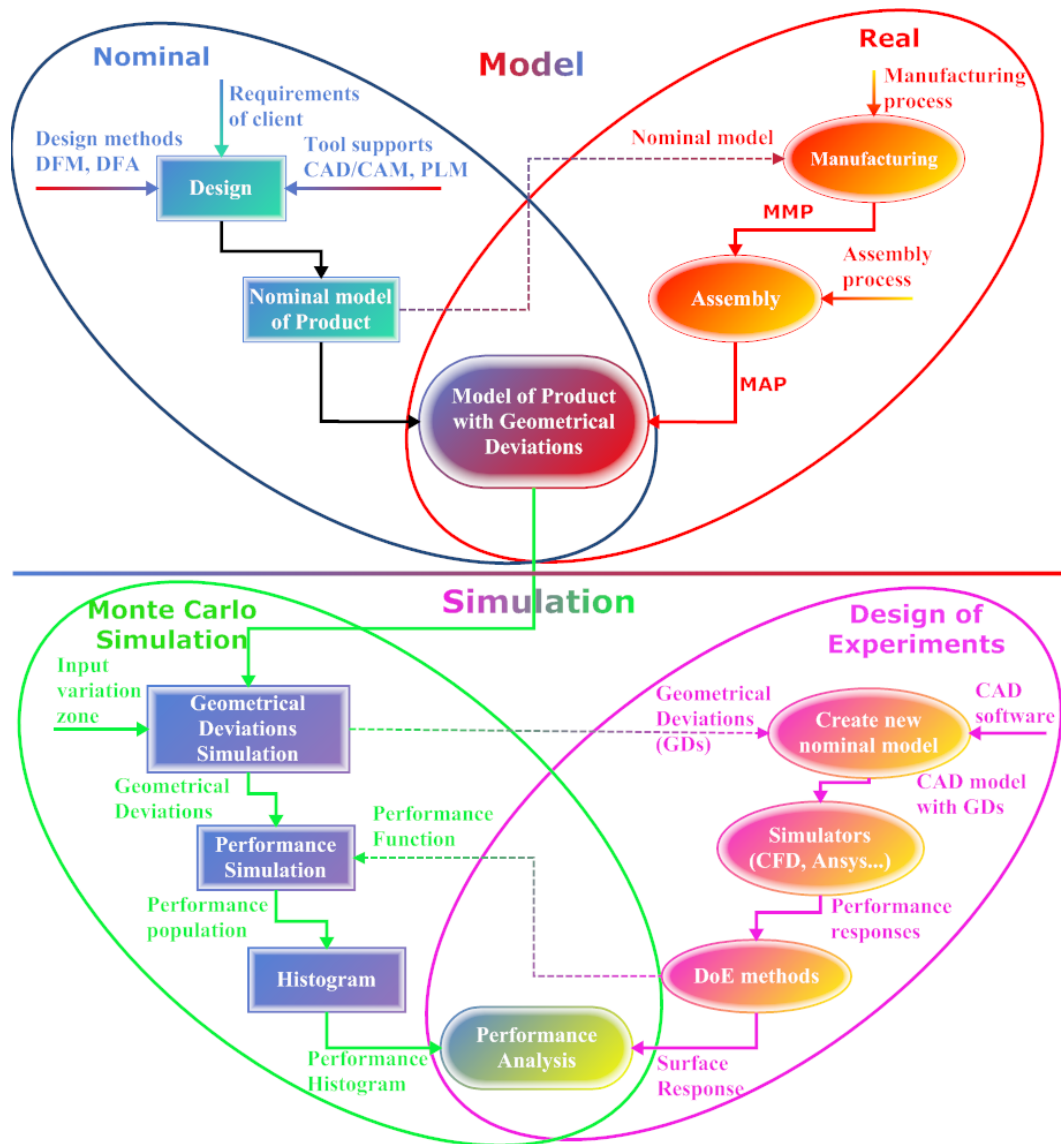


Figure 1.1: The overview of method

ation and simulation of GDM are presented in chapter 3.

The second one is a method that allows to integrate these deviations into the product performance simulation based on different approaches. Firstly, the relationship between the product performance and the parameters of the geometrical deviations is established. Then, the performance of the population of product from Monte-Carlo simulation is determined in order to verify the compliance of the designed product with customer's requirements. This method will be presented in chapter 4. The chapter 5 will present a method that allows to identify and classify the influence of the geometrical deviation parameters on the product performance. In

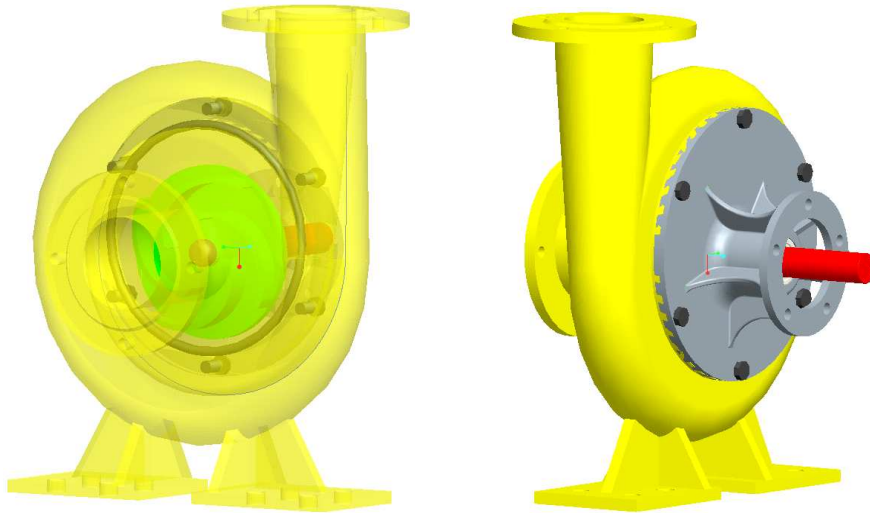


Figure 1.2: The nominal model of the centrifugal pump

addition, this method allows to determine the variance of the performance of the product relative to these parameters. Robust solution can be found from previous results by minimizing the variance of the product performance. Finally, the conclusion and the new research axes will be concluded in chapter 6.

To illustrate the methods presented in this thesis, a case study is proposed all along the dissertation. I used this case study all along my research to develop the methods and tools that are proposed in this manuscript. The proposed case is a centrifugal pump (see figure 1.2) with specifications:

- Flowrate: $250m^3/h$
- Total Head: $100m$
- Revolution speed: $2000RPM$
- Liquid: Water
- Temperature: $20^{\circ}C$

Chapter 2

STATE OF ART AND SCIENTIFIC QUESTIONS

THE goal of this chapter is to provide a general overview of the academic research around the scientific issues in the thesis. The comprehensive review of existing methodologies for modelling geometrical deviations of a product generated and accumulated along manufacturing and assembly processes will be presented in the first section. Then the general survey of robust design methodology will be introduced in the second section of this chapter. Their advantages and disadvantages among them are discussed in the third section. The research questions of the thesis are constructed in order to deal with the existences.

2.1 Manufacturing Stage

Many researches work about machining error sources and link between manufacturing parameters such as workpiece materials, tooling, machining, cutting speed, cutting feed, etc., and resulting errors such as surface roughness, surface deviation, surface hardness, etc., have been done. Ramesh et al. [RMP00a, RMP00b] have studied the effect of cutting force and thermal effect on geometrical deviation

of the surfaces of the part. Thangavel et al. [TS08] have studied the influence of turning parameters, such as cutting speed, feed rate, depth of cut and tool nose radius on the surface roughness. Sahoo et al. [SBR08] have studied the quality of milled surfaces affected by parameters, such as spindle speed, depth of cut and feed rate, workpiece materials, etc. They proposed a second order mathematical models using Response Surface Methodology (RSM) to allow the optimisation of cutting conditions according to surface quality. Mohanasundararaju et al. [MSA08] worked on the quality of grinded surfaces and the influence of grinding parameters, such as wheel speed, work speed, traverse speed, in-feed, dress depth and dressing lead and developed a mathematical model for surface prediction. Ghasempoor et al. [GYX07] proposed a geometrical method to model surface finish in grinding. This model takes into account the stochastic nature of the grinding process and the kinematics of chip generation. Given the grinding wheel specifications and cutting conditions, the model can produce the expected surface topography. The proposed model was evaluated by comparing the predictions with measured surface roughness obtained through grinding experiments. The results showed the predictions were consistent with the measurements, hence proving the effectiveness of the model. All these studies are experimental and deal with variations generated on one surface in one set-up. They have been done for process optimisation and error compensation. However, it is not a main topic of the related works. We will only consider models that allow to model geometrical defects generated and accumulated over successive set-up.

2.1.1 State Space Approach

Many models of dimensional error propagation along multistage machining processes are proposed. Many of these models are based on a state space model that is, firstly, mentioned by Whitney [Whi68]. There are many researches representing this approach that will be presented in this section, especially Zhou et al. [ZHS03]

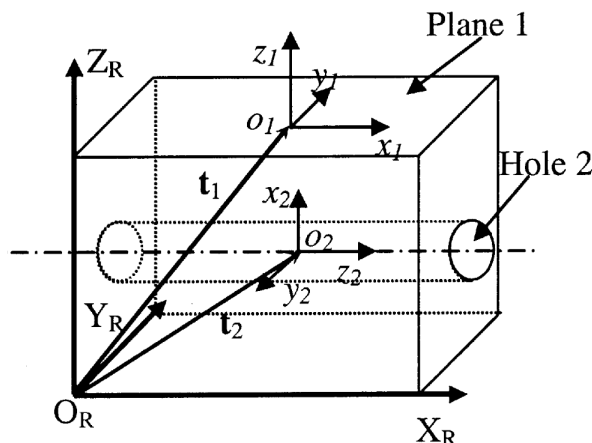


Figure 2.1: Illustration of feature representation [ZHS03]

and Huang et al. [HSY03].

2.1.1.1 Zhou et al. (2003)

Zhou et al. [ZHS03] used a state space model to describe the dimensional variation propagation of multistage machining processes. When the workpiece passes through multiple stages, machining errors at each stage are accumulated and transformed onto the workpiece. Differential motion vector, a concept from the robotics field, is used in this model as the state vector to represent the geometrical deviation of the workpiece. The deviation accumulation and transformation are quantitatively described by the state transition in the state space model.

The workpiece feature is represented by a location vector and a vector that consists of three rotating Euler angles. The part representation is illustrated in figure 2.1. $O_R X_R Y_R Z_R$ is the reference coordinate system (*RCS*). Plane 1 and Hole 2 are represented by local coordinate systems (*LCSs*) that are attached on them, respectively. The position and orientation of Plane 1 can be represented by a vector $[t_1^T, \omega_1^T]$. t_1 is the location vector that points to the origin of LCS_1 . ω_1 is a vector containing roll, pitch, and yaw Euler rotating angles between the coordinate systems LCS_1 and *RCS*. The deviation of a *LCS* can be represented by a differential

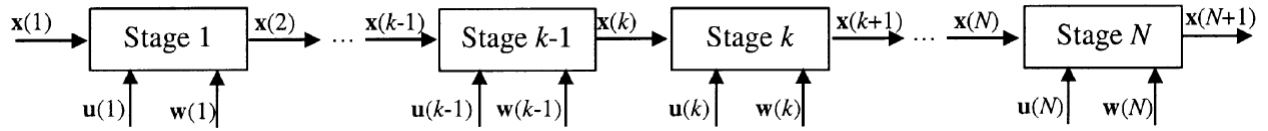


Figure 2.2: Diagram of a multistage machining process [ZHS03]

$$\text{motion vector } X_n^R = \begin{bmatrix} d_n^R \\ \theta_n^R \end{bmatrix}.$$

The deviation of the workpiece before stage k can be represented by a state vector $x(k)$. It is a stack of differential motion vectors for all key features of the workpiece. The deviation of the workpiece at stage k results from three sources: the datum-induced deviation caused in previous stages, the machining inaccuracy at the current stage, and unmodeled noise. The deviation propagation can be written in the linear discrete state space format, as shown in equation 2.1.

$$\begin{aligned} x(k+1) &= A(k)x(k) + B(k)u(k) + w(k) \\ y(k) &= C(k)x(k) + v(k) \end{aligned} \quad (2.1)$$

Where $A(k)x(k)$ represents the deviations of previously machined features and the deviation of newly ones that is only contributed by the datum error, $B(k)u(k)$ represents the workpiece deviation caused by the relative deviation between the workpiece and the cutting tool (this deviation is caused by the fixture error and the imperfection of the tool path), $y(k)$ is the measurement, $w(k)$ is the unmodeled system noise, and $v(k)$ is the measurement noise. Thus the accumulation of geometrical deviation of the workpiece in a multistage machining process can be described by figure 2.2.

The state vector $x(k)$ is defined as a stack of differential motion vectors corresponding to each feature with respect to RCS . There are three major components in $x(k)$:

- Machining error, which is defined as the deviation of the cutting tool from its nominal path with respect to Fixture Coordinate System (FCS).

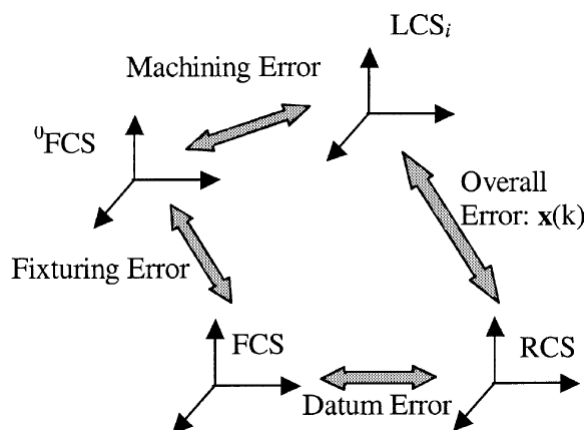


Figure 2.3: Composition of overall feature deviation [ZHS03]

- Fixturing error, which is caused by the imperfection of the locators.
- Datum error, which is the deviation of FCS with respect to RCS .

The relationships among these coordinate systems and errors are shown in figure 2.3. The geometrical deviations of all features of the manufactured part are described by the vector $x(N)$, as a stack of differential motion, at the final stage N of the multiprocess (see figure 2.2).

2.1.1.2 Huang et al. (2003)

Huang et al. [HSY03] proposed to use a state space model to describe the variation stack-up in multi-operational machining processes ($MMPs$). The final product variation is an accumulation or stack-up of variation from all machining operations. The error propagation in a machining process with N operations is shown in figure 2.4.

The main error sources at operation k can be classified as:

- Fixture error e_k^f representing the geometrical inaccuracy of locating elements
- Datum errors e_k^d caused by the imperfection of datum surfaces
- Machine tool errors e_k^m

- Noise $w(k)$ caused by process natural variations.

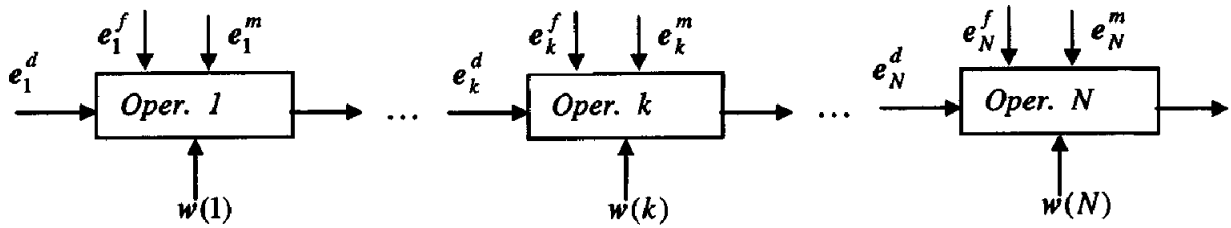


Figure 2.4: Error propagation in MMPs [HSY03]

Part model: The author assumed that part models need only to describe features relevant to part deviation. Therefore, they use a revised version of vectorial surface model developed by Martinsen [Mar93]. In the revised model, a part has n surfaces related to the error propagation. Those n surfaces include surfaces to be machined, design datums, machining datums and measurement datums. In a coordinate system, the i^{th} surface can be described by its surface orientation $n_i = [n_{ix}, n_{iy}, n_{iz}]^T$, location $p_i = [p_{ix}, p_{iy}, p_{iz}]^T$, and size $D_i = [d_{i1}, d_{i2}, \dots, d_{im}]^T$. By stacking up n_i , p_i and D_i , X_i is represented as a vector with the dimension $(6 + m)$, as described in equation 2.2.

$$X_i = [n_i^T, p_i^T, D_i^T]^T \quad (2.2)$$

Thus the part is modelled as a vector by stacking up all surface vectors that are expressed by equation 2.3.

$$X = [X_1^T, X_2^T, \dots, X_n^T]^T \quad (2.3)$$

Part deviation: The manufactured part features can differentiate from their ideal counterparts caused by operational errors and natural process variation. The feature deviation can be expressed by equation 2.4.

$$\Delta X_i = [\Delta n_i^T, \Delta p_i^T, \Delta D_i^T]^T \quad (2.4)$$

Where $\Delta n_i = [\Delta n_{ix}, \Delta n_{iy}, \Delta n_{iz}]^T$, $\Delta p_i = [\Delta p_{ix}, \Delta p_{iy}, \Delta p_{iz}]^T$, and $\Delta D_i = [\Delta d_{ix}, \Delta d_{iy}, \Delta d_{iz}]^T$.

The part deviation is a set of all feature deviations of the part. It is described by

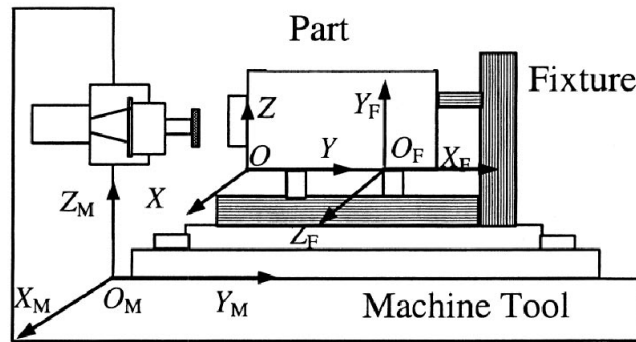


Figure 2.5: Coordinate systems[HSY03]

equation 2.5.

$$x = [\Delta X_1^T, \Delta X_2^T, \dots, \Delta X_n^T]^T \quad (2.5)$$

The intermediate part deviation after operation k can be noted $x(k)$. Part deviation is mainly caused by setup and machining operations. During each operation, the part is fixed in a fixture and then cut by the machine tool. Three coordinate systems are introduced as references to describe the part deviation and operational errors. They are shown in figure 2.5 including:

- M-Coordinate: the machine tool coordinate (x_M, y_M, z_M) , in which the fixture is located and oriented on the machine table.
- F-Coordinate: the fixture coordinate (x_F, y_F, z_F) , built in the fixture in which the part is located and oriented.
- P-Coordinate: the part coordinate (x, y, z) , in which the part surfaces are represented.

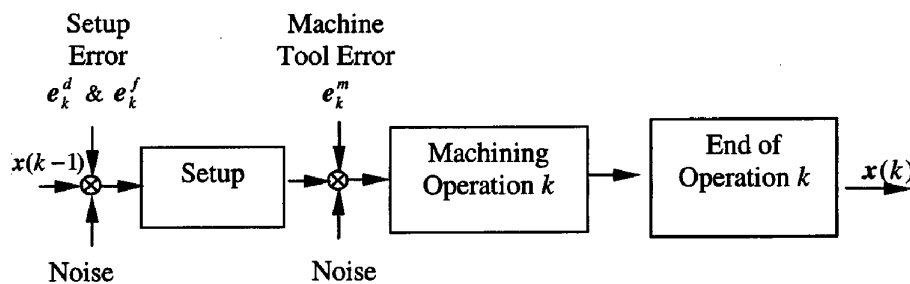


Figure 2.6: Error propagation [HSY03]

The authors assume that X , X_F and X_M are the part represented in the P-Coordinate, F-Coordinate and M-Coordinate respectively. The homogeneous transformation is used to model the part transformation among coordinates through rotation and translation transformations. The procedure is modelled as transforming the part from P-Coordinate to F-Coordinate and then from F-Coordinate to M-Coordinate. The mathematical expression is given by equation 2.6.

$$\begin{bmatrix} X_F \\ 1 \end{bmatrix} = \begin{bmatrix} {}^F R_P & {}^F T_P \\ 0 & 1 \end{bmatrix} \begin{bmatrix} X \\ 1 \end{bmatrix} \quad \text{and} \quad \begin{bmatrix} X_M \\ 1 \end{bmatrix} = \begin{bmatrix} {}^M R_F & {}^M T_F \\ 0 & 1 \end{bmatrix} \begin{bmatrix} X_F \\ 1 \end{bmatrix} \quad (2.6)$$

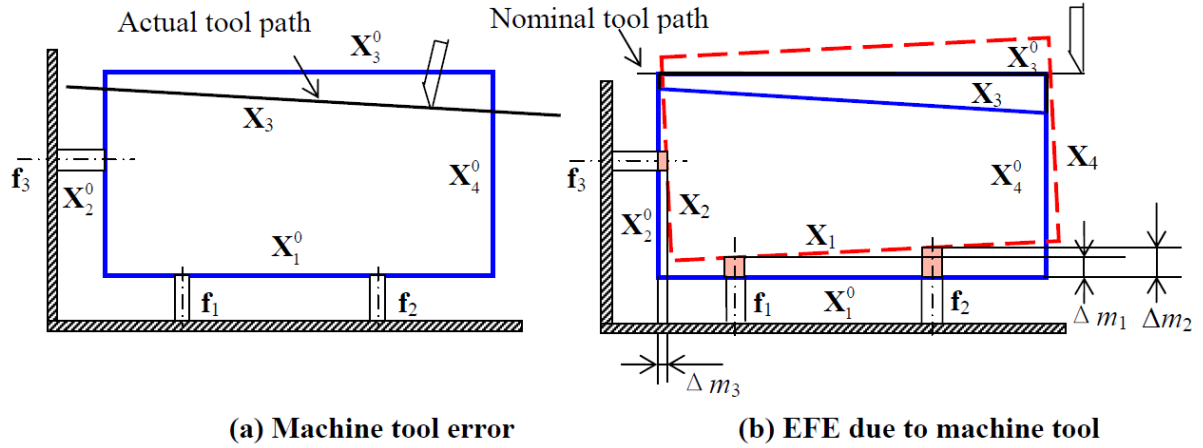
The figure 2.6 describes how the datum errors, fixture errors, and machine tool errors cause part deviation for each operation. The error propagation model after operation k in the multi-operational machining process is expressed by equation 2.7.

$$\begin{aligned} x(k) = & A(k)x(k-1) + {}^P R_M(k)B(k)x_M^u(k) + [{}^P R_M(k)B(k)M R_P^0(k) - B(K)]X^0(k) \\ & - {}^P R_M(k)B(k)\Delta^M T_P(k) + w(k) \end{aligned} \quad (2.7)$$

Where $B(k)$ is a representation of the process sequence, while $A(k)$ is defined as $A(k) = I - B(k)$, labeling uncut surfaces at operation k and $w(k)$ is a noise term, including neglected high order error terms and natural process variation.

2.1.1.3 Other researches

Djurdjanovic and Ni [DN03] proposed procedures for expressing the influence of errors in fixtures, locating datum features and measurement datum features on dimensional errors in machining based on the linear state space. These procedures are essential in the derivation of the Stream of Variation model [HS04] of dimensional machining errors using the CAD/CAPP parameters of the machining process. This model only considered the fixture errors and locating datum features on the workpiece and does not take into account machining cutting errors.



(a) Machine tool error

(b) EFE due to machine tool

Figure 2.7: Equivalent fixture error [WHK05]

Wang et al. [WHK05] formulated the variation propagation model using the proposed equivalent fixture error concept based on the error propagation error model in *MMPs* proposed by Huang et al. [HSY03]. With this concept, datum error and machine tool error are transformed to equivalent fixture locator errors at each operation. The concept of EFE¹ is based on the observation that datum and machine tool errors can generate the same error pattern on machined surfaces as fixture error. The figure 2.7a shows that the machined surface X_3 deviates from the designed position X_3^0 due to machine tool errors. The EFE transforms the workpiece from the nominal position $(X_1^0, X_2^0, X_3^0, X_4^0)$ to dashed line position shown in 2.7b. A nominal cutting operation can yield to the same surface deviation as machine tool error does in 2.7a. In figure 2.7b, the equivalent fixture locator deviation Δm_1 and Δm_2 is determined by the difference between surfaces X_1^0 and X_1 at locating point 1 and 2. Δm_3 can be computed by the difference between surfaces X_2^0 and X_2 at locating point 3. As a result, variation propagation modeling using EFE can be modelled. The machined surface j in the set-up k is expressed by equation 2.8.

$$[X_j^T(k) \ 1]^T = {}^F H_P^{-1}(k) H_d^{-1}(k) H_f^{-1}(k) H_m^{-1}(k) {}^F H_P(k) [X_j^{0T}(k) \ 1]^T \quad (2.8)$$

Where ${}^F H_P(k)$ is a homogeneous transformation matrix that transforms $X_j^0(k)$ from the nominal part coordinate system (PCS^0) to the nominal fixture coordinate sys-

¹Equivalent Fixture Error

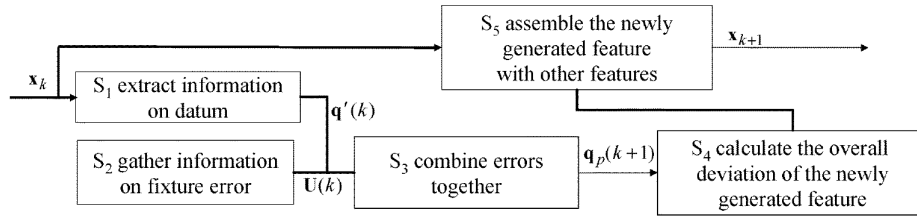


Figure 2.8: Steps of the derivation of variation propagation model [LZC07]

tem (FCS^0); $H_d(k)$ and $H_f(k)$ are homogeneous transformation matrices that transform $X_j^0(k)$ in FCS^0 caused by fixture error and datum error, respectively; $H_m(k)$ is a homogeneous transformation matrix to represent the transformation of the tool path from nominal to the real one caused by machine tool error.

Loose et al. [LZC07] established the relationships among fixture error, datum error, machine geometric error, and the dimensional quality of the product based on the dimensional variation model proposed by Zhou et al. [ZHS03]. One salient feature of the proposed technique is that the interactions among different operations with general fixture layouts are captured systematically through the modeling of setup errors. This model has a great potential to be applied to fault diagnosis and process design evaluation for a complex machining process. The steps of the variation propagation model are shown in figure 2.8. The vector of x_k is a collection of quality deviations of all key features on the product after the k^{th} stage. The deviation of each feature is represented by a 6 by 1 differential vector. If a feature has not been generated after the k^{th} stage, the corresponding components of that feature in x_k are set to be zero, and after it has been generated, the zero components are replaced by nonzero deviations. The detailed procedure explaining each step is presented below:

- S1: Only the dimensional quality of the datum features will have an influence on the deviation of the newly generated feature.
- S2: Gather the in-process information on the fixture nominal position and fixture error $U(k)$.

- S3: From the $q'(k)$ and the fixture error $U(k)$, find $q_p(k+1)$.
- S4: Calculate the dimensional error for all newly generated features q'_i .
- S5: Assemble the deviations of the newly generated features and x_k together (i.e., replace the components corresponding to each i^{th} newly generated features in x_k by their deviation q'_i to obtain the vector x_{k+1}).

Loose et al. [LZZC10] have continued to develop this model to specify and analyse the workpiece tolerances in terms of GD&T. It is valuable to evaluate a process since it gives an analytical representation of a design specification defined in the early design stage as well as the product dimensional quality measured in-line.

Liu et al. [LJ09] used the linear error propagation model proposed by Zhou et al. [ZHS03] and Huang et al. [HSY03] to establish a form-feature-based quality control model for *MMPs*. This model allows to map a relationship between machining errors of quality attributes and machining process elements. As a result, it is able to quantify the influences of datum error, fixture error and machine tools on the quality attributes of the workpiece based on a statistical model. The aim is to provide an analysis tool for machining error to help operator and manager to improve the process quality.

2.1.2 Small Displacement Torsor Approach

The concept of small displacement torsor (SDT) is first mentioned by Bourdet [Bou87] to solve the general problem of fitting of a geometrical surface model to a set of points (a cloud of points) in three-dimensional metrology. The definition of SDT will be presented in detail in section 3.1 in chapter 3. This approach is actively supported by many researchers, especially by a group of scientists in France. It is used in different research domains classified by Hong et al. [HC02] as below:

- 3D Tolerance propagation model: [GDTA92], [GPS99], [BB95], [BB98], [TCG96], [TCG99].
- 3D tolerance transfer techniques: [TCG98], [LVB99], [VLL01].

Moreover, this approach is also used to model geometrical deviations generated and accumulated by manufacturing processes. The first models of workpiece, set-ups and machining operations based on SDT is mentioned by Villeneuve et al. [VLL01] and then they have been developed by many French researchers in GRT², such as Tichadou et al. [TLH05] and Vignat et al. [VV07], etc.

2.1.2.1 Villeneuve et al. (2001)

Villeneuve et al. [VLL01] used the concept of small displacement to model the process. The authors provided a 3D geometrical deviation model of workpiece, set-ups and machining operations. The geometrical deviation of surface P_i of the manufactured part by machining operation Mk in set-up S_j is described by the SDT T_{P,P_i} , as given in equation 2.9.

$$T_{P,P_i} = -T_{R,P(S_j)} + T_{R,P_i(S_j)} \quad (2.9)$$

Where:

- $T_{R,P_i(S_j)}$ is a SDT modelling the deviation of surface P_i caused by the machining operation Mk . This torsor depends on the variation of the machining operation Mk (see figure 2.9):
- $T_{R,Mk(S_j)}$: SDT of a machining operation relative to its nominal position in set-up j . This torsor is the result of the cinematic variations of the machine tool.

²Group de Recherche en Tolérancement

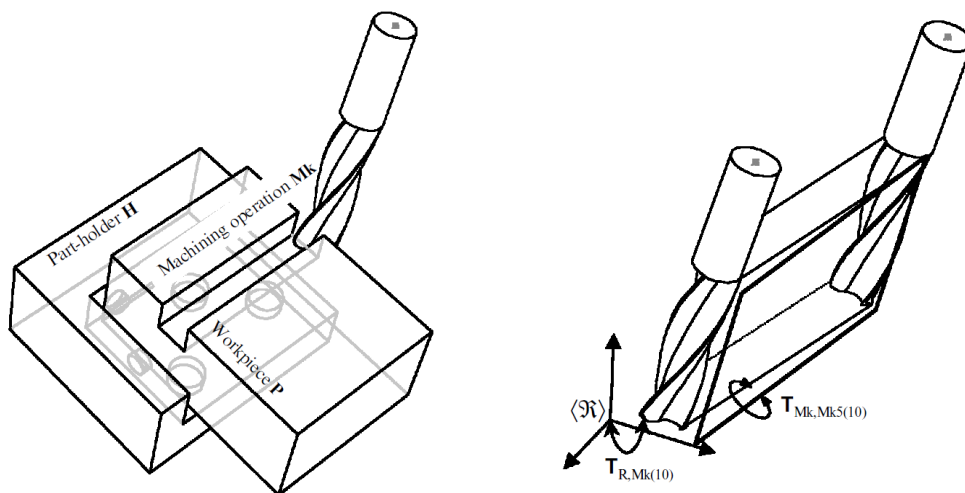


Figure 2.9: SDT of a machining operation (set-up 10) [VLL01]

- $T_{R,Mk(S_j)}$: deviation torsor of the surface Mk_i relatively to its nominal position in the machining operation Mk in set-up j . This torsor is the result of the geometric variations and deformations of the tool.

$T_{R,P_i(S_j)}$ is the positioning torsor of the part modelling the deviation of the workpiece relative to its nominal position in the set-up S_j . It depends on the quality of the part-holder and the link between the surface of the workpiece and the part-holder surface (see figure 2.10):

- $T_{R,H(S_j)}$: global SDT of the part-holder H relatively to its nominal position in set-up j .
- $T_{H,H_i(S_j)}$: deviation torsor of the surface H_i relatively to its nominal position on the part-holder in set-up j . This deviation expresses the geometrical variations of the part-holder.
- $T_{H_i,P_i(S_j)}$: gap torsor that expresses the characteristics of the interface between the workpiece and the part-holder at the level of the joint H_i/P_i . In the context of machining, these joints are organized hierarchically, i.e. the main support is ensured before the secondary one and so on. The present authors will hereafter consider that the parts do not interpenetrate at the contacts. Each fixed component of the torsors is thus considered as nil.

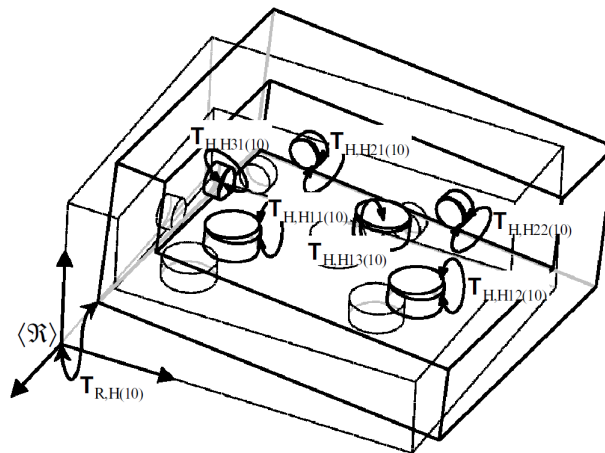


Figure 2.10: SDT of a part-holder (set-up 10) [VLL01]

2.1.2.2 Vignat et al. (2005)

Vignat et al. [Vig05, VV07] developed a model of manufactured parts (MMP) based on the SDT for simulating and storing the manufacturing defects in 3D based on the model of [VLL01]. It collects the deviations generated during a virtual manufacturing process. The defects generated by a machining process are considered to be the result of two independent phenomena: positioning and machining. The deviations due to these phenomena are accumulated over the successive set-ups. The positioning deviation is the deviation of the nominal part relative to the nominal machine while the machining deviation is the deviation of the manufactured surface relative to the nominal machine. The positioning operation of the part on the part-holder is realized by a set of hierarchically organized elementary connections. The deviations of the manufactured surface relative to its nominal position in MMP are expressed by parameters of a SDT. The MMP will be detailed in section 3.2 in chapter 3.

2.1.2.3 Tichadou et al. (2005)

Tichadou et al. [TLH05, Tic05] proposed a chart representation of the manufacturing process (see figure 2.11). This chart model the successive set-up and for each set-up the positioning surface and their hierarchy and the machined surfaces. It

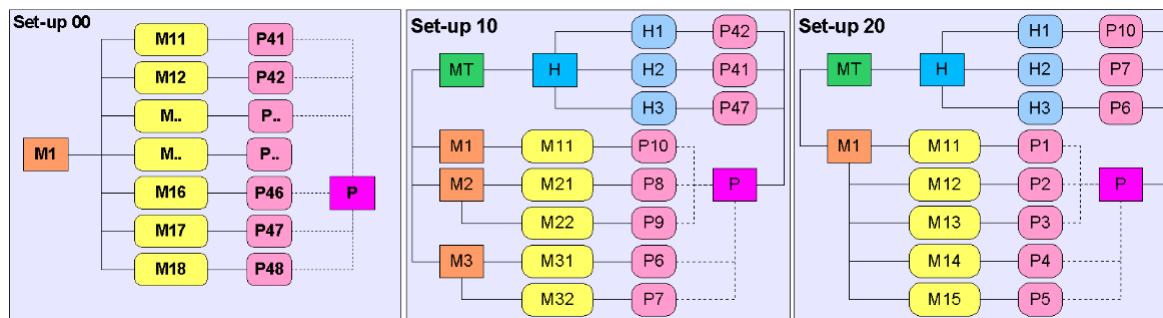


Figure 2.11: Charts of three set-ups [TLH05]

makes it possible to highlight the influential paths. They propose then two analysis methods. The first one uses a small displacement torsor model. The second one is based on the use of CAD software in which they model a manufacturing process with defects. They then virtually measure the realized part and check its conformity.

The data structure defined in those charts follow the following rules:

- Part-holder surface Hh : the number h indicates the hierarchy of the contacts (i.e. $H1$ is the main contact surface and so on).
- Machining operations Mm : m indicates the machining operation sequencing ($M1$ is machined first).
- Machining operation surfaces Mmj : j is only a surface number, a different one for each surface.

2.2 Assembly Stage

A product is made up of parts assembled by the way of connections. Each part has to pass through the manufacturing stage where geometrical deviations are generated. Then the product has to pass through assembly stage. Assembly stage of the product life cycle is an essential stage of its life cycle, and it obviously brings its share of deviations to the product. Thus it is necessary to manage the dimensional

and geometrical variations on the final product. Because they influence the quality of the products when they come to customers and users. Many researches for analysis of dimensional variation in an assembly process have been done based using different approaches.

2.2.1 State Transition Model Approach

2.2.1.1 Mantripragada and Whitney (1999)

Mantripragada and Whitney [MW99] propose algorithms to propagate and control variation in mechanical assemblies using the State Transition Model approach. It exploits the modeling environment and uses concepts from control theory to model variation propagation and control during assembly. The assembly process is modeled as a multistage linear dynamic system. Two types of assemblies are addressed:

- **Type-1:** It comprises typical machined or molded parts that have their mating features fully defined by their respective fabrication process prior to the final assembly. The variation in the final assembly is determined completely by the variation contributed by each part in the assembly. The assembly process merely puts the parts together by joining their predefined mates. The mating features are almost always defined by the desired function of the assembly, and the assembly process designer has almost no freedom in selecting mating features.
- **Type-2:** The second type of assembly includes aircraft and automotive body parts that are usually given some or all of their assembly features or relative locations during the assembly process. Assembling these parts requires placing them in proximity and then drilling holes or bending regions of parts, as well as riveting or welding. The locating scheme for these parts must include

careful consideration of the assembly process itself. Final assembly quality depends crucially on achieving desired final relative locations of the parts, something that is by no means assured because at least some of the parts lack definite mating features that tie them together unambiguously. A different datum flow logic, assembly sequence, etc., will result in quite different assembly configurations, errors and quality.

The state of an assembly at any assembly station is described by a 6x1 vector $\tilde{X}(k)$. It describes the total deviation in position and orientation of a coordinate frame on a mating feature on the k^{th} part, measured from its nominal or zero mean location, expressed in the coordinate frame of the part at the base of the chain. It is given in equation 2.10.

$$\tilde{X}(k) = \begin{bmatrix} dp_k \\ d\theta_k \end{bmatrix} = \begin{bmatrix} dp_k^x \\ dp_k^y \\ dp_k^z \\ d\theta_k^x \\ d\theta_k^y \\ d\theta_k^z \end{bmatrix} \quad (2.10)$$

Where dp_k is the first order differential error in the Cartesian position of the k^{th} frame and $d\theta_k$ the corresponding error in orientation.

Then state transition equation is used to express relations between two processes at k^{th} assembly station:

- Type-1:

$$\tilde{X}(k+1) = A(k)\tilde{X}(k) + F(k)\tilde{w}(k) \quad (2.11)$$

- Type-2:

$$\tilde{X}(k+1) = A(k)\tilde{X}(k) + B(k)\tilde{U}(k) + F(k)\tilde{w}(k) \quad (2.12)$$

Where:

$\tilde{w}(k)$: 6x1 vector describing the variation associated with the part being assembled at the k^{th} assembly station, expressed in local part coordinates.

$F(k)$: 6x6 matrix that transforms the variation associated with the incoming part at the k^{th} assembly station from part $k's$ coordinate frame to the base coordinate frame of the DFC (Data Flow Chain).

$A(k), B(k)$: identify matrix.

$\tilde{U}(k)$: 6x1 vector describing the property of the absorption zone modelling the contact between fixture and part.

Finally, all dimensional variations from successive assembly station are accumulated into vector $\tilde{X}(k)$ at the final assembly station.

2.2.2 Stream of Variation Model Approach

Ceglarek and Shi [CS95] proposed a model of dimensional variation applied to the sheet metal assembly. They apply their model to the automotive body assembly with the aim of making diagnosis and reduction of source of dimensional variability. Shiu et al. [SCS96] proposed a model of the multi-station assembly process in order to diagnose the automotive body dimensional faults. This model is based on the design information from the CAD system and allows a system behaviour determination based on in-line measurements of the final product. The model is only applied for the automotive sheet metal assembly.

2.2.2.1 Jin and Shi (1999)

Jin and Shi [JS99] introduced a state space model for dimensional control of sheet metal assembly processes. According to the authors, the dimensional variation of sheet metal assembly is caused by fixture error and part variation:

- **Fixture error:** the fixture error in station i is represented by equation 2.13.

$$\Delta P(i) = (\Delta x_{P_1}(i), \Delta z_{P_1}(i), \Delta z_{P_2}(i))^T \quad (2.13)$$

Where $\Delta P(i)$ is the fixture error vector for locator P_1 and P_2 of station i ; $\Delta x_{P_1}(i)$ and $\Delta z_{P_1}(i)$ represent the locating errors for 4-way pin P_1 in the X and Z directions respectively; $\Delta z_{P_2}(i)$ represents the locating error for 2-way pin P_2 in the Z direction.

- **Part variation:** the part error in station i represented by a vector at a point A is given by equation 2.14.

$$\Delta X_A(i) = (\Delta x_A(i), \Delta z_A(i), \Delta \alpha(i))^T \quad (2.14)$$

Where $\Delta x_A(i)$, $\Delta z_A(i)$ are the deviation errors at a point A in the X and Z directions in the body coordinate system at station i^{th} ; $\Delta \alpha(i)$ is the part orientation angle error of this part at station i .

A state space model is developed by Jin et al. [JS99] to describe part dimensional variations during the assembly process. A state variable vector $X(i)$ describing all assembly part error vectors is represented by equation 2.15.

$$X(i) = \begin{pmatrix} X_{A_1}(i) \\ \vdots \\ X_{A_n}(i) \end{pmatrix} \quad (2.15)$$

Where $i(i = 1, 2, \dots, N)$ is the index of the assembly station, N is the total number of assembly stations in the assembly process; n is the total number of parts to be assembled during the whole assembly process; $X_{A_1}(i)$ is the part error vector of part j expressed in part point A_1 in assembly station i^{th} . The state equation at

station i is expressed by equation 2.16.

$$X(i) = [I + T(i - 1)]X(i - 1) + B(i)U(i) + V(i) \quad (2.16)$$

Where $T(i - 1)$ is a part reorientation error vector representing the part reorientation movement occurring when the stack-up variations (up to the previous assembly station $i - 1$) at locator points of the current station i is reset to zero; $V(i)$ is the model noise term representing the modeling imperfections; $B(i)$ is a control matrix; $U(i)$ is the control vector at station i , which is defined as the fixture error vector for both subassembled parts at station i .

2.2.2.2 Camelio et al. (2003)

Camelio et al. [CHC03] introduced a methodology to evaluate dimensional variation propagation in a multi-station compliant assembly system based on linear mechanics and state space representation, as shown in figure 2.12. According to the authors, the variation sources in compliant assembly result from three sources: part variation, fixture variation and welding gun variation. The state space model considering the part variation, fixture variation ($N - 2 - 1$ fixturing principle) and welding gun variation can be represented by equation 2.17.

$$\begin{cases} X'(k - 1) = X(k - 1) + M(k) \cdot (X(k - 1) - U_{t_{3-2-1}}) \\ X(k) = (S(k) - P(k) + I) \cdot X'(k - 1) - (S(k) - P(k)) \cdot (U_g + U_{t_{(N-3)}}) + U(k) \end{cases} \quad (2.17)$$

Where $X(k - 1)$, $X(k)$ are the state vectors representing the dimensional deviation of the part in the station $k - 1$ and k respectively; $X'(k - 1)$ is a state vector representing the fixture variation at the re-location process caused by the $(3 - 2 - 1)$ locating fixtures $U_{t_{3-2-1}}$; $U_{t_{(N-3)}}$ is a state vector representing the $(N - 3)$ additional holding fixture variation; U_g is a state vector representing the welding gun deviation; $M(k)$, $P(k)$ and $S(k)$ are matrices representing re-location/re-orientation effect, the part

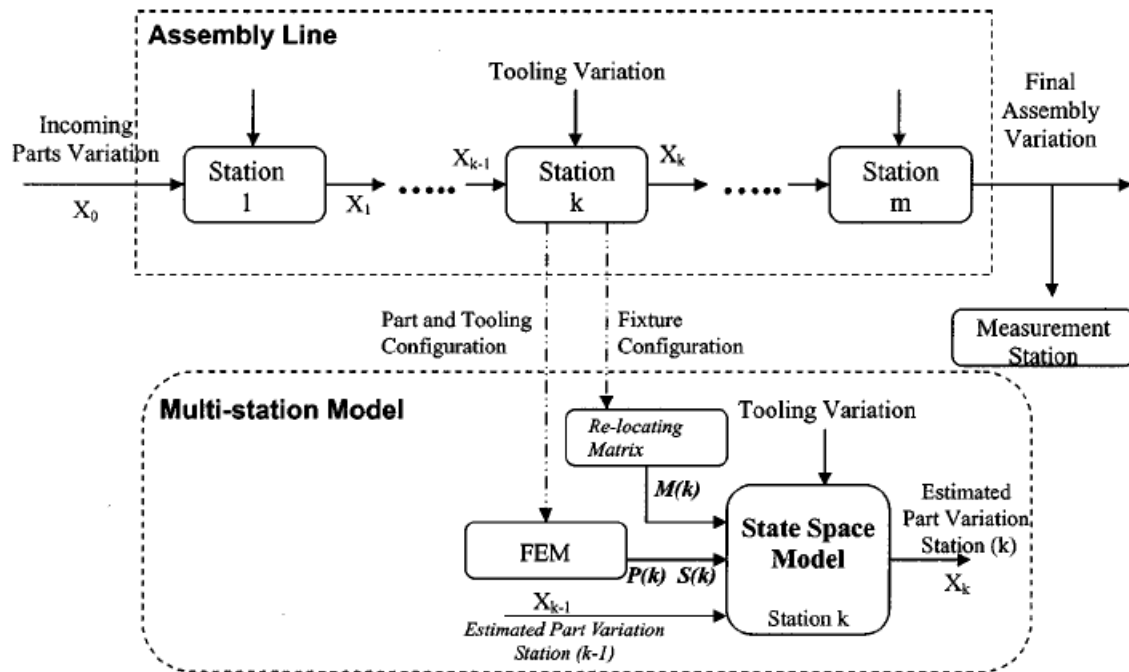


Figure 2.12: Multi-station assembly modeling methodology [CHC03]

deformation before welding and springback for unit deviations, respectively.

2.2.2.3 Huang et al. (2007)

Huang et al. [HLB⁺07, HLKC07] proposed a Stream-of-Variation Model (SOVA) for 3D rigid assemblies' dimensional variation propagation analysis in multi-station processes. This model is also based on State Space Model approach [JS99]. This approach is not only applied to the rigid-body assembly in single station assembly processes but also to multistation assembly processes. The stream of variation in multistage manufacturing systems (MMS) is illustrated in figure 2.13.

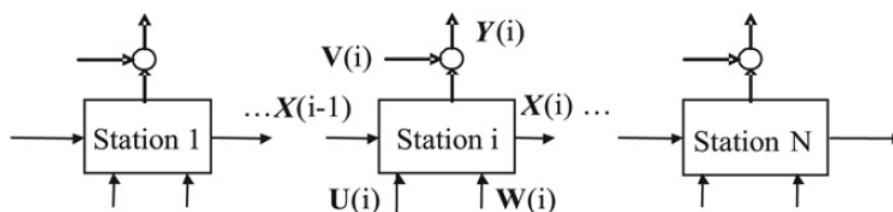


Figure 2.13: An assembly process with N stations [HLKC07]

The stream of variation in this MMP is characterized by equation 2.18.

$$X(i) = A(i-1)X(i-1) + B(i)P(i) + W(i) \quad i = 1, 2, \dots, N \quad (2.18)$$

Where $X(i) = [X^1(i), X^2(i), \dots, X^k(i), \dots, X^{nt}(i)]^T$ is a state vector representing the dimensional deviation of the final part in the station i and $X(i-1)$ represents the dimensional deviation of the subassembled part coming from the station $i-1$; $V(i)$ and $W(i)$ are the matrices representing independent noise in the station i ; $A(i)$ and $B(i)$ are transformation matrices between the global coordinate system and the local coordinate system.

2.2.3 Small Displacement Torsor Approach

2.2.3.1 Ballot et al. (1997, 2000) and Thiebaut (2001)

Ballot et al. [BB97, BB00] introduced a model of geometric deviation for part and mechanism based on the concept of small displacement torsor [BMLB96]. The deviation torsor expresses the variation between the nominal surface and the substitute surface, which is an ideal representation of the real one. This torsor is built upon two small displacement torsors: the small displacement torsor of the surface and the torsor of intrinsic feature variation. For example, the deviation torsor between a substitute S and a nominal N cylinder with a z axis is given in equation 2.19.

$$T_{S,N} = \left\{ \begin{array}{cc} \alpha_{S,N} & u_{S,N} \\ \beta_{S,N} & v_{S,N} \\ Ind_{rzS,N} & Ind_{tzS,N} \end{array} \right\}_{(O,xyz)} \quad and \quad T_{Intrinsic} = \left\{ \begin{array}{cc} 0 & dr_{S,N} \cdot \cos\theta \\ 0 & dr_{S,N} \cdot \sin\theta \\ 0 & 0 \end{array} \right\}_{(O,xyz)} \quad (2.19)$$

They also introduced the gap torsor that represents the gap between two substitute surfaces from different parts, which are nominally in contact. Finally, the part torsor is used to describe the part's displacement within the mechanism in relation

with geometric errors, gaps and its the nominal position of the part. A part torsor is associated to each part.

The propagation of deviation from a link i between surface 2 of part B and surface 1 of part A is directly computed from the composition of torsors from one part to another, as given in equation 2.20.

$$T_{B/R}^{(i)} = T_{A/R} + T_{1/A} - T_{2/R} - T_{1/2} \quad (2.20)$$

Where $T_{B/R}^{(i)}$ and $T_{1/A}$ represent the deviation of part B and part A in the common reference frame R , respectively; $T_{2/R}$ represents the deviation of the surface 2 of the part B in the reference frame R ; $T_{1/2}$ represents the deviation of the link between the surface 1 and surface 2. Moreover, the part B is positioned by n parallel links. Thus the deviation of part B is calculated by a set of $n - 1$ equalities, as given in equation 2.21.

$$T_{B/R}^{(1)} = T_{B/R}^{(2)} = \dots = T_{B/R}^{(i)} = \dots = T_{B/R}^{(n)} \quad (2.21)$$

In conclusion, the deviation of part B includes the deviation of part A , the deviation of the surfaces of the connection and the deviation of the link between the part A and the part B . All deviations are accumulated over on part B , as expressed in equation 2.20.

Thiebaut [Thi01] develops a model to allow to analyse the variation of the part in the assembly based on the concept of small displacement torsor and the research work of Ballot et al. [BB97, BB00]. The positioning variation of the part relative to its nominal position in the global coordinate system is expressed by equation 2.22.

$$D(A/R) = E(A/S_A) + T(S_A/S_B) + E(S_A/B) + D(B/R) \quad (2.22)$$

Where:

$D(A/R)$ is the variation of the position of part A relative to its nominal position in the global coordinate system R .

$E(A/S_A)$ is the variation of surface S_A of the part A relative to its nominal position.

$T(S_A/S_B)$ is the variation of the link between the surface S_A of the part A and the surface S_B of the part B .

$E(S_A/B)$ is the variation of surface S_B of the part B relative to its nominal position.

$D(B/R)$ is the variation of part B relative to its initial nominal position in the global coordinate system R .

The linear system of equations is created along all connections between the part A and B . The positioning variation of the part A is determined by resolution of the linear system of equations based on the Gauss-Pivot method.

2.3 Robust Design Methodology

The concept of robust design methodology (RDM) evolved during the second half of the twentieth century. The significant contributions of Taguchi [Tag86], Phadke [Pha89], Kacker [Kac85], Box and Jones [GJ92] established RDM as a methodology to improve product and process quality. The fundamental principle in robust design is mentioned by Taguchi [Tag86]. He summarised the quality loss function by equation 2.23.

$$L = k(y - m)^2 \quad (2.23)$$

Where y represents the performance parameter of the system, m represents the target or the nominal value of y , L represents the quality loss and k is a constant.

Taguchi breaks the design process into three stages:

- System design - involves creating a working prototype
- Parameter design - involves experimenting to find which factors influence product performance most

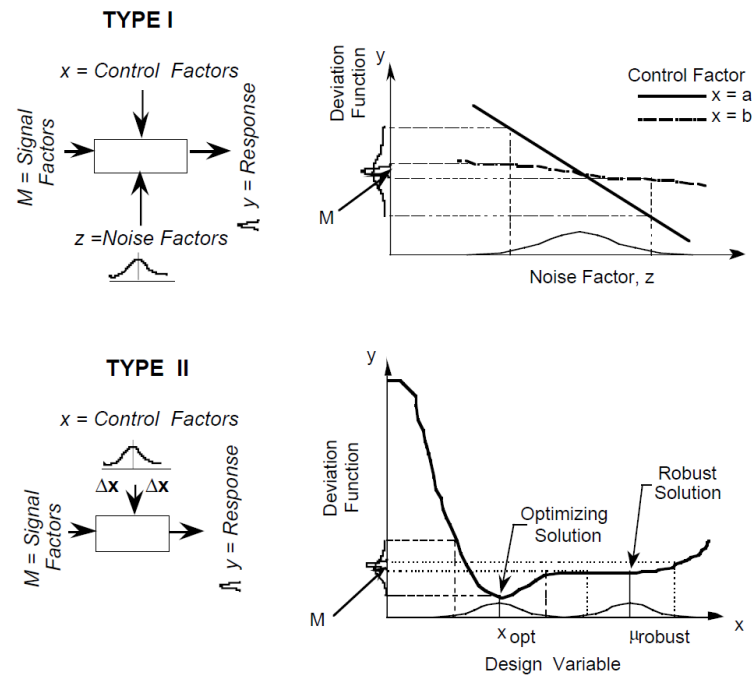


Figure 2.14: A comparison of two types of robust design [CATM96]

- Tolerance design - involves setting tight tolerance limits for the critical factors and looser tolerance limits for less important factors.

2.3.1 Chen et al. (1996)

Chen et al. [CATM96] defined robust design to be to improve the quality of a product by minimizing the effects of variation without eliminating its causes. The authors classified the effect of the variation source on the performance variations into two general following categories (see figure 2.14):

- Type I: minimizing variations in performance caused by variations in noise factors (uncontrollable parameters), such as ambient temperature, operating environment, or other natural phenomena, etc.
- Type II: minimizing variations in performance caused by variations in control factors (design variables), such as material properties, manufacturing quality variations, etc.

They also developed a robust design procedure that integrates the response surface methodology with a compromise decision support problem in order to overcome the limitations of Taguchi's methods. This procedure includes three steps:

- Step 1: Build response surface models to relate each response to all important control- and noise-factors using the Response Surface Methodology (RSM). The response surface is established by the design of experiments method and fitting a response model. This model can be expressed by equation 2.24.

$$\hat{y} = f(x, z) \quad (2.24)$$

Where \hat{y} is the estimated response and x and z are control and noise variables.

- Step 2: Derive functions for mean and variance of the responses based on the type of robust design applications. For the Type I, the mean and variance of the response are described by equations 2.25, respectively.

$$\begin{aligned} \mu_{\hat{y}} &= f(x, \mu_z) \\ \sigma_{\hat{y}}^2 &= \sum_{i=1}^n \left(\frac{\partial f}{\partial z_i} \right)^2 \sigma_{z_i}^2 \end{aligned} \quad (2.25)$$

For the Type II, the mean and variance of the response are described by equations 2.26, respectively.

$$\begin{aligned} \mu_{\hat{y}} &= f(x) \\ \sigma_{\hat{y}}^2 &= \sum_{i=1}^m \left(\frac{\partial f}{\partial x_i} \right)^2 \sigma_{x_i}^2 \end{aligned} \quad (2.26)$$

- Step 3: Use the compromise decision support problem (DSP) to find the robust design solution.

The response-model approach is used to minimize the variance in equation 2.25 or 2.26 and bring the mean to the target. Because the classical RSM is restricted to unconstrained searching for a local optimum of a single response (or the variance of that response) a compromise Decision Support Problem is introduced to handle multiple aspects of quality and engineering constraints.

2.3.2 Vlahinos et al. (2003)

Vlahinos et al. [VKDS03] proposed to use probabilistic FEA analysis in order to identify the effects of material and manufacturing variations on the product performance. The authors then proposed a method that allows to take material and

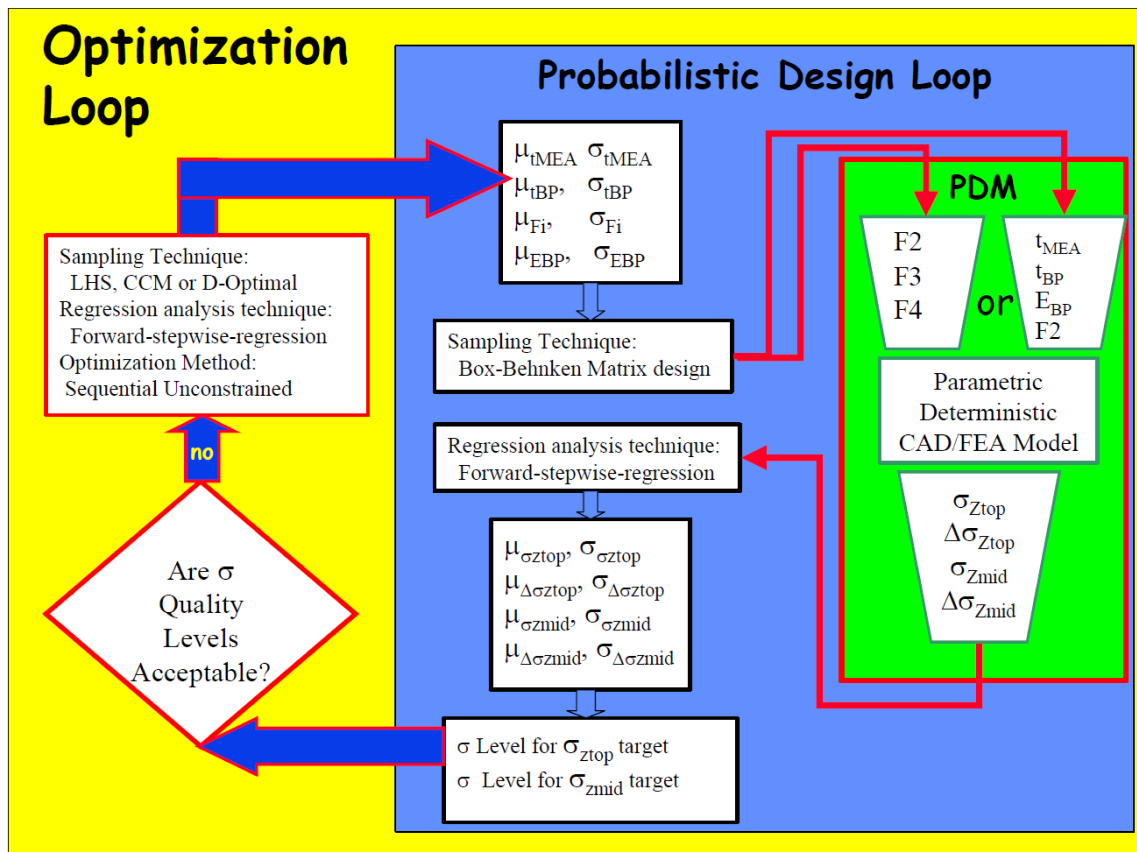


Figure 2.15: Workflow for Robust Optimization [VKDS03]

manufacturing variations, occurring during the product life cycle, into account for robust design optimization. The robust design optimization process shown in figure 2.15 has been implemented to evaluate the effect of the bolt stack loading on the MEA pressure distribution. The effect of variation in the material properties such as the modulus of elasticity of the bi-polar plates E_{bp} , the bi-polar plate thickness t_{bp} , the MEA thickness t_{mea} and the bolt loading F have also been assessed. This robust optimization workflow includes three different processes: the parametric deterministic model (PDM), the probabilistic design loop, and the design optimization loop.

2.3.3 Gu et al. (2004)

Gu et al. [GLS04] proposed a new approach for robust design of mechanical systems. This approach integrates the independent analysis based on axiomatic design [Suh01] and the traditional robust technique. The sensitivity of the functional domain Fr to variations in the physical domain Dp is measured by the sensitivity index S , as expressed by equation 2.27.

$$S = \left| \frac{\Delta Fr / Fr}{\Delta Dp / Dp} \right| = \left| \frac{\Delta Fr / \Delta Dp}{Fr / Dp} \right| \simeq \left| \frac{\partial Fr / \partial Dp}{Fr / Dp} \right| \quad (2.27)$$

The authors then defined the sensitivity matrix S_v by equation 2.28.

$$S_v = s_v^2 \cdot D \cdot D^T \quad (2.28)$$

Where $s_v^2 = \frac{\sigma_F^2}{\sigma_D^2}$ is a ratio between variance of output Fr and variance of input Dp .

The variance of output Fr is defined by equation 2.29.

$$\begin{aligned} V(Fr) &= \sigma_F^2 = V(D \cdot \Delta Dp) = D \cdot V(\Delta Dp) \cdot D^T \\ &= D \cdot \sigma_D^2 \cdot D^T \end{aligned} \quad (2.29)$$

The authors expressed the conditions for a design to be robust being that the sensitivity matrix S_v satisfies the two following requirements:

- Sensitivity matrix S_v has to be a diagonal matrix
- All elements on the main diagonal have to be identical.

This approach is continuously developed by Gang et al. [ZBZG09, ZLB⁺10] to apply on nonlinear mechanical systems and the determination of tolerances of mechanical products.

2.3.4 Other Researches

Since many successful applications in engineering industry are being expanded to different fields. All the robust design study according to Li et al. [LAB06] can be classified into two categories: the stochastic approaches and the deterministic approaches. The stochastic approaches use probabilistic information of the design variables and the design parameters, such as their mean and variance, to analyse the system robustness. Parkinson [Par95] proposed to use engineering models to develop robust design in order to reduce the sensitivity of the design to variation. This method was used in tolerancing in order to solve the problem of determining optimum nominal dimensions of manufactured components and improving assembly quality without tightening tolerances. Du et al. [DC00] proposed a statistical method to allow checking several feasibility modelling techniques for robust optimization. Kalsi et al. [KHL01] proposed a technique to reduce the effects of uncertainty and incorporate flexibility in the design of complex engineering systems involving multiple decision-makers. Al-Widyan et al. [AWA05] formulated the robust design problem based on the minimization of a norm of the covariance matrix. This matrix links the variations in performance functions with the variations in the design-environment parameters, considering the stochastic nature of the design-environment parameters.

The deterministic approaches often use the gradient information of the variations and employ the Euclidean norm method and the condition number method to improve the system robustness. Ting et al. [TL96] determined sensitivity Jacobian and Rayleigh quotient of the sensitivity Jacobian to measure the robustness of the system. Zhu et al. [ZT01] presented the theory of the performance sensitivity distribution in order to find the robust design, i.e. less sensitive to variation sources. Caro et al. [CBW05] proposed a new robust design method to dimension a mechanism and to synthesize its dimensional tolerances. Lu et al. [LL09] proposed a novel robust design approach to improve system robustness upon variations in

design variables as well as model uncertainty.

Both are based on a study of impact of source variation on performance variation. These covariations are expressed by matrix and restricted to geometry versus geometry. By modelling the manufacturing and assembly process sink of geometrical variations and using the resulting geometrical model in numerical simulations (structure, fluid, dynamics...), the covariations can be expressed upon non geometrical performances of the product and the robust design methodology can be applied.

2.4 Conclusion and Scientific Questions

Today, product designers work on a numerical model of the product within a CAx system. This model only represents nominal product information. Most of the simulations for predicting the behavior (kinematics, dynamics...) and evaluating the product quality are carried out on this nominal model. However, according to Kimura [Kim07] there are many kinds of disturbances in the product life cycle, such as forming and machining errors in manufacturing stage; assembly inaccuracy in assembly stage and material deterioration, wear, fatigue, corrosion, temperature, environment and condition of use in product usage stage. These disturbances obviously affect the “real” performance of the designed product. Thus, it is necessary to take them into account the product design stage.

Some research works exist today in the academic research for each stage of the product life cycle separately. In the manufacturing stage, there are many approaches as presented in this chapter and summarised in table 2.1 in order to model geometrical deviations generated by variation sources from the manufacturing process. In the assembly stage, the geometrical deviations of the final product are similarly modelled by many approaches, as presented in this chapter and summarised in table 2.2.

	State space approach			Small displacement torsor	
	Zhou et al. (2003)	Huang et al. (2003)	Wang et al. (2005)	Villeneuve et al. (2001)	Vignat et al. (2005)
Fixture errors	Yes	Yes	Yes	Yes	Yes
Machining tool errors	Yes	Yes	Yes	Yes	Yes
Multioperation	Yes	Yes	Yes	Yes	Yes
2D/3D	3D	3D	3D	3D	2D and 3D

Table 2.1: The geometrical deviation models in manufacturing stage.

The main principle of the models proposed by Mantripragada and Whitney [MW99], Jin and Shi [JS99], Huang et al. [HLKC07] and Thiebaut [Thi01] is to model the variation of the part in each stage along the assembly process. These models take into account the geometrical deviations of the part but these deviations are not linked to deviations from the manufacturing stage. They are not linked to any model proposed by Zhou et al. [ZHS03], Huang et al [HSY03], Wang et al. [WHK05], Villeneuve et al. [VLL01] and Vignat et al. [Vig05] which model the variation from the manufacturing stage. Thus, it is necessary to develop a global model that can cover the whole production stages of the product life cycle.

Moreover, all robust design methodologies as presented in section 2.3 only work for an accurate model since they need to know the mathematical relationship between the performance of the product and the variation sources during its life cycle. This accurate model is difficult to obtain due to complex process (manufacturing and assembly process), complex dynamics, complex geometrical boundary conditions. Therefore, it is necessary to integrate the deviation into numerical simulation of the product performance, and then to establish the relationship between the performance and these deviations.

For these reasons, we need to find out a complete answer for the following scientific questions:

- **How to model the geometrical deviations of a product corresponding to all the stage of its life cycle?**
- **How to integrate geometrical deviations into the product performance simulation?**
- **How to manage the causes and consequences of these deviations in the design stage and identify the variation sources that affect on the performance of the product?**

My thesis focuses on developing a model of geometrical deviations of the product that has to be consistent with all the stages of the product life cycle and a method that allows the integration of these deviations into the simulations of the product performance. We propose several analysis methods in order to classify and identify the variation sources that influence the performance of the product and to determine the variance of the product performance variation. As a result, the robust solution can be found by determining a design solution that minimizes the performance variability.

	State transition approach	State space approach			Small displacement torsor	
	Mantripragada and Whitney (1999)	Jin and Shi (1999)	Camelio et al. (2003)	Huang et al. (2007)	Ballot et al. (1997)	Thiebaut (2001)
Fixture errors	No	Yes	Yes	Yes	Yes	Yes
Part deviation	Yes	No	Yes	Yes	Yes	Yes
Machining tool errors	N/A	N/A	N/A	N/A	N/A	N/A
Multistation	No	Yes	Yes	Yes	N/A	Yes
2D/3D	N/A	2D	3D	3D	3D	3D

Table 2.2: The geometrical deviation models in assembly stage

Chapter 3

GDM¹ FOR PRODUCT LIFE CYCLE ENGINEERING

THE purpose of this chapter is to propose a geometrical deviation model (GDM) based on the small displacement torsor concept. This model allows to model geometrical deviations of a product generated and accumulated through manufacturing and assembly stage of its life cycle. The Monte-Carlo simulation method is then used in this chapter to provide a set of products representative of the population of the real product by using the proposed GDM. After then, product designers can measure and verify any geometrical functional requirements on the virtual products.

3.1 Small Displacement Torsors

The concept of small displacement torsor (SDT) was developed by Bourdet [Bou87], in order to solve the problem of fitting a model of ideal geometrical surface with a cloud of points in three-dimensional metrology. This concept is based on the rigid

¹GEOMETRICAL DEVIATION MODEL

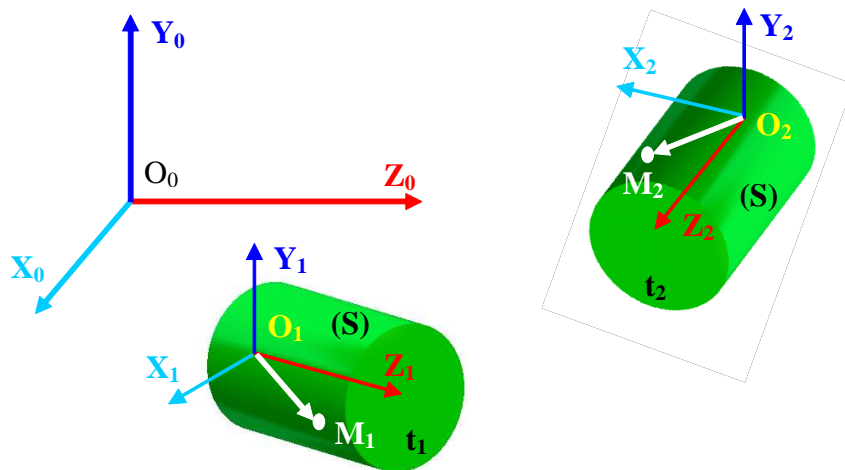


Figure 3.1: Displacement of a rigid body

body movements. It has widely been used in software for coordinate measuring machines to process measured data. It was also used in kinematic simulation software taking into account geometrical defects and for analysis and transfer of manufacturing tolerances [VLL01]. The concept allows to simplify the three-dimensional problem by linearization of the transformation matrix to express the movement of a solid.

3.1.1 Definition

The SDT is defined based on the displacement of a point of the rigid body in space. We consider the displacement of the point M of the rigid body (S) at the instant t_1 and t_2 represented by points M_1 and M_2 respectively (see figure 3.1).

The vector $\overrightarrow{\delta M} = \overline{M_1 M_2}$ is called the displacement vector of the point M of the rigid body (S) between the instant t_1 and t_2 . The displacement of the point M in the global coordinate system $R_0(O_0, X_0 Y_0 Z_0)$ is expressed by equation 3.1.

$$\overline{M_1 M_2} = \overline{M_1 O_1} + \overline{O_1 O_2} + \overline{O_2 M_2} \quad (3.1)$$

Then the displacement $\overrightarrow{\delta M}$ in the local reference $R_1(O_1, X_1 Y_1 Z_1)$ is calculated by

relation 3.2.

$$\overrightarrow{\delta M}_{/R_1} = \overrightarrow{\delta O}_{/R_1} + \overrightarrow{O_2 M_2}_{/R_1} - \overrightarrow{O_1 M_1}_{/R_1} \quad (3.2)$$

Where $\overrightarrow{\delta O}$ is the displacement of the origin of the local coordinate system $R_1(O_1, X_1 Y_1 Z_1)$.

The relation 3.2 can also be expressed by equation 3.3.

$$\overrightarrow{\delta M}_{/R_1} = \overrightarrow{\delta O}_{/R_1} + (P_{12} - I) \overrightarrow{O_1 M_1}_{/R_1} \quad (3.3)$$

Where P_{12} is a transformation matrix from the local reference $R_1(O_1, X_1 Y_1 Z_1)$ to local reference $R_2(O_2, X_2 Y_2 Z_2)$. It is a general rotation matrix that can be decomposed into three rotation matrices around the three axis X_1, Y_1, Z_1 of the local reference R_1 . P_{12} can be obtained by multiplication of the three rotation matrices 3.4.

$$P_{12} = \begin{pmatrix} 1 & 0 & 0 \\ 0 & \cos\theta_1 & -\sin\theta_1 \\ 0 & \sin\theta_1 & \cos\theta_1 \end{pmatrix} \begin{pmatrix} \cos\theta_2 & 0 & \sin\theta_2 \\ 0 & 1 & 0 \\ -\sin\theta_2 & 0 & \cos\theta_2 \end{pmatrix} \begin{pmatrix} \cos\theta_3 & -\sin\theta_3 & 0 \\ \sin\theta_3 & \cos\theta_3 & 0 \\ 0 & 0 & 1 \end{pmatrix} \quad (3.4)$$

The result of matrix product can be written by equation 3.5.

$$P_{12} = \begin{pmatrix} \cos\theta_2 \cos\theta_3 & -\cos\theta_2 \sin\theta_3 & \sin\theta_2 \\ \cos\theta_1 \sin\theta_3 + \sin\theta_1 \sin\theta_2 \cos\theta_3 & \cos\theta_1 \sin\theta_3 - \sin\theta_1 \sin\theta_2 \sin\theta_3 & -\sin\theta_1 \cos\theta_2 \\ \sin\theta_1 \sin\theta_3 - \cos\theta_1 \sin\theta_2 \cos\theta_3 & \sin\theta_1 \cos\theta_3 + \cos\theta_1 \sin\theta_2 \sin\theta_3 & \cos\theta_1 \cos\theta_2 \end{pmatrix} \quad (3.5)$$

In the case of small displacement, the value of the angles θ_1, θ_2 and θ_3 are very small. The transformation matrix P_{12} is thus simplified and written as in equation 3.6.

$$P_{12} = \begin{pmatrix} 1 & -\theta_3 & \theta_2 \\ \theta_3 & 1 & -\theta_1 \\ -\theta_2 & \theta_1 & 1 \end{pmatrix} \quad (3.6)$$

The relation 3.3 can then be rewritten as in equation 3.7.

$$\overrightarrow{\delta M}_{/R_1} = \overrightarrow{\delta O}_{/R_1} + \begin{pmatrix} 0 & -\theta_3 & \theta_2 \\ \theta_3 & 0 & -\theta_1 \\ -\theta_2 & \theta_1 & 0 \end{pmatrix} \overrightarrow{O_1 M_1}_{/R_1} \quad (3.7)$$

Finally, the small displacement of the point M of the rigid body (S) between the instant t_1 and t_2 is expressed by equation 3.8.

$$\overrightarrow{\delta M}_{/R_1} = \overrightarrow{\delta O}_{/R_1} + \overrightarrow{\delta \theta}_{/R_1} \wedge \overrightarrow{O_1 M_1}_{/R_1} \quad (3.8)$$

Where $\overrightarrow{\delta \theta}_{/R_1} = \begin{pmatrix} \theta_1 \\ \theta_2 \\ \theta_3 \end{pmatrix}$ is called small rotation vector relative to reference frame R_1 .

In conclusion, the small displacement of any point M of the rigid body (S) is determined by the displacement one point of the solid and a small rotation vector. Thus, the small displacement of the rigid body (S) is determined by the small displacement torsor T and this torsor is expressed at point M by two vectors, including rotation vector $\overrightarrow{\delta \theta}_{/R_1}$ and displacement vector $\overrightarrow{\delta M}_{/R_1}$, as shown in equation 3.9.

$$T = \left\{ \begin{array}{c} \overrightarrow{\delta \theta} \\ \overrightarrow{\delta M} \end{array} \right\}_{(M, X_1 Y_1 Z_1)} \quad (3.9)$$

3.1.2 Torsor Transformations

Each torsor is expressed at a point and in a coordinate system. In order to realise torsor operations (addition or subtraction), each torsor must be described at the same point and in the same coordinate system. Thus, it is necessary to transform the torsor from a point to another point or from a coordinate system to another coordinate system. The torsor transformations between the local and the global coordinate system are presented in figure 3.2.

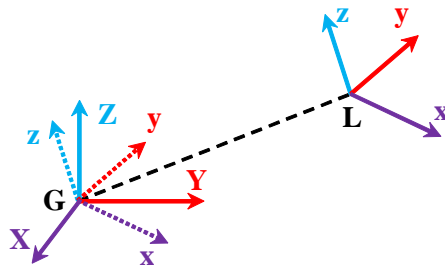


Figure 3.2: Torsor transformations – Local to Global

A small displacement torsor $\{T\}$ is defined at a point L by its elements $\left\{ \begin{matrix} R & D_L \end{matrix} \right\}_{(L,xyz)}$ in the local coordinate system (L, xyz) and at a point G by $\left\{ \begin{matrix} R & D_G \end{matrix} \right\}$ in the same local coordinate system and the relation between two elements is given in equation 3.10.

$$\begin{bmatrix} R^T & D_G^T \end{bmatrix} = [P] \begin{bmatrix} R^T & D_L^T \end{bmatrix}^T \quad (3.10)$$

Where $[P]$ is a 6x6 transformation matrix, as given in equation 3.11.

$$[P] = \begin{bmatrix} 1 & 0 & 0 & 0 & 0 & 0 \\ 0 & 1 & 0 & 0 & 0 & 0 \\ 0 & 0 & 1 & 0 & 0 & 0 \\ 0 & -\Delta z & \Delta y & 1 & 0 & 0 \\ \Delta z & 0 & -\Delta x & 0 & 1 & 0 \\ -\Delta y & \Delta x & 0 & 0 & 0 & 1 \end{bmatrix} \quad (3.11)$$

Where $\Delta = (\Delta x, \Delta y, \Delta z)^T = (X_L - X_G, Y_L - Y_G, Z_L - Z_G)^T$ is a vector from point G to L in the global coordinate system (G, XYZ) . Let the local coordinate system (L, xyz) be defined by the three unit vectors $x = (q_{xX}, q_{xY}, q_{xZ})$, $y = (q_{yX}, q_{yY}, q_{yZ})$ and $z = (q_{zX}, q_{zY}, q_{zZ})$ in the global coordinate system (G, XYZ) . Thus, the local coordinate system could be represented by the matrix $[Q]$, as given in equation 3.12.

$$[Q] = \begin{bmatrix} q_{xX} & q_{yX} & q_{zX} \\ q_{xY} & q_{yY} & q_{zY} \\ q_{xZ} & q_{yZ} & q_{zZ} \end{bmatrix} \quad (3.12)$$

The torsor $\{T\}$ is a can be expressed in the global coordinate system (G, XYZ) as shown in equation 3.13.

$$\{T\} = \left\{ \begin{array}{cc} R_G & D_G \end{array} \right\}_{(G,xyz)} = \left\{ \begin{array}{cc} [Q].R_G & [Q].D_G \end{array} \right\}_{(G,XYZ)} \quad (3.13)$$

3.1.3 Surface Deviation Torsor

From the definition of the small displacement torsor presented in section 3.1.1, Bourdet et al. [BB95] defined a surface deviation torsor by combining two torsors, one for the reference elements of the surface and one for the intrinsic characteristics of the surface. A SDT for a surface describes the deviation of an associated surface relative to the nominal one. The associated surface is an ideal surface associated to the real surface by using a minimum distance criterion such as the least square. The characteristic variation torsor takes into account the variation of the intrinsic characteristics of the surface such as the radius of a cylinder or a sphere or the top angle of a cone. For example, the deviation torsor of a plane (see figure 3.3) at a point O in the reference frame $R(O, XYZ)$ is expressed by equation 3.14. In this case, the characteristic variation torsor of the plane is null because the plane does not have intrinsic characteristics.

$$T_{Plan} = \left\{ \begin{array}{cc} rx & 0 \\ ry & 0 \\ 0 & tz \end{array} \right\}_{(O,XYZ)} \quad (3.14)$$

Where rx and ry are the components of the rotation vector describing the rotational variation of the associated plane relative to the nominal plane around the X, Y axis. tz is a component of the displacement vector of the point O describing the translational variation of point O on the associated plane relative to its nominal position along Z axis. The plane, in this case, has three invariant characteristics (i.e. cannot be measured due to the surface class) and the value of these charac-

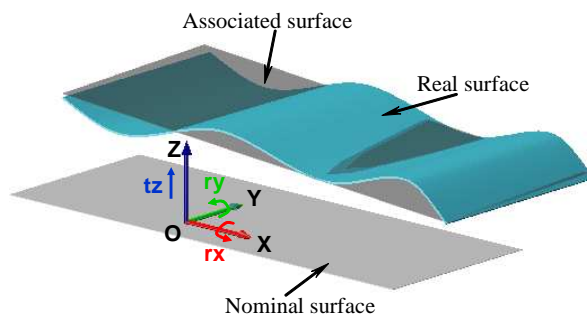


Figure 3.3: Deviation torsor of a plane [NVV09]

teristics can be set to 0. The deviation torsors of the usual elementary surfaces are summarised in table 3.1.

3.1.4 Link Deviation Torsor

A link deviation torsor T_{Link} describes the deviation of the relative position of two associated surfaces coming from different parts as shown in figure 3.4. A link deviation torsor is associated to each couple of surfaces of a mechanism that builds up a connection and thus are possibly in contact. The components of the link torsor are divided into determined component (lr, lt) and undetermined one (Ulr, Ult) . The undetermined components (Ulr, Ult) of the link torsor express the relative degrees of mobility of the two connected surfaces. In other words, they are the degrees of freedom of the connection. The link deviation torsors of the usual elementary connections are summarised in table 3.2. For example, the link deviation torsor of the planar connection (in table 3.2) is expressed by equation 3.15.

$$T_{Plane-Plane} = \left\{ \begin{array}{cc} lrx & Ultx \\ lry & Uly \\ Ulrz & ltz \end{array} \right\}_{(O,XYZ)} \quad (3.15)$$

In this case, there are three undetermined components $Ulrz, Ultx, Uly$ because the planar connection has three degrees of freedom (one rotation around Z axis, two translations along X, Y axis).

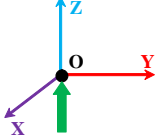
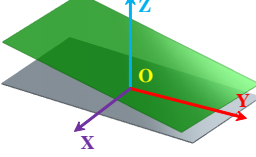
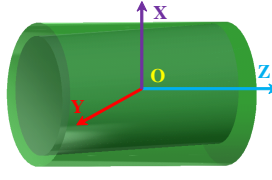
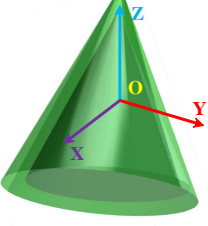
Elementary surfaces		Deviation torsor
Point		$T_{Point} = \begin{Bmatrix} 0 & 0 \\ 0 & 0 \\ 0 & tz \end{Bmatrix}_{(O,XYZ)}$
Plane		$T_{Plan} = \begin{Bmatrix} rx & 0 \\ ry & 0 \\ 0 & tz \end{Bmatrix}_{(O,XYZ)}$
Cylinder		$T_{Cylinder} = \begin{Bmatrix} rx & tx \\ ry & ty \\ 0 & 0 \end{Bmatrix}_{(O,XYZ)}$ <p style="text-align: center;">radius variation ra</p>
Cone		$T_{Cone} = \begin{Bmatrix} rx & tx \\ ry & ty \\ 0 & tz \end{Bmatrix}_{(O,XYZ)}$ <p style="text-align: center;">radius variation ra and angle variation α</p>

Table 3.1: Deviation torsor of elementary surfaces

3.1.5 Part Deviation Torsor

A part deviation torsor T_{Part} is a small displacement torsor associated to each part. It describes the positioning deviation of a nominal part in the associated assembly relative to its nominal position in the nominal assembly as shown in figure 3.4. This part deviation torsor expresses the assembly deviation due to part surfaces' deviations and links' deviations among part surfaces. The part torsor expresses this deviation in the 3D space and thus contains six parameters (three rotations

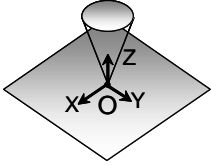
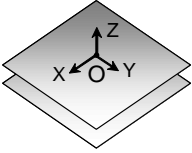
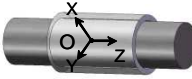
Elementary connection	Coordinate system	Link deviation torsor
Punctual		$T_{Punctual} = \left\{ \begin{array}{cc} U_{lrx} & U_{ltx} \\ U_{lry} & U_{lty} \\ U_{lrz} & t_z \end{array} \right\}_{(O,XYZ)}$
Plane -Plane		$T_{Planar} = \left\{ \begin{array}{cc} l_{rx} & U_{ltx} \\ l_{ry} & U_{lty} \\ U_{lrz} & t_z \end{array} \right\}_{(O,XYZ)}$
Cylinder-Cylinder		$T_{Cylinder} = \left\{ \begin{array}{cc} l_{rx} & l_{tx} \\ l_{ry} & l_{ty} \\ U_{lrz} & U_{ltz} \end{array} \right\}_{(O,XYZ)}$

Table 3.2: Link deviation torsors of elementary connections. [Vig05]

and three translations), as given in equation 3.16.

$$T_{Part} = \left\{ \begin{array}{cc} r_x & t_x \\ r_y & t_y \\ r_z & t_z \end{array} \right\}_{(O,XYZ)} \quad (3.16)$$

3.2 Geometrical Deviation Model

Some models of geometrical deviations generated and accumulated during the manufacturing and assembly processes already exist and are presented in chapter 2. However, these models are not consistent with the whole production stage (manufacturing and assembly) of the product life cycle. Thus, it is necessary to develop a model of geometrical deviations covering all processes from manufacturing stage to assembly stage.

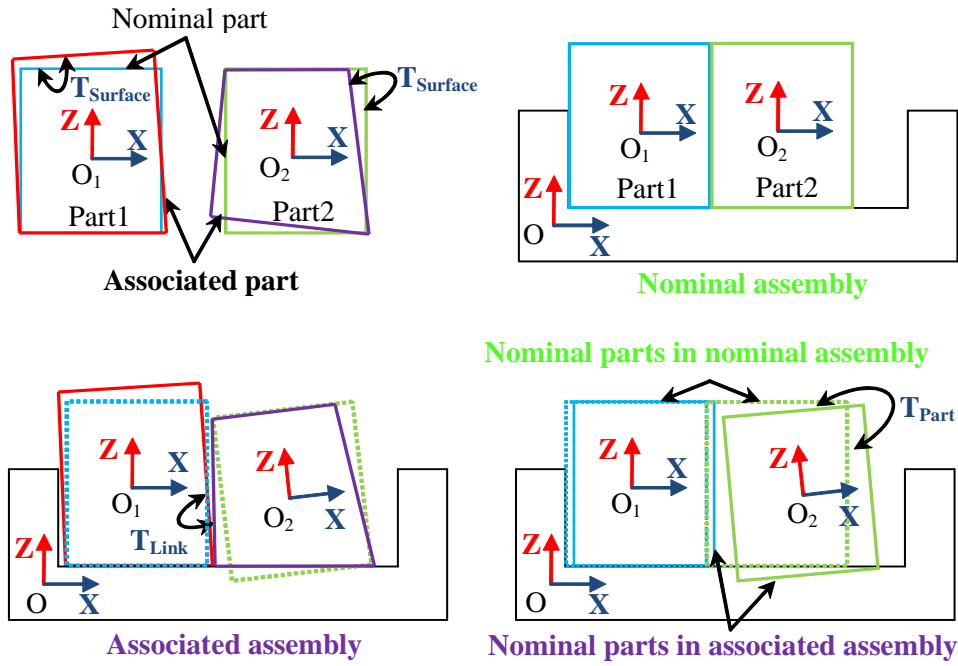


Figure 3.4: Deviation of associated part and nominal part

3.2.1 Model of Manufactured Part

The geometrical deviation model for the manufacturing stage is based on the model of manufactured part (MMP) developed by Vignat and Villeneuve [VV07]. It describes the geometrical deviations generated and accumulated on each surface of the manufactured part relative to its nominal position. The deviations of surface k of manufactured part i , manufactured in set-up S_j , relative to its nominal position can be expressed by equation 3.17.

$$T_{P^i, P_k^i} = -T_{S_j, P^i} + T_{S_j, P_k^i} \quad (3.17)$$

T_{S_j, P_k^i} is a SDT modelling the machining deviation of the machined surface k realised in set-up S_j . This deviation expresses the deviation of machined surfaces relative to the nominal machine. This torsor merges deviations of the surface swept by the tool and cutting local deformations.

T_{S_j, P^i} is a part deviation torsor modelling the positioning deviation of workpiece i in set-up S_j . This deviation is a function of the MMP surface deviations generated

by previous set-ups, the fixture surface deviations and the link fixture/part surfaces. This SDT is the result of the sum of the three mentioned deviations and is calculated by equation 3.18.

$$T_{S_j, P^i} = -T_{P^i, P_m^i} + T_{S_j, H_i S_j} + T_{H_i S_j, P_m^i} \quad (3.18)$$

T_{P^i, P_m^i} is a surface deviation torsor modelling the deviation of surface m of part i which has been manufactured in previous set-up S_{j-1} ($j \geq 1$). The set-up S_0 is normally a set-up to prepare the raw part.

$T_{H_i S_j, P_m^i}$ is a link deviation torsor between surface m of part i and the corresponding surface of the fixture in phase S_j . This torsor is written the same as in table 3.2.

$T_{S_j, H_i S_j}$ is a SDT modelling the deviations of the fixture surfaces. It is a combination of fixture surface deviations and fixture deviation relative to their nominal position in set-up S_j . It is calculated by equation 3.19.

$$T_{S_j, H_i S_j} = T_{S_j, H} + T_{H, H_i S_j} \quad (3.19)$$

$T_{S_j, H}$ is a part deviation torsor modelling the positioning deviations of the fixture relative to its nominal position in the machine.

$T_{H, H_i S_j}$ is a surface deviation torsor modelling the deviations of surface i of the fixture relative to its nominal position in the fixture in phase S_j .

For a specific elementary connection, the undetermined components (Ulr , Ult) of the link deviation torsor $T_{H_i S_j, P_m^i}$ remain in the part deviation torsor T_{S_j, P^i} . They express the degrees of freedom of this elementary connection. However, the workpiece is completely positioned on the part-holder in set-up S_j by a set of parallel elementary connections. These results are fully constrained and over-constrained assembly. The mathematical expression of the unique position of the workpiece in set-up S_j is obtained by elimination of the undetermined components of the link

torsors. In order to eliminate these components (Ulr, Ult), the part deviation torsor $T_{Sj, Pi}$ is calculated from each elementary connection between the workpiece and the part-holder in set-up Sj .

$$T_{Sj, Pi} = -T_{Pi, Pn} + T_{Sj, HkSj} + T_{HkSj, Pn} \quad (3.20)$$

The torsor $T_{Sj, Pi}$ coming from each connection expresses the same positioning deviation of the workpiece on the part-holder in set-up Sj . Using these equalities, the undetermined components (Ulr, Ult) and the determined ones (lr, lt) are calculated by using “unification” method proposed by Bourdet et al. [BB95]. The procedure of calculation is also presented in depth by Villeneuve and Vignat [VV05b]. The relationship between the undetermined components (Ulr, Ult) and the determined ones (lr, lt) is established by Gauss-elimination method. The elimination of the undetermined components (Ulr, Ult) is then realised by replacing these relations in the part deviation torsor $T_{Sj, Pi}$.

Finally, the whole deviations generated and accumulated by the manufacturing process are collected in the MMP and the deviations of each surface k of the manufactured part i are expressed by a SDT. The variation of the parameters of the MMP is limited and this limitation is managed by constraints. The constraints on the part-holder surface deviations (CH) are relative to its quality (precision of its surface). The constraints on the machining deviations (CM) are relative to the machine capabilities. The constraints on the links between part and part-holder surfaces (CHP) represent assembly rules. They constrain determined components (lr, lt) of the link deviation torsor. These constraints depend on the type of connection (floating or slipping). The first constraint expresses non-penetration between part and part-holder conditions. In other words, workpiece material must not penetrate fixture material. For floating contact, the determined components (lr, lt) need only to comply with the non-penetration condition between the workpiece and the part-holder. In the case of slipping contact, it is necessary to bring the surfaces

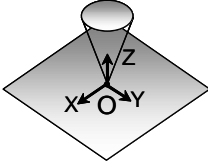
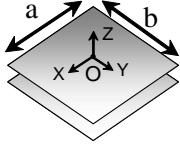
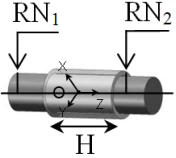
Elementary connection	Coordinate system	Non-penetration conditions	Positioning function
Punctual		$ltz \geq 0$	$-ltz$
Plane-Plane		$-\frac{b}{2}lrx - \frac{a}{2}lry + ltz \geq 0$ $-\frac{b}{2}lrx + \frac{a}{2}lry + ltz \geq 0$ $\frac{b}{2}lrx - \frac{a}{2}lry + ltz \geq 0$ $\frac{b}{2}lrx + \frac{a}{2}lry + ltz \geq 0$	$-ltz$
Cylinder-Cylinder		$RN_2 - RN_1 + r_2 - r_1 + \sqrt{\frac{(ltx - \frac{H}{2}lry)^2 + (ltx + \frac{H}{2}lry)^2}{2}} \geq 0$ $RN_2 - RN_1 + r_2 - r_1 + \sqrt{\frac{(ltx + \frac{H}{2}lry)^2 + (ltx - \frac{H}{2}lry)^2}{2}} \geq 0$	$-RN_2$

Table 3.3: Non-penetration conditions and positioning functions of elementary connections

close to each other. To do that a positioning function is defined. This function expresses the displacement of a point of the workpiece along a direction relevant to the contact. The function increases when the surfaces of the connection move closer.

For example, plane-plane connection (see table 3.3), this positioning function $-ltz$ expresses the displacement of a point of the workpiece along a direction normal to the plane and in a direction that brings the two planes closer. Thus, for this kind of contact, the displacement function has to be maximized, respecting the non-penetration conditions between workpiece and part-holder as shown in equation

3.21.

$$\left\{ \begin{array}{l} -\frac{b}{2}lrx - \frac{a}{2}lry + ltz \geq 0 \\ -\frac{b}{2}lrx + \frac{a}{2}lry + ltz \geq 0 \\ \frac{b}{2}lrx - \frac{a}{2}lry + ltz \geq 0 \\ \frac{b}{2}lrx + \frac{a}{2}lry + ltz \geq 0 \end{array} \right. \quad (3.21)$$

3.2.2 Model of Assembled Part

The geometrical deviations of each part of a product generated in the manufacturing stage are already modelled by MMP. Then each part making up the product will be assembled by each set-up of the assembly process in the assembly stage. In other words, each part with geometrical deviations corresponding to each MMP is assembled by each set-up. The assembly process is described in figure 3.5. The model of geometrical deviations generated in each set-up is called model of sub-assembled part (MSP). Finally, the model of geometrical deviations accumulated on the product is called model of assembled part (MAP). The geometrical deviations of surface k of part i in the set-up j relative to the global coordinate system of the product are expressed by equation 3.22.

$$T_{P^i, P_k^i} = T_{P, P^i} + T_{P^i, P_k^i} \quad (3.22)$$

Where is T_{P^i, P_k^i} a surface deviation torsor modelling the deviation of surface k of part i relative to its nominal position in the local coordinate system of the part i . It comes from MMP i .

T_{P, P^i} is a part deviation torsor modelling the positioning deviations of part i relative to its nominal position in the global coordinate system of the product. It depends not only on the deviations of the surfaces of part i , but also the links between the surfaces of part i and the surfaces of another connected part t , the deviation of the concerned surfaces of part t and the positioning deviation of part t relative to the

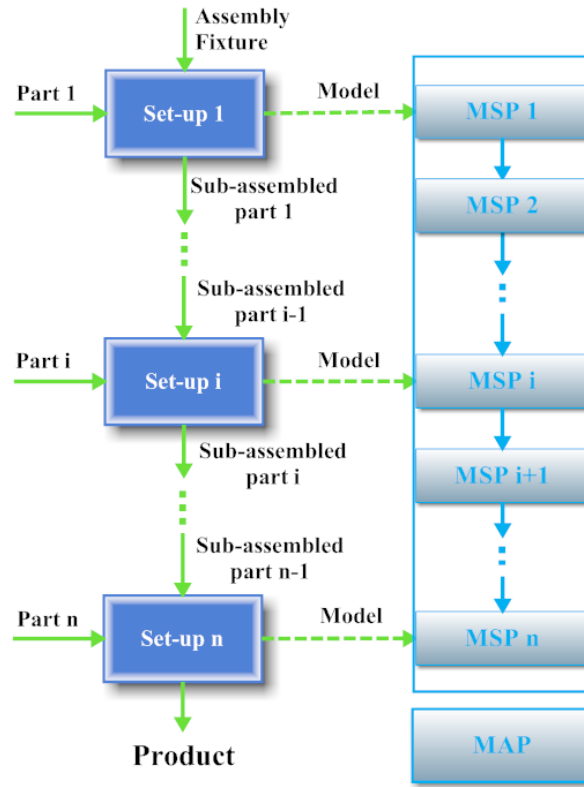


Figure 3.5: Assembly process and MAP generation

global coordinate system of the product. Torsor T_{P,P^i} is determined based on the law of mechanisms as proposed by Thiébaud [Thi01]. It is calculated by equation 3.23 for an elementary connection between part i and part t , which is a part of the subassembled part $i - 1$ coming from the previous set-up $i - 1$ of the assembly process.

$$T_{P,P^i} = T_{P,P^t} + T_{P^t,P_n^t} + T_{P_n^t,P_m^i} - T_{P^i,P_m^i} \quad (3.23)$$

Where $T_{P_n^t,P_m^i}$ is a link deviation torsor between surface m of MMP i and surface n of MMP t . T_{P,P^t} is a part deviation torsor modelling the positioning deviations of part t relative to its nominal position in the global coordinate system of the product.

The position of part i depends on several of these elementary connections who link part i with the part t and others parts making up the sub-assembly. For each elementary connection, the positioning deviation of part i is calculated as in equation 3.23 which results in a set of equations 3.24, 3.25 and 3.26, one per elementary connection between the part i and the other parts from the assembly.

Link 1:

$$T_{P,P^i} = T_{P,P^t} + T_{P^t,P_m^t} + T_{P_m^t,P_n^i} - T_{P^i,P_n^i} \quad (3.24)$$

Link 2:

$$T_{P,P^i} = T_{P,P^t} + T_{P^t,P_q^t} + T_{P_q^t,P_p^i} - T_{P^i,P_p^i} \quad (3.25)$$

...

Link n:

$$T_{P,P^i} = T_{P,P^t} + T_{P^t,P_z^t} + T_{P_z^t,P_y^i} - T_{P^i,P_y^i} \quad (3.26)$$

As far as the part is rigid and its position is unique, it is possible to write a linear system of equation 3.27.

$$\left\{ \begin{array}{l} Link\ 1 = Link\ 2 \\ Link\ 1 = Link\ 3 \\ \dots \\ Link\ n - 1 = Link\ n \end{array} \right. \quad (3.27)$$

The resolution of this system by Gauss-elimination method is similar to the resolution presented for MMP positioning. It is also called unification and aims to eliminate the undetermined components of the link torsors between part i and the other parts. The positioning deviation of the part i can then be completely determined and expressed by the torsor T_{P,P^i} . It is a function of determined links, surfaces deviations parameters and part deviation torsor of the other parts it is connected to. It is calculated in the setup t of the assembly process.

Finally, all part deviation torsors of part i assembled in set-up j of the assembly process are collected in the MSP i . Similarly, the MSP n is generated at the end of setup n of the assembly process. Finally, the model of assembled part (MAP) is created based on a set of n MSP generated throughout the assembly process. The GDM of the product collects all the geometrical deviations generated and accumu-

lated along the manufacturing and assembly stages. It is built on the MMP and the MAP, as given in equation 3.28.

$$GDM_{/Product} = MMP_{/Product} + MAP_{/Product} \quad (3.28)$$

As a result, the geometrical deviations of surface k of part i in the global coordinate system of the product, expressed as in equation 3.22, can be decomposed into the geometrical deviations of surface k of MMP i and the positioning deviations of MAP i in the global coordinate system of the product.

To summarize, all geometrical deviations of all surfaces of the product relative to their nominal positions in the global coordinate system are collected by GDM. The variation parameters of the GDM are limited by manufacturing constraints (CH , CM , CHP) and assembly constraints (CA). These constraints are presented in table 3.3 in section 3.2.1. The geometrical deviations of the product generated by the manufacturing and assembly processes during its life cycle have been calculated and stored.

3.3 Geometrical Deviation Simulation

3.3.1 Monte-Carlo Simulation

The GDM generated at previous step gives the mathematical expression of the deviations and the constraints representing the process capabilities. For the verification of functional requirements and the integration of deviations into performance simulation, a quantitative evaluation of these deviations is necessary. To this aim, Monte-Carlo simulation is used to predict the amount of variations generated and accumulated throughout the product life cycle. This is the second step of the proposed method. The Monte-Carlo methods are based on the use of random generators to simulate the stochastic phenomenon. An image of the real production with

geometrical deviations is generated by using this kind of method. The overview of the algorithm for realising the Monte-Carlo simulation is shown in figure 3.6.

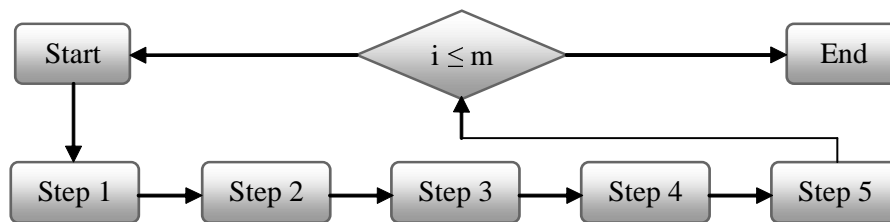


Figure 3.6: The algorithm diagram of the Monte-Carlo simulation

A population of M products is virtually manufactured through the following steps:

- Step 1. Define the probability distribution type or the variation zone of the input variables.

The input variables are the parameters of the torsors that represent the quality of the manufacturing fixtures and the capabilities of the machine tool. They are the parameters of the part-holder surfaces' deviation torsors and the machining deviation torsors. The determination of the distribution of these variables is based on experimental measurements or manufacturing process knowledge [TNVL07]. In the second case, it can come from Statistical Process Control (SPC) which is a technique used to monitor a manufacturing process. The strategies to bound the variation zones of the input parameters are presented by Kamali Nejad [NVV09]. In the case of a plane, the deviation torsor $T_{Sj,HiSj}$ modelling the deviations of the plane of the part-holder in the set-up Sj is expressed by equation 3.29.

$$T_{Sj,HiSj} = \left\{ \begin{array}{cc} rx_{Sj} & 0 \\ ry_{Sj} & 0 \\ 0 & tz_{Sj} \end{array} \right\}_{(O_{Hi},XYZ)} \quad (3.29)$$

To define the variation zone of the parameters of this torsor, the strategy of independent parameters defined in [NVV09] will be used. Thus their variation zone can mathematically be defined by equation 3.30, where maximum

and minimum values for each parameter come from measurement or process knowledge.

$$\left\{ \begin{array}{l} rx_{Sj\ min} \leq rx_{Sj} \leq rx_{Sj\ max} \\ ry_{Sj\ min} \leq ry_{Sj} \leq ry_{Sj\ max} \\ tz_{Sj\ min} \leq tz_{Sj} \leq tz_{Sj\ max} \end{array} \right. \quad (3.30)$$

- Step 2. Generate randomly a set of input values according to their distributions and variation zone.

The set of input values are randomly generated by a cellular automata algorithm in relation with the defined distributions and variations zone. The cellular automata defined by Wolfram [Wol83] is a simple mathematical idealization of natural systems. For example, two parameters rx_{Sj} and ry_{Sj} of the torsor $T_{Sj,HiSj}$ are uniformly distributed in the variation zone 3.31.

$$\left\{ \begin{array}{l} -0.001 \leq rx_{Sj} \leq 0.001 \\ -0.0015 \leq ry_{Sj} \leq 0.0015 \end{array} \right. \quad (3.31)$$

The figure 3.7 represents 10000 samples generated by the cellular automata algorithm.

- Step 3. Calculate the surface deviations of each manufactured part of the product based on the MMPs.

In order to calculate the deviations of the surfaces of the manufactured part, it is necessary to determine the values of the parameters of the link deviation torsor of the MMP model. These values determine the position of the manufactured part in the fixture of the current set-up. The determination based on the non-penetration constraints and positioning functions is explained in [NVV09].

In the case of floating contact, the determined components (lr, lt) are randomly chosen in the interval bounded by the non-penetration constraints. For

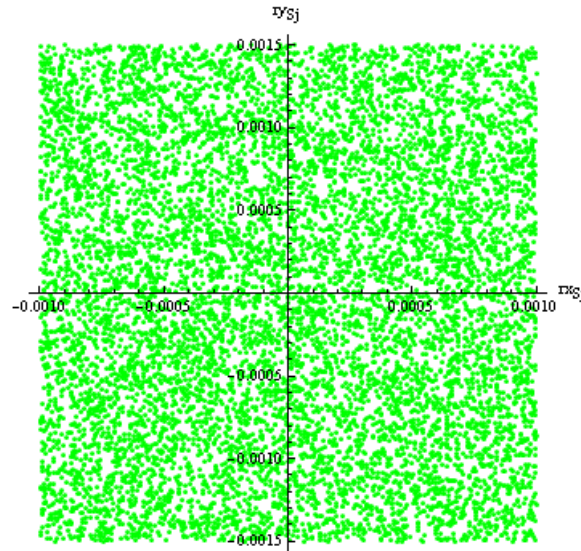


Figure 3.7: Random sample numbers

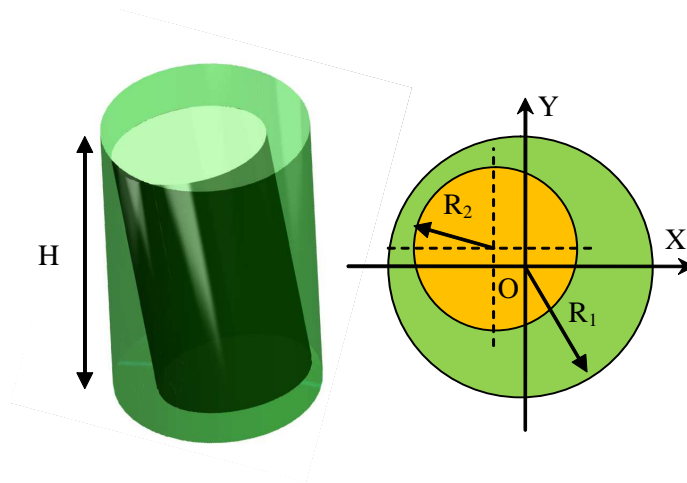


Figure 3.8: Floating cylindrical contact

a cylinder-cylinder connection (see figure 3.8), the components of the link tor-
sor T_{HiSj,P_m^i} are described as in 3.32.

$$T_{HiSj,P_m^i} = \left\{ \begin{array}{cc} lrx_{sj} & ltx_{sj} \\ lry_{sj} & lty_{sj} \\ Ulrz_{sj} & Ultz_{sj} \end{array} \right\}_{(O,XYZ)} \quad (3.32)$$

We make the assumption that the determined components (lr , lt) are uni-
formly distributed in the interval bounded by the inequalities 3.33 represent-
ing the maximum clearance between the two cylinders.

$$\left\{ \begin{array}{l} |lrx_{Sj}| \leq \frac{2(R_1 - R_2)}{H} \\ |lry_{Sj}| \leq \frac{2(R_1 - R_2)}{H} \\ |ltx_{Sj}| \leq R_1 - R_2 \\ |lty_{Sj}| \leq R_1 - R_2 \end{array} \right. \quad (3.33)$$

The determined components must also satisfy the non-penetration constraints described by inequalities 3.34. The respect of this condition is thus checked and the values of the component are rejected in the case of non-satisfaction. In case of rejection a new set of parameters is randomly generated according to constraints expressed in 3.33.

$$\left\{ \begin{array}{l} R_1 - R_2 + \sqrt{(ltx_{Sj} - \frac{H}{2}lry_{Sj})^2 + (lty_{Sj} + \frac{H}{2}lrx_{Sj})^2} \geq 0 \\ R_1 - R_2 + \sqrt{(ltx_{Sj} + \frac{H}{2}lry_{Sj})^2 + (lty_{Sj} - \frac{H}{2}lrx_{Sj})^2} \geq 0 \end{array} \right. \quad (3.34)$$

Where R_1 , R_2 and H are the radius of the two cylinder and the height of the cylindrical link, respectively.

In the case of a slipping contact, the determined components (lr , lt) are calculated by maximizing the positioning function subject to non-penetration constraints. For the plane-plane connection (see figure 3.9), the components of the link torsor T_{HiSj, P_m^i} are expressed as in 3.35.

$$T_{HiSj, P_m^i} = \left\{ \begin{array}{ll} lrx_{Sj} & U ltx_{Sj} \\ lry_{Sj} & U lty_{Sj} \\ U lrx_{Sj} & ltx_{Sj} \end{array} \right\}_{(O, XYZ)} \quad (3.35)$$

The determined components (lr , lt) are calculated according to the procedure

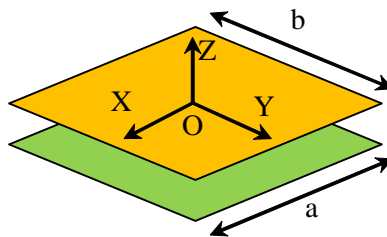


Figure 3.9: Slipping planar contact

3.36.

Maximize : $-ltz_{S_j}$

Subject to

$$\left\{ \begin{array}{l} -\frac{b}{2}lrx_{S_j} - \frac{a}{2}lry_{S_j} + ltz_{S_j} \geq 0 \\ -\frac{b}{2}lrx_{S_j} + \frac{a}{2}lry_{S_j} + ltz_{S_j} \geq 0 \\ \frac{b}{2}lrx_{S_j} - \frac{a}{2}lry_{S_j} + ltz_{S_j} \geq 0 \\ \frac{b}{2}lrx_{S_j} + \frac{a}{2}lry_{S_j} + ltz_{S_j} \geq 0 \end{array} \right. \quad (3.36)$$

The deviation torsor T_{P^i, P_j^i} of the surface j of the manufactured part i is then calculated by replacing the determined parameters of the link deviation torsor.

- Step 4. Assemble the manufactured part of the product based on verification of the assembly constraints (CA).

During this step, the determined components (lr , lt) of the link deviation torsor are calculated based on verification of the assembly constraints. The determination is realized as for MMP fixture links by the method presented in step 3.

- Step 5. Calculate the surface deviations of the product in the global coordinate system of the product.

The surface deviations of the product in the global coordinate system are determined by replacing all input parameters generated in the step 2 and all determined components of the link deviation torsors calculated in the step 3 and 4 into the GDM. All parameters of the model are collected at the end of

this step. Then the procedure will be restarted from step 1 until the desired number of product is reached.

A set of M products with geometrical deviations are generated by the Monte-Carlo simulation method. All parameters of the model from the Monte-Carlo simulation are collected in matrix data. The matrix data are used to simulate the performance of the product, as presented in chapter 4 and identify and classify the effect of the parameters on the performance of the product, as given in chapter 5.

3.4 A Case Study

3.4.1 A Centrifugal Pump

3.4.1.1 CAD² model of the centrifugal pump

A geometrical deviation model for product life cycle engineering has been presented in section 3.2. In order to illustrate this method, an example of centrifugal pump design is developed. The theory of fluid mechanics used to determine the behaviour of the product is based on [LR92]. The characteristics of the designed centrifugal pump are:

- Flowrate: $250m^3/h$
- Total Head: $100m$
- Revolution speed: $2000RPM$
- Liquid: Water

The CAD model (nominal model) of the designed centrifugal pump is represented in figure 3.10.

²Computer Aided Design

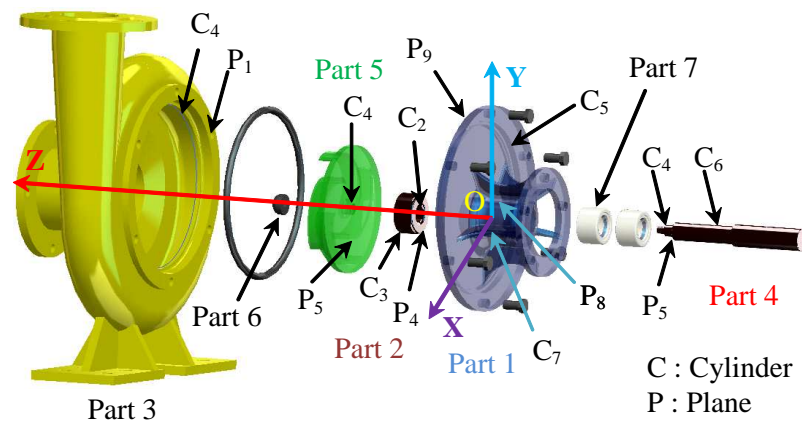


Figure 3.10: The parts of designed centrifugal pump

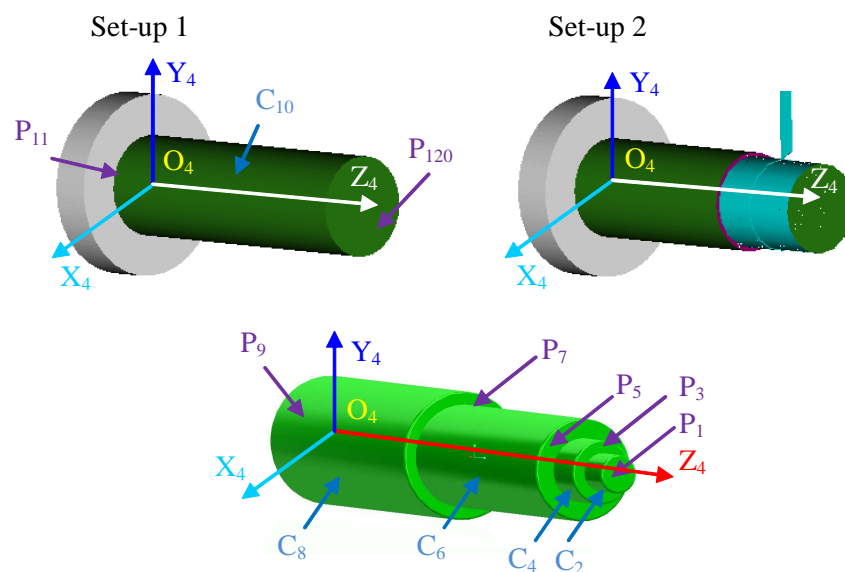


Figure 3.11: Model of manufactured shaft of the pump

3.4.1.2 MMP of the centrifugal pump

In order to manufacture the pump, a manufacturing process, an assembly process and the associated resources are proposed. As a result, the geometrical deviation model of this centrifugal pump from manufacturing and assembly stages of its life cycle is generated by the method presented in section 3.2. For example, the shaft (part 4) of the pump is realised by a turning process on a lathe machine (see figure 3.11) according to the process plan described in table 3.4.

The geometrical deviation of each surface j of the shaft is expressed by a SDT. In order to calculate this torsor, it is necessary to determine the positioning deviation

of workpiece in set-up 1 and 2. For example, the positioning deviation of the workpiece in set-up $S1$ is determined by the connection between the surface C_{10} and the corresponding part-holder surface. It is expressed by equation 3.37.

$$T_{S1,P^4} = T_{S1,H10S1} + T_{H10S1,P_{10}^4} - T_{P^4,P_{10}^4} \quad (3.37)$$

Where T_{P^4,P_{10}^4} is a surface deviation torsor modelling the deviations of cylinder C_{10} of the workpiece. It comes from previous set-up 0 where the rough part has been manufactured. It is described at the center point O_{C10} of the cylinder C_{10} in the local coordinate system $(O_4, X_4Y_4Z_4)$ of part 4 by equation 3.38.

$$T_{P^4,P_{10}^4} = \left\{ \begin{array}{cc} rx_{4,10} & tx_{4,10} \\ ry_{4,10} & ty_{4,10} \\ 0 & 0 \end{array} \right\}_{(O_{C10}, X_4Y_4Z_4)} \quad (3.38)$$

$T_{S1,H10S1}$ is a SDT modelling the deviations of the part-holder surface. It is described at the point O_{C10H} of the part-holder in the local coordinate system $(O_4, X_4Y_4Z_4)$ by equation 3.39.

$$T_{S1,H10S1} = \left\{ \begin{array}{cc} rx_{4,10S1} & tx_{4,10S1} \\ ry_{4,10S1} & ty_{4,10S1} \\ 0 & 0 \end{array} \right\}_{(O_{C10H}, X_4Y_4Z_4)} \quad (3.39)$$

T_{H10S1,P_{10}^4} is a link deviation torsor modelling characteristic link between cylinder C_{10} of the workpiece and the surface H_{10} of the part-holder. It is expressed at the point O_{C10L} in the local coordinate system $(O_4, X_4Y_4Z_4)$ by equation 3.40.

$$T_{H10S1,P_{10}^4} = \left\{ \begin{array}{cc} lrx_{4,10S1} & ltx_{4,10S1} \\ lry_{4,10S1} & lty_{4,10S1} \\ Ulrz_{4,10S1} & Ultz_{4,10S1} \end{array} \right\}_{(O_{C10L}, X_4Y_4Z_4)} \quad (3.40)$$

Set-up 1	
Positioning	Cylinder on C_{10} Plane on P_{11}
Machining	Surface C_8, P_9
Set-up 2	
Positioning	Cylinder on C_{10} Plane on P_{11}
Machining	Surface $P_1, C_2, P_3, C_4, P_5, C_6, P_7$

Table 3.4: Turning process

The positioning deviation of workpiece in set-up 1 can similarly be calculated by another connection between the surface P_{11} and the corresponding part-holder surface, as shown in equation 3.41.

$$T_{S1,P4} = T_{S1,H11S1} + T_{H11S1,P_{11}^A} - T_{P4,P_{11}^A} \quad (3.41)$$

T_{H10S1,P_{10}^A} is a link deviation torsor modelling characteristic link between the plane P_{11} of the workpiece and the surface H_{11} of the part-holder. It is expressed at the point $O_{P_{11}L}$ in the local coordinate system $(O_4, X_4Y_4Z_4)$ by equation 3.42.

$$T_{H11S1,P_{10}^A} = \left\{ \begin{array}{cc} lrx_{4,11S1} & Ultx_{4,11S1} \\ lry_{4,11S1} & Ulty_{4,11S1} \\ Ulrz_{4,11S1} & ltz_{4,11S1} \end{array} \right\}_{(O_{P_{11}L}, X_4Y_4Z_4)} \quad (3.42)$$

In order to calculate the link deviation torsor $T_{S1,P4}$, it is necessary to eliminate the undetermined components Ulr, Ult . This elimination is based on the unification method. The equation 3.37 and 3.41 describe the same positioning deviation of part 4 in the part-holder in set-up 1. Thus we can write the linear system of equation

3.43 by writing this equality.

$$\left\{ \begin{array}{l}
 \text{lr}_{x_{4,10S1}} - \text{lr}_{x_{4,11S1}} - \text{rx}_{4,10} + \text{rx}_{4,11} + \text{rx}_{4,10S1} - \text{rx}_{4,11S1} = 0 \\
 \text{lr}_{y_{4,10S1}} - \text{lr}_{y_{4,11S1}} - \text{ry}_{4,10} + \text{ry}_{4,11} + \text{ry}_{4,10S1} - \text{ry}_{4,11S1} = 0 \\
 \text{Ulr}_{z_{4,10S1}} - \text{Ulr}_{z_{4,11S1}} = 0 \\
 -300\text{lr}_{y_{4,10S1}} + 350\text{lr}_{y_{4,11S1}} + \text{lt}_{x_{4,10S1}} + 300\text{ry}_{4,10} - 350\text{ry}_{4,11} + \\
 -300\text{ry}_{4,10S1} + 350\text{ry}_{4,11S1} - \text{tx}_{4,10} + \text{tx}_{4,10S1} - \text{Ult}_{x_{4,11S1}} = 0 \\
 300\text{lr}_{x_{4,10S1}} - 350\text{lr}_{x_{4,11S1}} + \text{lt}_{y_{4,10S1}} - 300\text{rx}_{4,10} + 350\text{rx}_{4,11} + \\
 300\text{rx}_{4,10S1} - 350\text{rx}_{4,11S1} - \text{ty}_{4,10} + \text{ty}_{4,10S1} - \text{Ult}_{y_{4,11S1}} = 0 \\
 -\text{lt}_{z_{4,11S1}} + \text{tz}_{4,11} - \text{tz}_{4,11S1} + \text{Ult}_{z_{4,10S1}} = 0
 \end{array} \right. \quad (3.43)$$

The elimination of the undetermined components Ulr, Ult is solved by Gauss-elimination method. The solution is shown in equation 3.44.

$$\left\{ \begin{array}{l}
 \text{Ulr}_{z_{4,10S1}} = \text{Ulr}_{z_{4,11S1}} \\
 \text{Ult}_{x_{4,11S1}} = -300\text{lr}_{y_{4,10S1}} + 350\text{lr}_{y_{4,11S1}} + \text{lt}_{x_{4,10S1}} + 300\text{ry}_{4,10} - 350\text{ry}_{4,11} \\
 \quad - 300\text{ry}_{4,10S1} + 350\text{ry}_{4,11S1} - \text{tx}_{4,10} + \text{tx}_{4,10S1} \\
 \text{Ult}_{y_{4,11S1}} = 300\text{lr}_{x_{4,10S1}} - 350\text{lr}_{x_{4,11S1}} + \text{lt}_{y_{4,10S1}} - 300\text{rx}_{4,10} + 350\text{rx}_{4,11} \\
 \quad + 300\text{rx}_{4,10S1} - 350\text{rx}_{4,11S1} - \text{ty}_{4,10} + \text{ty}_{4,10S1} \\
 \text{Ult}_{z_{4,10S1}} = \text{lt}_{z_{4,11S1}} - \text{tz}_{4,11} + \text{tz}_{4,11S1}
 \end{array} \right. \quad (3.44)$$

The undetermined components $Ulr_{z_{4,10S1}}, Ulr_{z_{4,11S1}}$ describe the rotational mobility of the workpiece (part 4) in the part-holder in the set-up 1. However, the workpiece, in this case, is fixed by clamping force and friction in the chuck jaws on the turning machine and thus does not have angular reference. Thus their value remains undetermined and for the purpose of simplicity be assigned a null value. Finally, the torsor T_{S1, P^4} modelling the positioning deviation of workpiece in set-up

1 is completely determined as in equation 3.45.

$$T_{S1,P^4} = \left\{ \begin{array}{cc} lrx_{4,10S1} - rx_{4,10} + rx_{4,10S1} & -300lry_{4,10S1} + ltx_{4,10S1} + 300ry_{4,10} \\ & -300ry_{4,10S1} - tx_{4,10} + tx_{4,10S1} \\ lry_{4,10S1} - ry_{4,10} + ry_{4,10S1} & 300lrx_{4,10S1} + lty_{4,10S1} - 300rx_{4,10} \\ & +300rx_{4,10S1} - ty_{4,10} + ty_{4,10S1} \\ 0 & ltz_{4,11S1} - tz_{4,11} + tz_{4,11S1} \end{array} \right\}_{(O_4, X_4 Y_4 Z_4)} \quad (3.45)$$

The torsor T_{S2,P^4} modelling the positioning deviation of workpiece in set-up 2 can be determined by the same way as for set-up 1. The machining deviations in the case of manufacturing the cylinder C_8 are described by a SDT, as shown in equation 3.46. This torsor expresses the machining defects due to the imperfections of tool and machine.

$$T_{S1,P_8^4} = \left\{ \begin{array}{cc} rx_8 & tx_8 \\ ry_8 & ty_8 \\ 0 & 0 \end{array} \right\}_{(O_{C8M}, X_4 Y_4 Z_4)} \quad (3.46)$$

Finally, the geometrical deviations of any surface j of the shaft are modelled by the surface deviation torsor T_{P^4,P_j^4} . For example, the surface deviations of the plane P_1 (see figure 3.11) of the shaft relative to its nominal position expressed at the point O_4 in the local coordinate system $(O_4, X_4 Y_4 Z_4)$ is described by the torsor T_{P^4,P_1^4} , as shown in equation 3.47. In this torsor, the parameters $rx_{4,1}$, $rx_{4,8}$, $rx_{4,10}$, $ry_{4,1}$, $ry_{4,8}$, $ry_{4,10}$, $tz_{4,1}$, $tz_{4,9}$ and $tz_{4,11}$ represent the machining deviations of the surfaces (P_1 , P_9 , P_{11} , C_8 , C_{10}) of the shaft. The parameters $rx_{4,10S1}$, $rx_{4,8S2}$, $ry_{4,10S1}$, $tx_{4,10S1}$, $tx_{4,8S2}$, $ty_{4,10S1}$, $ty_{4,8S2}$, $tz_{4,11S1}$ and $tz_{4,9S2}$ represent the deviations of the fixture surfaces in set-up 1 and set-up 2. The parameters $lrx_{4,10S1}$, $lrx_{4,8S2}$, $lry_{4,10S1}$, $lry_{4,8S2}$, $ltx_{4,10S1}$, $ltx_{4,8S2}$, $lty_{4,10S1}$, $lty_{4,8S2}$, $ltz_{4,11S1}$ and $ltz_{4,9S2}$ represent the link between the fixture

surfaces and the surfaces of workpiece in the set-up 1 and set-up 2.

$$T_{P^4, P_1^4} = \left\{ \begin{array}{l} \text{lr}_{x_{4,10S1}} + \text{lr}_{x_{4,8S2}} + \text{rx}_{4,1} \quad -300\text{ry}_{4,10S1} - 50\text{ry}_{4,8S2} + \text{lt}_{x_{4,10S1}} \\ -\text{rx}_{4,8} - \text{rx}_{4,10} \quad +\text{lt}_{x_{4,8S2}} - 350\text{ry}_{4,1} + 81\text{ry}_{4,8} \\ +\text{rx}_{4,10S1} + \text{rx}_{4,8S2} \quad +300\text{ry}_{4,10} - 300\text{ry}_{4,10S1} - 50\text{ry}_{4,8S2} \\ \quad \quad \quad -\text{tx}_{4,8} - \text{tx}_{4,10} + \text{tx}_{4,10S1} + \text{tx}_{4,8S2} \\ \\ \text{lry}_{4,10S1} + \text{lry}_{4,8S2} + \text{ry}_{4,1} \quad 300\text{lr}_{x_{4,10S1}} + 50\text{lr}_{x_{4,8S2}} + \text{lt}_{y_{4,10S1}} \\ -\text{ry}_{4,8} - \text{ry}_{4,10} \quad +\text{lt}_{y_{4,8S2}} - 350\text{ry}_{4,1} + 81\text{ry}_{4,8} \\ +\text{ry}_{4,10S1} + \text{ry}_{4,8S2} \quad +300\text{ry}_{4,10} - 300\text{ry}_{4,10S1} - 50\text{ry}_{4,8S2} \\ \quad \quad \quad -\text{tx}_{4,8} - \text{tx}_{4,10} + \text{tx}_{4,10S1} + \text{tx}_{4,8S2} \\ \\ 0 \quad \quad \quad \text{lt}_{z_{4,11S1}} + \text{lt}_{z_{4,9S2}} + \text{tz}_{4,1} - \text{tz}_{4,9} \\ \quad \quad \quad -\text{tz}_{4,11} + \text{tz}_{4,11S1} + \text{tz}_{4,9S2} \end{array} \right\}_{(O_4, X_4 Y_4 Z_4)} \quad (3.47)$$

3.4.1.3 MAP of the centrifugal pump

The manufactured parts of the pump are then assembled according to the selected assembly process. The assembly process is shown in figure 3.12. The positioning deviation of the newly assembled part relative to its nominal position in each set-up is modelled by the model of subassembled part (MSP). In set-up 1, the MSP 1 includes a torsor T_{P, P^2} modelling the positioning deviation of the ball bearing (part 2) relative to its nominal position in the global coordinate system that is placed relative to the casing back (part 1). The torsor T_{P, P^2} is expressed by equation 3.48 based on the connections between the surfaces (cylinder C_4 and plane P_3) of the ball bearing and the surfaces of the casing back (cylinder C_8 and plane P_7). These

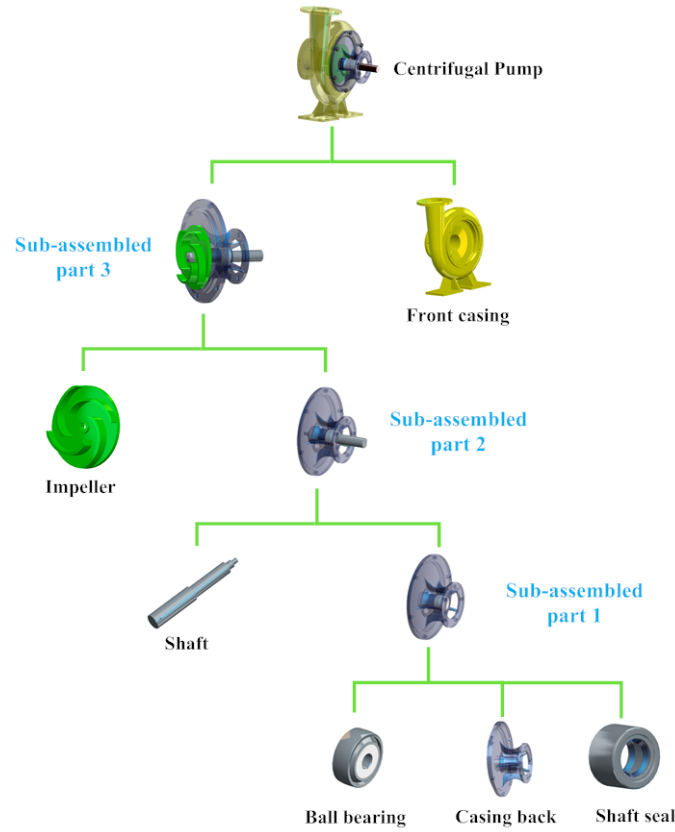


Figure 3.12: Assembly process of the pump

connections are described by the assembly graph, as shown in figure 3.13.

$$\begin{aligned}
 T_{P,P^2} &= T_{P,P^1} + T_{P^1,P_8^1} + T_{P_8^1,P_4^2} - T_{P^2,P_4^2} \\
 T_{P,P^2} &= T_{P,P^1} + T_{P^1,P_7^1} + T_{P_7^1,P_3^2} - T_{P^2,P_3^2}
 \end{aligned}
 \tag{3.48}$$

The undetermined components (Ulr , Ult) of the link deviation torsor $T_{P_8^1,P_4^2}$ and $T_{P_7^1,P_3^2}$ modelling the deviation of the link between the part 2 and the part 1 are eliminated by Gauss-elimination method. Then the part deviation torsor T_{P,P^2} of the part 2 is calculated by replacing the undetermined components (Ulr , Ult) in equation 3.48. The part deviation torsor T_{P,P^1} models the positioning deviations of the part 1 of the pump relative to its nominal position in the global coordinate system of the pump (O, XYZ) (see figure 3.10). The global coordinate system of the pump is positioned on part 1, thus part deviation torsor T_{P,P^1} is equal zero. The part deviation torsor T_{P,P^2} is then expressed by equation 3.49. In this torsor, the parameters $lrx_{1,7 \rightarrow 2,3}$, $lry_{1,7 \rightarrow 2,3}$, $ltx_{1,7 \rightarrow 2,3}$ and $lty_{1,7 \rightarrow 2,3}$ are the determined compo-

nents of the link deviation torsor $T_{P_7^1, P_3^2}$ representing the link between the cylinder C_7 of part 1 and the cylinder C_3 of part 2. The parameter $ltz_{1,8 \rightarrow 2,4}$ is a determined component of the link deviation torsor $T_{P_8^1, P_4^2}$ representing the link between the plane P_8 of part 1 and the plane P_4 of part 2. The torsor T_{P, P^2} is then collected in MSP 1 for set-up 1.

$$T_{P, P^2} = \left\{ \begin{array}{ll} -lrx_{1,6S1} + rx_{1,6} + rx_{1,7} & -35lry_{1,6S1} - ltx_{1,4S1} + 35ry_{1,6} \\ -rx_{1,6S1} - rx_{2,3} + lrx_{1,7 \rightarrow 2,3} & + \frac{45}{2}ry_{1,7} - 35ry_{1,6S1} - \frac{45}{2}ry_{2,3} \\ & + tx_{1,4} + tx_{1,7} - tx_{1,4S1} - tx_{2,3} \\ & + \frac{45}{2}lry_{1,7 \rightarrow 2,3} + ltx_{1,7 \rightarrow 2,3} \\ -lry_{1,6S1} + ry_{1,6} + ry_{1,7} & 35lrx_{1,6S1} - lty_{1,4S1} - 35rx_{1,6} \\ -ry_{1,6S1} - ry_{2,3} + lry_{1,7 \rightarrow 2,3} & - \frac{45}{2}rx_{1,7} + 35rx_{1,6S1} + \frac{45}{2}rx_{2,3} \\ & + ty_{1,4} + ty_{1,7} - ty_{1,4S1} - ty_{2,3} \\ & - \frac{45}{2}lrx_{1,7 \rightarrow 2,3} + lty_{1,7 \rightarrow 2,3} \\ 0 & -ltz_{1,6S1} + tz_{1,6} + tz_{1,8} \\ & -tz_{1,6S1} - tz_{2,4} + ltz_{1,8 \rightarrow 2,4} \end{array} \right\}_{(O_4, X_4 Y_4 Z_4)} \quad (3.49)$$

Similarly, the positioning deviation of the shaft (part 4) in set-up 2 is described by the part deviation torsor T_{P, P^4} . It is expressed by equation 3.50 based on the connections between the part 4 and the part 2.

$$\begin{aligned} T_{P, P^4} &= T_{P, P^2} + T_{P^2, P_2^2} + T_{P_2^2, P_6^4} - T_{P^4, P_6^4} \\ T_{P, P^4} &= T_{P, P^2} + T_{P^2, P_1^2} + T_{P_1^2, P_7^4} - T_{P^4, P_7^4} \end{aligned} \quad (3.50)$$

The positioning deviation torsor T_{P, P^4} of the part 4 explicitly depends on the positioning deviation torsor T_{P, P^2} of the part 2. Thus, the positioning deviation of part 2 in the set-up 1 participate in the deviation of the part 4 in the set-up 2. The torsor T_{P, P^4} is then collected in MSP 2 for the set-up 2. Finally, the model of assembled part (MAP) of the pump is created based on a set of MSP (MSP 1, MSP 2, MSP 3)

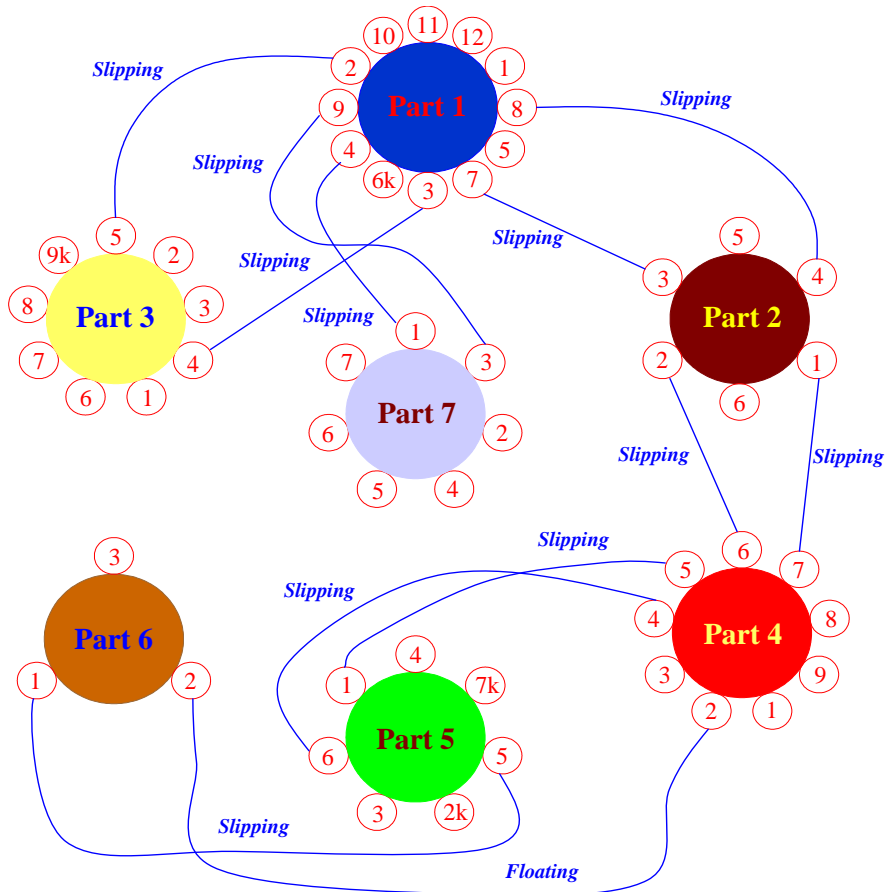


Figure 3.13: Assembly graph of the pump

generated throughout the assembly process (see figure 3.12).

The geometrical deviation model (GDM) of the pump gathers the MMP and MAP of the pump according to the selected manufacturing and assembly processes and the associated resources. The geometrical deviations of each surface of the pump relative to its nominal position in the global coordinate system (O, XYZ) of the pump is modelled by the GDM of the pump. As a result, the gap deviation torsor $T_{P_8^3, P_4^5}$ between the casing (part 3) and the impeller (part 5) of the pump (see figure 3.14) can be calculated based on the GDM by equation 3.51.

$$T_{P_8^3, P_4^5} = -T_{P, P_8^3} + T_{P, P_4^5} \quad (3.51)$$

Where T_{P, P_8^3} and T_{P, P_4^5} are surface deviation torsors modelling the geometrical deviations of the conic surface C_8 of the casing and the conic surface C_4 of the impeller

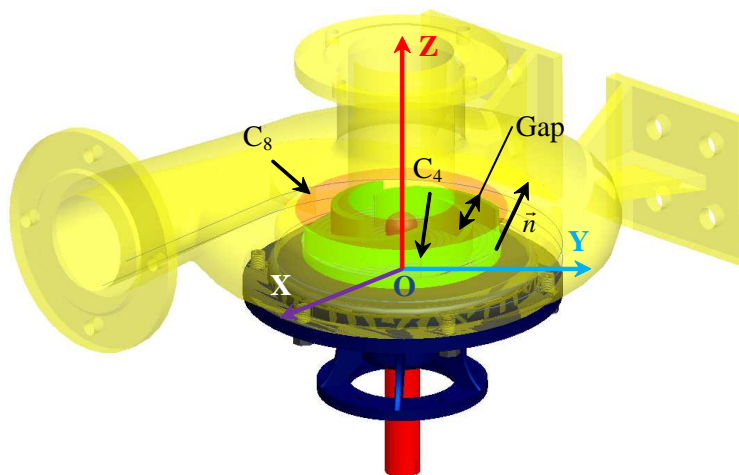


Figure 3.14: The gap between the casing and the impeller of the pump

of the pump, respectively. These torsors are modelled by the GDM of the pump. They are calculated based on the MMP and MAP of the pump, as shown in equation 3.52.

$$\begin{aligned} T_{P,P_8^3} &= T_{P,P^3} + T_{P^3,P_8^3} \\ T_{P,P_4^5} &= T_{P,P^5} + T_{P^5,P_4^5} \end{aligned} \quad (3.52)$$

The torsor $T_{P_8^3,P_4^5}$ at the point O in the global coordinate system (O, XYZ) of the pump is described by rotational vector $\delta\vec{\theta}$ and translational vector $\delta\vec{O}$, as shown in equation 3.9. Thus, the deviation of the gap between the casing and the impeller of the pump is used to verify a non contact condition between the moving surface of the impeller and the motionless surface of the casing, as shown in inequality 3.53.

$$Deviation\ Gap = \delta\vec{O} \cdot \vec{n} \geq 0 \quad (3.53)$$

Where \vec{n} is a unit vector along the normal direction of the gap.

Moreover, this model is also used to analyse assemblability and geometrical requirements as non contact between moving and motionless surface, etc. and later performance as flowrate, velocity of fluid, pressure.

Set-up 2	
Fixture	
Plane 4,9S2	$rx_{4,9S2}, ry_{4,9S2}$ variation range 0.001 $tz_{4,9S2}$ variation range 0.02
Cylinder 4,8S2	$rx_{4,8S2}, ry_{4,8S2}$ variation range 0.002 $tx_{4,8S2}, ty_{4,8S2}$ variation range 0.01 radius $ra_{4,8S2}$ variation range 0.01
Machining	
Plane 4,5	$rx_{4,5}, ry_{4,5}$ variation range 0.005 $tz_{4,5}$ variation range 0.01
Cylinder 4,4	$rx_{4,4}, ry_{4,4}$ variation range 0.0025 $tx_{4,4}, ty_{4,4}$ variation range 0.01 radius $ra_{4,4}$ variation range 0.025
Plane 4,7	$rx_{4,7}, ry_{4,7}$ variation range 0.0015 $tz_{4,7}$ variation range 0.02
...	...

Table 3.5: Variation range of the input variables

3.4.1.4 Geometrical deviation simulation for the centrifugal pump

The Monte-Carlo simulation method is applied to calculate the values of the geometrical deviations of the pump based on the GDM, as presented in section 3.4.1.4. The input variables are the parameters of the torsors that represent machining inaccuracy and deviation of the fixture surface, such as $rx_{i,j}, ry_{i,j}, tx_{i,j}, ty_{i,j}, tz_{i,j}$ for the manufacturing operation of the surface j of the part i and $rx_{i,jSk}, ry_{i,jSk}, tx_{i,jSk}, ty_{i,jSk}, tz_{i,jSk}$ for the surface j of the fixture in the set-up Sk . As explained in subsection 3.3.1, the input variables are considered as independent variables. The probability distributions and the variation range of the input variables need to be determined. A uniform distribution is chosen for the current case. The variation ranges are determined according to the capability of the associated resources. For example, the variation ranges of the input parameters in the set-up 2 of the manufacturing process for manufacturing the shaft are shown in table 3.5.

In order to obtain an image of the geometrical deviations of the pump, it is necessary to calculate the value of the determined components (lr, lt) of the link deviation torsor based on the assembly rules and function of machining and part holder deviation values, as explained in step 3 of the method presented in section 3.3.1.

The determined component $lrx_{4,9S2}$, $lry_{4,9S2}$ and $ltz_{4,9S2}$ of the link deviation torsor in the set-up 2 are determined by maximizing the positioning function $-ltz_{4,9S2}$ while verifying the non-penetration conditions between the surface of the part-holder and the surface of workpiece. This procedure is described in equation 3.54.

Maximize : $-ltz_{4,9S2}$

Subject to :

$$\left\{ \begin{array}{l} -25lry_{4,8S2} + ltz_{4,9S2} + 25ry_{4,8} - 25ry_{4,9} - 25ry_{4,8S2} + 25ry_{4,9S2} \geq 0 \\ -25lrx_{4,8S2} + ltz_{4,9S2} + 25rx_{4,8} - 25rx_{4,9} - 25rx_{4,8S2} + 25rx_{4,9S2} \geq 0 \\ 25lry_{4,8S2} + ltz_{4,9S2} - 25ry_{4,8} + 25ry_{4,9} + 25ry_{4,8S2} - 25ry_{4,9S2} \geq 0 \\ 25lrx_{4,8S2} + ltz_{4,9S2} - 25rx_{4,8} + 25rx_{4,9} + 25rx_{4,8S2} - 25rx_{4,9S2} \geq 0 \end{array} \right. \quad (3.54)$$

Where $rx_{4,8}$, $ry_{4,8}$, $rx_{4,9}$, $ry_{4,9}$, $rx_{4,8S2}$, $ry_{4,8S2}$, $rx_{4,9S2}$ and $ry_{4,9S2}$ are the machining and part holder surface deviation variables. They are randomly generated based on the uniform distribution and the variation range indicated in table 3.5. Similarly, we can determine other determined components (lr , lt) of the link deviation torsor of the MMPs and the MAPs of the pump. The geometrical deviations of each surface of the pump are then calculated based function of the values of link and surface deviation parameters. Then, the designer can numerically verify any geometrical requirement of the pump. For example, the gap necessary to guarantee the non contact condition between the moving surface of the impeller and the motionless surface of the casing (see figure 3.14) is calculated by equation 3.55 based on the definition of the gap in 3.53. If the gap is negative, the surface is in contact and the manufactured pump is unable to work. Thus this gap is an important geometrical requirement to verify to guarantee the quality of the pump.

$$\begin{aligned} Gap = 14.2291 + tz_{1,3} - tz_{1,8} + tz_{3,4} - tz_{3,8} - tz_{4,5} + tz_{4,7} + tz_{5,1} \\ - tz_{5,4} + ltz_{1,3 \rightarrow 3,4} - ltz_{1,8 \rightarrow 2,4} - ltz_{4,5 \rightarrow 5,1} \end{aligned} \quad (3.55)$$

In order to verify the quality of the one million of pumps, the designer can calculate

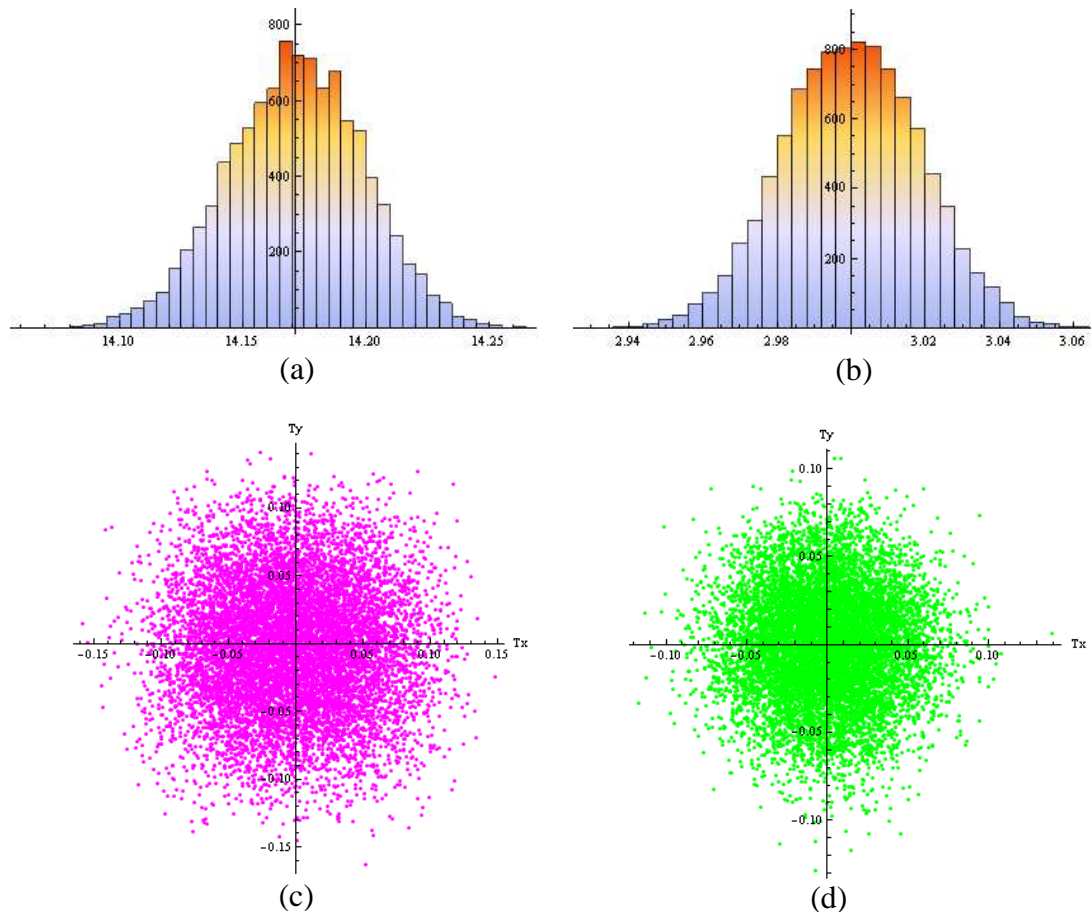


Figure 3.15: Monte-Carlo simulation results

one million value of the gap based on the Monte-Carlo simulation method. As a result, the designer can estimate the distribution of the value of the gap between the impeller and the casing of the pump which has to remain positive to avoid contact between the impeller and the casing of the pump. The distribution of the gap is shown in figure 3.15a (mean $\mu = 14.172$ mm, standard deviation $\sigma = 0.0274$ mm).

Further, the designer can also know the distribution of positioning deviation of each part of the pump. For example, the distribution of the gap between the plane of the impeller and the plane of the volute back casing is shown in figure 3.15b. The distribution of the impeller's center (green colour) and the distribution of the casing's center (magenta colour) according to two perpendicular axes X and Y are shown in figure 3.15c and 3.15d, respectively.

3.5 Conclusion

The model of geometrical deviations of all surfaces of the product proposed in this chapter is consistent with the machining and assembly stage of the product life cycle. It is called Geometrical Deviation Model (GDM) and is built on two models.

- Model of Manufactured Part (MMP) proposed by Vignat [Vig05] for modelling the geometrical deviation generated and accumulated during the manufacturing processes.
- Model of Assembled Part (MAP) for modelling the positioning deviations of each part of the product accumulated during the assembly process.

The GDM is thus able to model the geometrical deviations of all surfaces relative to their nominal position in the global coordinate system of the product generated and accumulated during the manufacturing and assembly stage of its life cycle. This model is used to analyse and verify the functional requirements (non contact condition, gap, etc.), assemblability conditions, etc. Moreover, an image of the population of products is calculated by using the parameters of the GDM and the Monte Carlo simulation method.

Chapter 4

INTEGRATION OF GD¹S INTO SIMULATION OF PRODUCT PERFORMANCE

THE objective of this chapter is to introduce a method that allows to integrate geometrical deviations into the simulation of the product performance. This method is able to determine the relationship between the product performance and the parameters of the geometrical deviations from the manufacturing processes. The result is an image of the population of the manufactured products and their performance calculated from the results of the Monte-Carlo simulation as presented in section 3.3. Some approaches for integration of the geometrical deviations into the simulation of the product performance are introduced in the first section of this chapter. Case studies are then presented in the second section in order to illustrate the proposed approaches.

¹GEOMETRICAL DEVIATION

4.1 Method Description

The set of M products with geometrical deviations being virtually manufactured, the product designers can be aware of the variation range of the geometrical deviation for each surface of the product. These deviations obviously have an influence on the performance of the product. However, the current product modelling technology is unable to take into account these deviations. Most of the simulations predicting the behaviour of the product (kinematics, dynamics, resistance, fluid flow, etc.) are carried out on the nominal model of the product. The result of the simulation of the designed product performance can thus be considered as nominal and consequently different from the real one. The risk is then that not all of the products meet the requirements of the customers and users. Thus it is necessary to integrate geometrical deviations into the simulation of the product performance in order to predict its “real” performance. We propose, in this chapter, two approaches to answer this issue. The first approach, called mathematical analysis approach, is based on the existence of a mathematical relationship between the product performance and the geometrical deviation parameters. This approach can only be used when the relationship is available or easy to set up, which does not occur often. Thus a second approach is proposed based on the design of experiment method (DOE). This method uses numerical simulations to establish the relation between product performance and the parameters of the geometrical deviations. The performance is then calculated for the set of product virtually manufactured as presented chapter 3.

4.1.1 Mathematical Analysis Approach

The relationship between performances Pr_i and design parameters p_i can mathematically be described by equation 4.1.

$$Pr_i = F_i(p_1, p_2, p_3, \dots, p_n) \quad (4.1)$$

The design parameters $\{p_i\}_{i=1..n}$ can be classified into geometrical parameters $\{\hat{p}_j\}_{j=1..m}$ and non-geometrical parameters $\{\tilde{p}_k\}_{k=1..n-m}$. We consider, in this thesis, the effect of geometrical parameters variation $\{\hat{p}_j\}_{j=1..m}$ on product performance variation, thus non-geometrical parameters variation $\{\tilde{p}_k\}_{k=1..n-m}$ is not taken into account. The deviation of the product performance ΔPr_i expresses the difference between the real performance and the nominal one. It is described in equation 4.2.

$$\Delta Pr_i = Pr_i - Pr_i^N \quad (4.2)$$

Where Pr_i^N represents the nominal performance of the product and is determined by equation 4.3.

$$Pr_i^N = F_i(\hat{\mu}_1, \hat{\mu}_1, \dots, \hat{\mu}_m, \tilde{\mu}_1, \tilde{\mu}_2, \dots, \tilde{\mu}_{n-m}) \quad (4.3)$$

The parameters $\{\hat{\mu}_j\}_{j=1..m}$ and $\{\tilde{\mu}_k\}_{k=1..n-m}$ express the nominal value of the geometrical parameters $\{\hat{p}_j\}_{j=1..m}$ and the non-geometrical parameters $\{\tilde{p}_k\}_{k=1..n-m}$. The deviation of the product performance ΔPr_i can be expressed by equation 4.4.

$$\Delta Pr_i = F_i(\hat{p}_1, \hat{p}_2, \dots, \hat{p}_m, \tilde{p}_1, \tilde{p}_2, \dots, \tilde{p}_{n-m}) - F_i(\hat{\mu}_1, \hat{\mu}_1, \dots, \hat{\mu}_m, \tilde{\mu}_1, \tilde{\mu}_2, \dots, \tilde{\mu}_{n-m}) \quad (4.4)$$

The expression of the performance Pr_i can be simplified by a polynomial function based on the Taylor series expansion principles [AS64] if the function F_i is continuous and high-order derivatives exist. It is expressed, at second order, by equation 4.5.

$$\begin{aligned} Pr_i &= F_i(\hat{\mu}_1, \hat{\mu}_1, \dots, \hat{\mu}_m, \tilde{\mu}_1, \tilde{\mu}_2, \dots, \tilde{\mu}_{n-m}) + \sum_{j=1}^m \frac{\partial F_i}{\partial \hat{p}_j} \Big|_{(\hat{\mu}_1, \dots, \hat{\mu}_m)} \cdot \Delta \hat{p}_j \\ &+ \sum_{j=n-m}^n \frac{\partial F_i}{\partial \tilde{p}_j} \Big|_{(\tilde{\mu}_{n-m}, \dots, \tilde{\mu}_n)} \cdot \Delta \tilde{p}_j + \sum_{j=1}^m \sum_{k=1}^m \frac{\partial^2 F_i}{\partial \hat{p}_j \partial \hat{p}_k} \Big|_{(\hat{\mu}_1, \dots, \hat{\mu}_m)} \cdot \Delta \hat{p}_j \cdot \Delta \hat{p}_k \\ &+ \sum_{j=1}^m \sum_{k=n-m}^n \frac{\partial^2 F_i}{\partial \hat{p}_j \partial \tilde{p}_k} \Big|_{(\hat{\mu}_1, \dots, \hat{\mu}_m, \tilde{\mu}_1, \dots, \tilde{\mu}_n)} \cdot \Delta \hat{p}_j \cdot \Delta \tilde{p}_k \\ &+ \sum_{j=n-m}^n \sum_{k=n-m}^n \frac{\partial^2 F_i}{\partial \tilde{p}_j \partial \tilde{p}_k} \Big|_{(\tilde{\mu}_1, \dots, \tilde{\mu}_n)} \cdot \Delta \tilde{p}_j \cdot \Delta \tilde{p}_k \end{aligned} \quad (4.5)$$

Where $\Delta \hat{p}_j = \hat{p}_j - \hat{\mu}_j (j = 1..m)$ represents the deviation of geometrical parameters \hat{p}_j . In this thesis, the variation of the non-geometrical parameters is not taken into

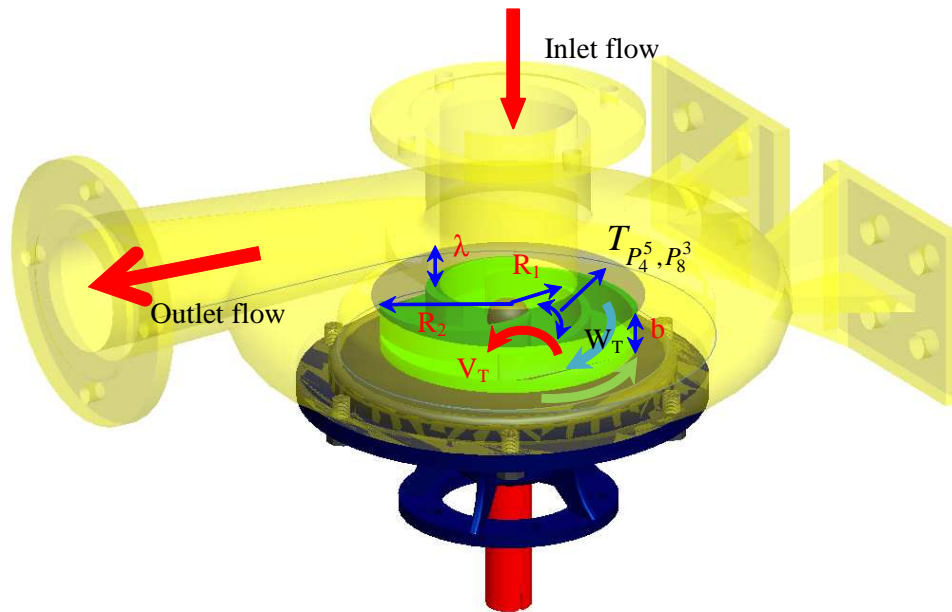


Figure 4.1: Cross section of the impeller passage

account. Thus the relationship between the deviation of product performance ΔPr_i and the deviations of geometrical parameters $\Delta \hat{p}_j$ can be expressed by equation 4.6.

$$\Delta Pr_i = f_i(\Delta \hat{p}_1, \Delta \hat{p}_2, \dots, \Delta \hat{p}_m) = \sum_{j=1}^m \left. \frac{\partial F_i}{\partial \hat{p}_j} \right|_{(\hat{\mu}_1, \dots, \hat{\mu}_m)} \cdot \Delta \hat{p}_j + \sum_{j=1}^m \sum_{k=1}^m \left. \frac{\partial^2 F_i}{\partial \hat{p}_j \partial \hat{p}_k} \right|_{(\hat{\mu}_1, \dots, \hat{\mu}_m)} \cdot \Delta \hat{p}_j \cdot \Delta \hat{p}_k \quad (4.6)$$

The geometrical deviations $\Delta \hat{p}_i$ can be determined from the geometrical deviation model of the product presented in chapter 3. The product performance can be determined from the relation 4.6 and the results of the geometrical deviation simulation as presented in section 3.3. Thus, the mathematical analysis approach can integrate geometrical deviations of the product, generated during its life cycle, into performance simulation.

The centrifugal pump (see figure 4.1) presented in chapter 3 is used to illustrate this approach. The considered performance is the flowrate of the pump. According to the model of Hoshide et al. [HN72], the mass flowrate \dot{m} of the centrifugal pump is described by equation 4.8.

$$\dot{m} = \rho (A_T W_T - A_L V_L) \quad (4.7)$$

Where $A_T = b_N dr$ and $A_L = \lambda_N dr$ with ρ being the mass density. W_T is the relative tangential velocity of the fluid within the volume control. V_L is the leakage velocity relative to the blade, b_N is the nominal blade width of the impeller and λ_N is the nominal clearance between the top surface of the impeller and the casing surface. Then the nominal flowrate can be calculated by equation 4.8.

$$\begin{aligned} dQ_{Nominal} &= (b_N W_T - \lambda_N V_L) dr \\ Q_{Nominal} &= \int_{R_1}^{R_2} (b_N W_T - \lambda_N V_L) dr \end{aligned} \quad (4.8)$$

The relative tangential velocity W_T can be determined by the Bernoulli's principle, as shown in equation 4.9.

$$W_T = \cos\beta \cdot \sqrt{2g(z_1 - z_r) - \frac{2\Delta P_T}{\rho} + (r - R_1)\omega^2} \quad (4.9)$$

Where β is the blade angle which is dependent on the radius r . The differential pressure between the inlet and the outlet of the blade ΔP_T is fitted to a second order polynomial form, as shown in equation 4.10.

$$\Delta P_T = P(r) - P(1) = \Delta P_{Tmax} (A_T + B_T r + C_T r^2 + \dots) \quad (4.10)$$

In addition, leakage velocity V_L is caused by the blade differential pressure from pressure to suction side of the blade. It is determined by equation 4.11.

$$V_L = K \sqrt{\frac{2\Delta P}{\rho}} \quad (4.11)$$

Where K is an equivalent orifice coefficient ($K = 0.98$, in the present case) and ρ is the density of the fluid. The differential pressure across the blade ΔP is also fitted to a polynomial form, as shown in equation 4.12.

$$\Delta P = \Delta P_{max} (A + B r + C r^2 + \dots) \quad (4.12)$$

The nominal blade width of the impeller is determined by equation 4.13.

$$b_N = -a_N r + a_N R_2 + b_2; a_N = \tan 10^\circ \quad (4.13)$$

Finally, the flowrate of the pump taking into account the geometrical deviation of the gap and blade width is determined by equation 4.14.

$$Q = \int_{R_1 + \Delta R_1}^{R_2 + \Delta R_2} (b_D W_T - \lambda_D V_L) dr \quad (4.14)$$

Where $\Delta b = b_D - b_N$ is the deviation of the blade width and $\Delta \lambda = \lambda_D - \lambda_N$ is the deviation of the gap. The deviation of the flow rate of the pump can be calculated by equation 4.15.

$$\Delta Q = \int_{R_1 + \Delta R_1}^{R_2 + \Delta R_2} (\Delta b W_T - \Delta \lambda V_L) dr \quad (4.15)$$

The non-geometrical parameters, in this case, including density of fluid ρ , pressure P and rotational velocity ω are fixed at their nominal value. Thus, the relationship between the deviation of flowrate and the deviation of geometrical parameters can be expressed by equation 4.16.

$$\Delta Q = f(\Delta b, \Delta \lambda, \Delta R_1, \Delta R_2) \quad (4.16)$$

$\Delta R_1, \Delta R_2$ are deviations of inlet and outlet radius of the impeller and $\Delta b, \Delta \lambda$ are deviation of the blade width and deviation of the gap between the impeller and the casing of the pump. They are determined based on the geometrical deviation model of the pump. For example, the gap deviation $\Delta \lambda$ is determined by equation 3.55. The value of coefficients ($A, B, C, A_T, B_T, C_T, \dots$) are determined by experimental measurement on a real model of the pump. In our case, the values from Hoshide et al. [HN72] for Mark 4 Pump model are used. The value of coefficients ($A, B, C, A_T, B_T, C_T, \dots$) are shown in equation 4.17.

$$(A = 1.013; B = 0.267; C = 0; A_T = 1.526; B_T = 0.577; C_T = 0) \quad (4.17)$$

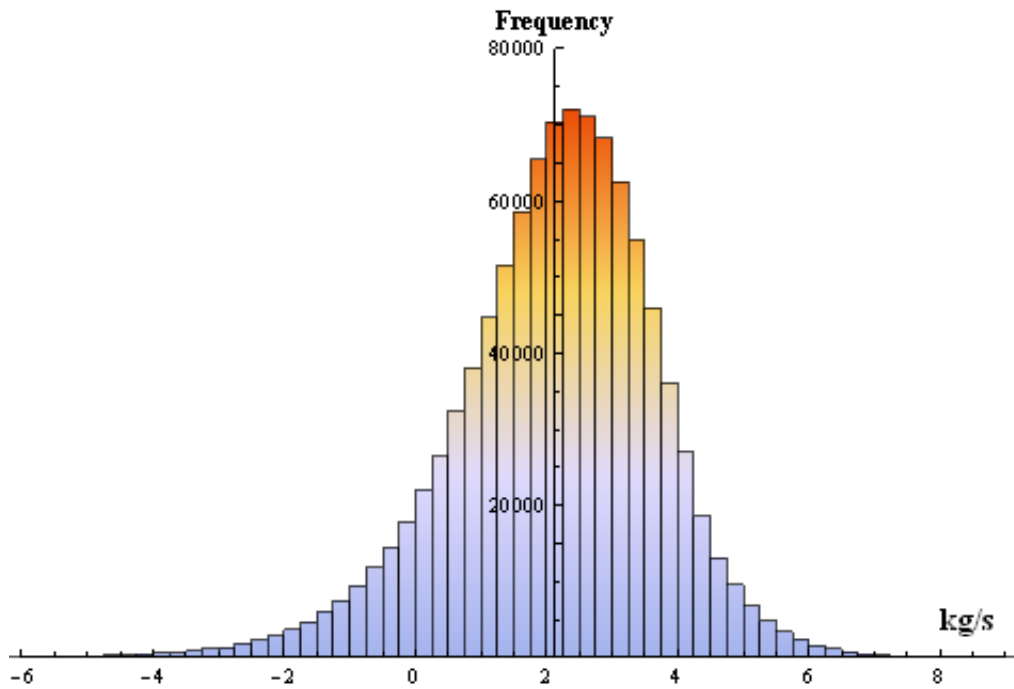


Figure 4.2: Distribution of deviation flowrate of the pump

These values do not fit exactly with our pump model. However, they are used in this case in order to illustrate the proposed approach. The distribution of the flowrate of one million of pumps is determined based on the result of ΔR_1 , ΔR_2 , Δb and $\Delta \lambda$ from the Monte-Carlo simulation, as shown in figure 4.2.

Finally, the mathematical analysis approach can take geometrical deviations of the product into account in the determination of its performance. As a result, the product designer can predict the “real” performance of the product and thus the satisfaction of the customers’ requirements. However, it is unable to take into account all geometrical deviations because it relies on the mathematical model of the product performance, i.e. the mathematical relationship between the performance and the geometrical parameters of the product. Thus, we propose, in the next section, another approach that allows to integrate more geometrical deviation sources. This second method, based on numerical simulations and design of experiments, avoid the necessity of finding a mathematical relationship, and it allows better consideration of geometrical variations.

4.1.2 Design of Experiment Approach

We propose, in this subsection, to use numerical simulation together with a design of experiment (DOE) approach to integrate geometrical deviation parameters into the performance prediction. The DOE method is based on the results of numerical simulation with deviated models and uses the regression model to establish an approximate relationship between the product performance and the geometrical deviation parameters. Three approaches are proposed in this section and the choice among them depends on the knowledge that the designer has about the product behaviour and the number of involved parameters.

4.1.2.1 From nominal model to deviated one in a CAD² software

To integrate the geometrical deviations into the simulation of the product performance, we need a deviated model, that allows to represent these deviations. Thus it is necessary to develop a method that permits to obtain the deviated model of the product based on its nominal model in the CAD software.

4.1.2.1.1 Nominal model Today, the engineering activities in product design involve CAD software. This software is a useful tool to model the nominal geometry of the product. The nominal model constructed in CAD system is mainly based on three techniques:

- Constructive solid geometry (CSG) is a technique used in solid modeling. It allows a modeler to create a complex surface or part by using Boolean operators (union, intersection and difference) to combine simple parts (cuboids, cylinders, prisms, pyramids, spheres, cones). The operations used to build a CSG are shown in figure 4.3.

²Computer Aided Design

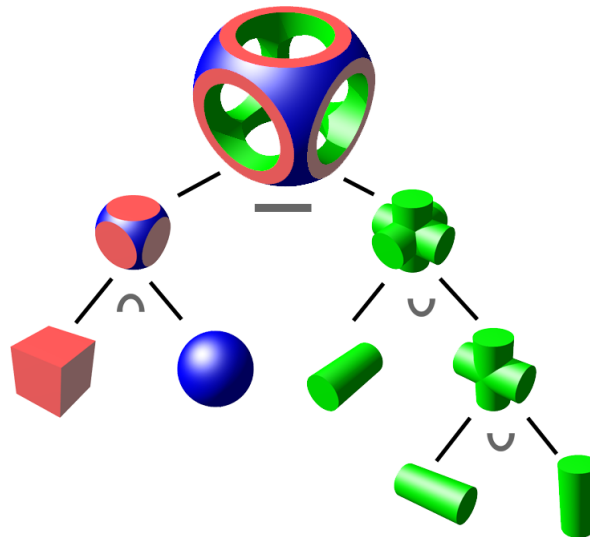


Figure 4.3: CSG operations [Wik10]

- Boundary Representation (B-REP) is a method for representing shapes using the limits. A solid is represented as a collection of connected surface elements, the boundary between solid and non-solid.
- TTRS (Technologically and Topologically Related Surface) model is proposed by Clément et al. [CRT94]. This model composes 7 classes of invariance surfaces, such as spheres, planes, prisms, cones, spirals, revolution. A part is defined by a set of boundary surfaces that are described relative to a coordinate system.

Whatever the technology used, the nominal model does not take into account the geometrical deviations or form defects of the surfaces. We propose, in next section, a method to create a deviated model of the product integrating the geometrical deviations of the surfaces.

4.1.2.1.2 Deviated model The geometrical deviations of each surface of the product are determined by a surface deviation torsor and the value of its component are calculated based on a Monte-Carlo simulation method. As presented in chapter 3, a surface deviation torsor expresses the positioning deviation of a surface relative to its nominal position. The nominal model of the product created

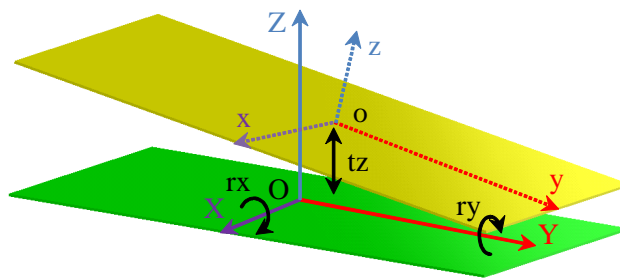


Figure 4.4: Deviated model of a plane

in the CAD software is built on a set of elementary surfaces (planes, cylinders, spheres, etc.). Thus it is possible to create a deviated model of a surface in the CAD software based on the nominal surface and the part deviation torsor. For example, the geometrical deviations of a plane relative its nominal position in a coordinate system (O, XYZ) are described by equation 4.18.

$$T_{Plane} = \left\{ \begin{array}{cc} rx & 0 \\ ry & 0 \\ 0 & tz \end{array} \right\}_{(O,XYZ)} \quad (4.18)$$

The deviated plane can be created by rotating the nominal plane of an angle rx and ry around OX , OY axis respectively and translating it of tz along OZ , as shown in figure 4.4. By the same way, the deviated model of a part or a product relative to its nominal model could be created in CAD software. The nominal part in CAD system includes a set of the boundary surfaces (elementary solids) based on B-REP or TTRS. The boundary surfaces are elementary surfaces, such as planes, cylinders, cones, spheres and spiral. The deviations of each elementary surface of a part or a product is modelled by a surface deviation torsor collected in the GDM, as presented in chapter 3. Thus the deviated model relative to its nominal model could be generated by displacing the boundary surfaces according to the value of the surface deviation torsor. The deviated model of the product is built on the deviated model of the parts. As a result, the deviated model of the product created in CAD software can be integrated into product performance simulation.

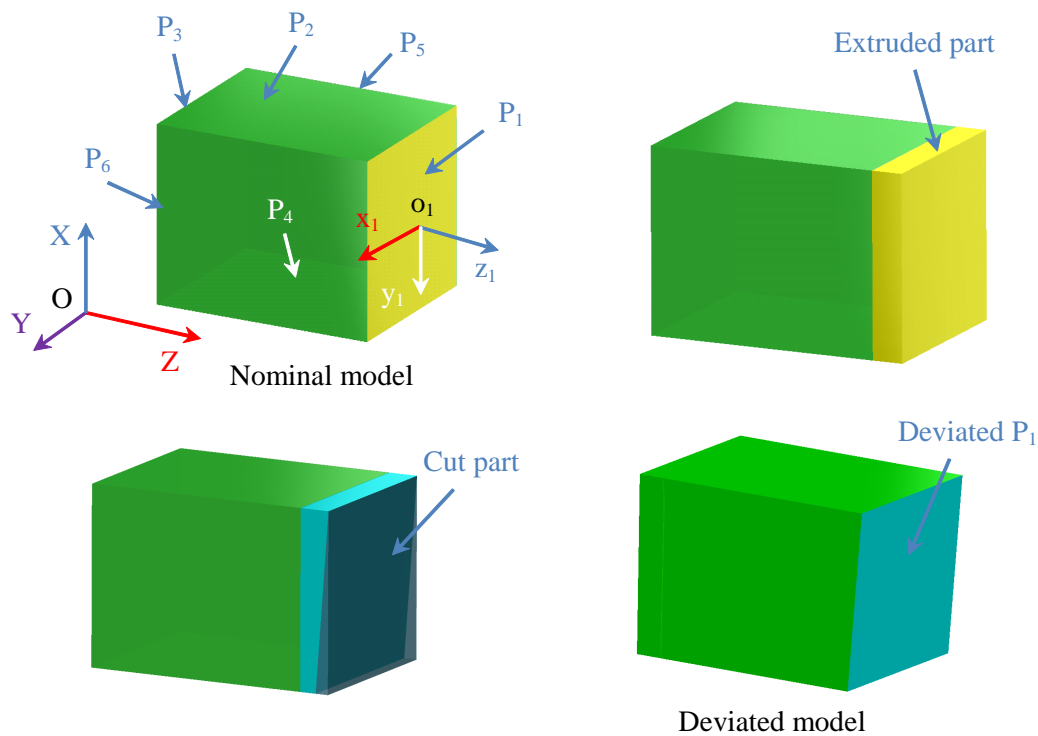


Figure 4.5: Deviated model of a part in PTC ProEngineer

However, we do not have the interface that allows to act on the geometry data in commercial CAD software (ProEngineer, Solidworks, Catia, etc.) and thus it is difficult to combine the deviated elementary surfaces of the deviated model of the part or the product. Therefore, we propose, in this thesis, to use the expert knowledge to filter the unessential surfaces and parameters of the geometrical deviations. The aim is to reduce time used to create the deviated model in CAD software. The selected geometrical deviations and surfaces must have a strong influence on the product performance according to expert knowledge.

The deviated model of the part or the product that is used, in the thesis, to make the simulation of the product performance is produced in a commercial CAD software (ProEngineer). This model is created by using some available techniques in this software, such as extrusion, revolution, sweep, blend, etc. For example, we use extrusion technique in PTC ProEngineer to displace the plane (see figure 4.5). The surface deviation torsor representing the geometrical deviations of the plane

P_1 comes from GDM and Monte-Carlo simulation, as given in equation 4.19.

$$T_{P_1} = \begin{pmatrix} rx_1 & 0 \\ ry_1 & 0 \\ 0 & tz_1 \end{pmatrix}_{(o_1, x_1 y_1 z_1)} \quad (4.19)$$

First, the plane P_1 is moved along axis o_1z_1 from a value l , $\{l \geq tz_1 + \frac{H}{2}(rx_1 + ry_1)\}$ by the extrusion technique. Then the deviated plane is created by cutting the extruded part by plane rotated around the axes o_1x_1 and o_1y_1 of rx_1 and ry_1 , respectively. Finally, we obtain the deviated part in PTC ProEngineer, as shown in figure 4.5.

4.1.2.2 Regression model

Regression analysis is used to approximate a relationship between dependent variables R and independent variables P . Regression models can be linear or non-linear. In this thesis, linear and non-linear regression models are used to find the relation between the performance of the product and the parameters of the variation sources, as presented in the next section.

The linear regression model presented by [RT95] is used to establish the relationship between the performance and the parameters. The relationship is linearly expressed as in equation 4.20.

$$f = p \cdot \beta + e \quad (4.20)$$

The equation 4.20 can be written under matrix form, as shown in equation 4.21.

$$\begin{bmatrix} r_1 \\ r_2 \\ \vdots \\ r_{2^n} \end{bmatrix} = \begin{bmatrix} p_{11} & p_{21} & \dots & p_{n1} \\ p_{12} & p_{22} & \dots & p_{n2} \\ \vdots & \vdots & \ddots & \vdots \\ p_{12^n} & p_{22^n} & \dots & p_{n2^n} \end{bmatrix} \begin{bmatrix} \beta_1 \\ \beta_2 \\ \vdots \\ \beta_{2^n} \end{bmatrix} + \begin{bmatrix} e_1 \\ e_2 \\ \vdots \\ e_{2^n} \end{bmatrix} \quad (4.21)$$

Where $\beta = \{\beta_1, \beta_2, \dots, \beta_{2^n}\}$ is the coefficient vector of the model. The vector $\hat{\beta}$ is an estimated vector of the vector β and is calculated by equation 4.22.

$$\hat{\beta} = (P^t P)^{-1} . P^t . R \quad (4.22)$$

$e = \{e_1, e_1, \dots, e_{2^n}\}$ is the experimental error vector. The estimated relationship \hat{f} between the performance of the product and the parameters is expressed by equation 4.23.

$$\hat{f} = p . \hat{\beta} + \varepsilon \quad (4.23)$$

Where ε is the residual vector as defined by equation 4.24.

$$e = f - \hat{f} \quad (4.24)$$

This relation \hat{f} being established, the performance of the population of virtual products (a set of M products) will be calculated by replacing the value of the selected factors, collected from the Monte-Carlo simulation results, into equation 4.27. The collection of performance data can then be analysed by using usual statistic and graphic tools.

4.1.2.3 Factorial design

A factorial design is usually used to understand the effect of two or more independent variables upon a single dependent variable. It is used, in the current case, to study the relationship between the geometrical deviations and a specific performance of the product. In order to initiate this method, it is necessary to create an experimental table, called design matrix, that includes design factors and their levels and corresponding experimental runs results (called response vector). These factors are non-geometrical or geometrical deviation parameters that obviously have an influence on its performance. The overview of this method is shown in figure 4.6.

The number of experimental runs depends on the number of factors and the associated number of levels and thus the number of factors and levels influence the computation time. k^n runs must be realized for n factors and k levels. To reduce the number of factors, key geometrical parameters are defined based on expert knowledge. Then the number of levels for these factors has to be defined depending on a compromise between the desired precision and the calculation time. The values of the key parameters are measured on the virtual product and are functions of the elementary deviation parameters. The variation range of these factors can be calculated based on the M Monte-Carlo simulation result. The value assigned to the levels of a parameter is calculated according to these range of variation. The k^n values of the n parameters are then gathered in a design matrix P , as shown in equation 4.25.

$$P = \begin{bmatrix} p_{11} & p_{21} & \cdots & p_{n1} \\ p_{12} & p_{22} & \cdots & p_{n2} \\ \vdots & \vdots & \ddots & \vdots \\ p_{1k^n} & p_{2k^n} & \cdots & p_{nk^n} \end{bmatrix} \quad (4.25)$$

This method is used when the relationship between geometrical deviation and product performance is not mathematically established. Thus simulation tools as FEA, CFD, etc., are used to calculate the performance of the product. A set of the k^n deviated models of the product, corresponding to the geometrical parameters p_{ij} of each line of the design matrix, has to be created in the CAD system, as presented in section 4.1.2.1.2. Each deviated model is used to simulate the performance of the product and the performance of k^n representative products are gathered in a response vector R . The response vector R corresponding to the design matrix P can then be filled, as expressed in equation 4.26.

$$R = \left\{ \begin{array}{c} r_1 \\ r_2 \\ \vdots \\ r_{k^n} \end{array} \right\} \quad (4.26)$$

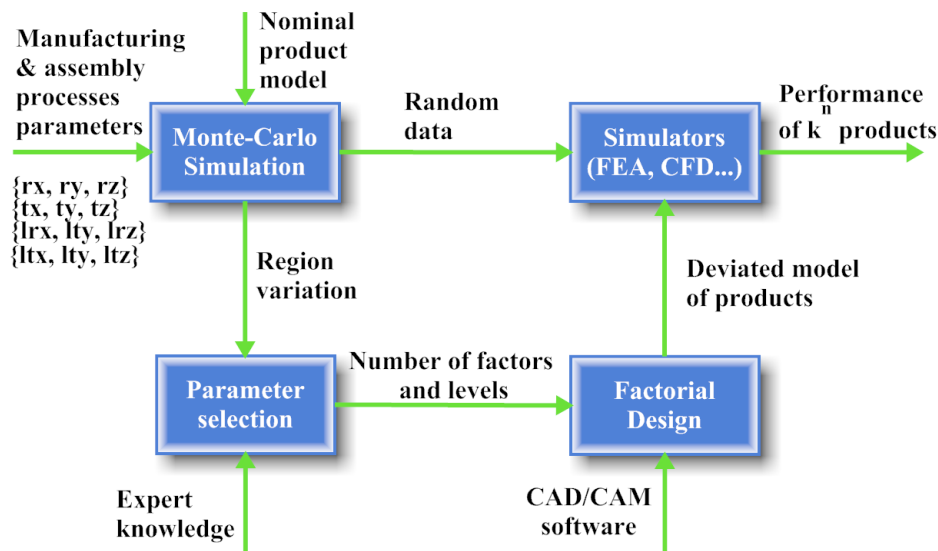


Figure 4.6: Performance simulation of the product with geometrical deviations

The relationship f between the performance of the product and the selected factors $\{p_1, p_2, \dots, p_n\}$ is established by a linear or non-linear regression model, as presented in section 4.1.2.2. This relationship can be expressed by equation 4.27.

$$Performance = f(p_1, p_2, \dots, p_n) \quad (4.27)$$

4.1.2.4 Taguchi design

The full factorial designs as presented in subsection 4.1.2.3 are used to establish the relationship between the performance and the geometrical deviation parameters of the product. However, the number of numerical simulations becomes too large when the numbers of selected factors and levels is increasing. For example, $3^4 = 81$ simulations are necessary in the case of four factors and three levels. Thus, we propose an alternative method based on Taguchi's orthogonal arrays in order to reduce the number of simulations. The overview of Taguchi design approach is shown in figure 4.7. Taguchi's orthogonal arrays are highly fractional orthogonal designs proposed by Taguchi. They are used to estimate the main effects with only a few experiments. They are applicable to investigate main effects from factors and levels. This approach is also suitable to apply for certain mixed level experiments

where the factors included do not have the same number of levels.

As for section 4.1.2.3, the number of factors is selected by the expert knowledge in order to filter the factors that have small effects on the performance of the product. The value associated to the levels of each factor are also defined from the results of the geometrical deviation simulation. Then the number of experimental runs is selected based on the Taguchi's orthogonal arrays, as shown in table 4.1. In the case of n factors and k levels, there are L_N experimental runs that must be realized according to Taguchi table. The design matrix P in this case is different from the one from factorial design. It is defined according to Taguchi table for each factor and level. For example, the design matrix P in the case of 7 factors and 2 levels (low level, high level) is defined according to Taguchi table L_8 , as given in equation 4.28.

$$P = \begin{bmatrix} p_1^- & p_2^- & p_3^- & p_4^- & p_5^- & p_6^- & p_7^- \\ p_1^- & p_2^- & p_3^- & p_4^+ & p_5^+ & p_6^+ & p_7^+ \\ p_1^- & p_2^+ & p_3^+ & p_4^- & p_5^- & p_6^+ & p_7^+ \\ p_1^- & p_2^+ & p_3^+ & p_4^+ & p_5^+ & p_6^- & p_7^- \\ p_1^+ & p_2^- & p_3^+ & p_4^- & p_5^+ & p_6^- & p_7^+ \\ p_1^+ & p_2^- & p_3^+ & p_4^+ & p_5^- & p_6^+ & p_7^- \\ p_1^+ & p_2^+ & p_3^- & p_4^- & p_5^+ & p_6^+ & p_7^- \\ p_1^+ & p_2^+ & p_3^- & p_4^+ & p_5^- & p_6^- & p_7^+ \end{bmatrix} \quad (4.28)$$

Where p_i^- and p_i^+ represent low and high level value for factor p_i respectively.

Then a set of L_N deviated model of the product, according to the values of the geometrical deviations p_i of each row of the design matrix P , has to be created in the CAD system, as presented in section 4.1.2.1.2. Each deviated model is used to simulate the performance of the product (FEA, CFD software, etc.) and the performance of the L_N representative products are gathered in a response vector

R , as expressed in equation 4.29.

$$R = \begin{Bmatrix} r_1 \\ r_2 \\ \vdots \\ r_{L_N} \end{Bmatrix} \tag{4.29}$$

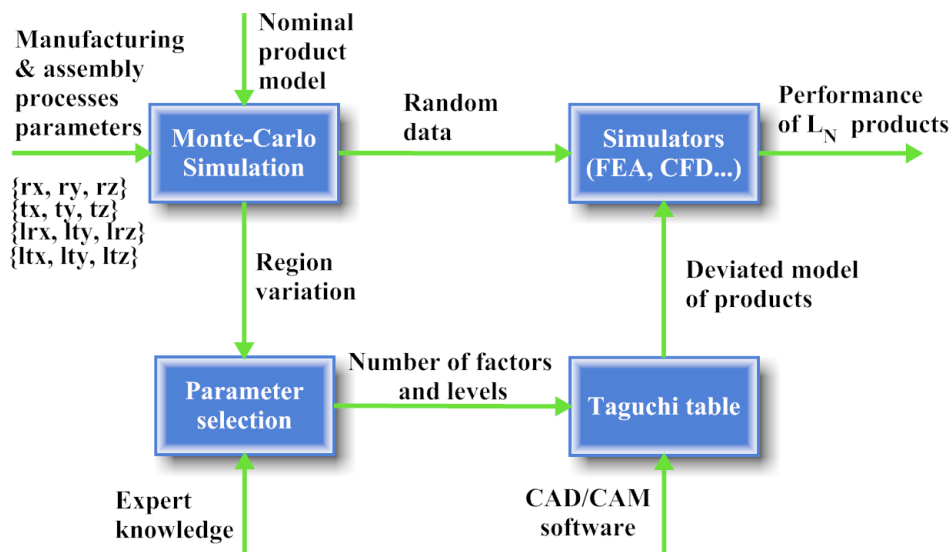


Figure 4.7: Performance simulation with Taguchi design

The relationship between the performance of the product and the factors is established by using a linear or non-linear regression based on the design matrix P and the response vector R . The procedure has already been presented in subsection 4.1.2.3. In comparison with factorial design, Taguchi design approach can take into account much more factors with a reasonable number of calculation.

		Number of Factors																					
		2	3	4	5	6	7	8	9	10	11	12	13	14	15	16	17	18	19	20	21	22	23
Number of Levels	2	L4	L4	L8	L8	L8	L8	L12	L12	L12	L12	L16	L16	L16	L16	L32	L32	L32	L32	L32	L32	L32	L32
	3	L9	L9	L9	L18	L18	L18	L18	L27	L27	L27	L27	L27	L36	L36	L36	L36	L36	L36	L36	L36	L36	L36
	4	L16	L16	L16	L16	L32	L32	L32	L32	L32													
	5	L25	L25	L25	L25	L25	L50	L50	L50	L50	L50	L50											

Table 4.1: Table of Taguchi design

For example, it is necessary to run 27 simulations in the case of 10 factors and 3

levels while we need to run $3^{10} = 59049$ simulations in the case of factorial design. This is one of the advantages of this approach. Thus this approach is usually used when the number of factors and levels is large.

4.1.2.5 Random design

In case of increasing complexity alongside with factors number, the number of necessary simulations to determine the relationship between performance and deviations can become too large and thus time consuming even using Taguchi design. Moreover, the use of expert knowledge to determine key factors filters the deviation sources and can lead to the lost of some influential factors. Factorial design and Taguchi's orthogonal arrays are not effective in this case. Thus, we propose a random design method in order to address these issues. All product geometrical deviations parameters, called factors $p_{i(i=1..n)}$, that have small effects on the performance of the product are taken into account. The variation range of each factor is determined based on the results of geometrical deviations Monte-Carlo simulations, as presented in chapter 3.

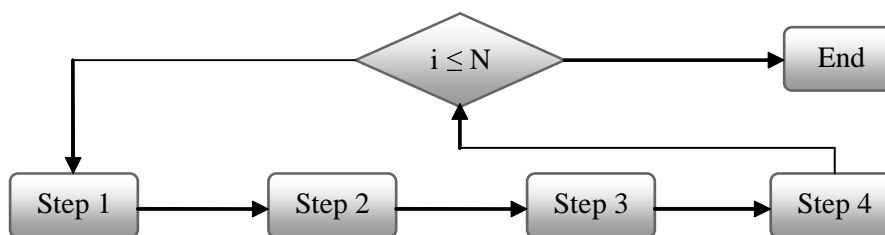


Figure 4.8: The algorithm diagram of random design method

The random design approach is realized in 4 steps (see figure 4.8):

- Step 1. Draw randomly a product with geometrical deviations in the set of product collected from the Monte-Carlo simulation.

A k^{th} product with geometrical deviations is randomly drawn in a set of M products collected from results of geometrical deviation simulation. The value

of each factor p_i is calculated based on the drawn product deviation parameters values. The set of values of the factors p_i is added into the k^{th} row of the design matrix P , as given in equation 4.30.

$$P = \begin{bmatrix} p_{11} & p_{21} & \cdots & p_{n1} \\ p_{12} & p_{22} & \cdots & p_{n2} \\ \vdots & \vdots & \ddots & \vdots \\ p_{1k} & p_{2k} & \cdots & p_{nk} \end{bmatrix} \quad (4.30)$$

- Step 2. Create the deviated CAD model.

The deviated model of k^{th} product will be created in the CAD software corresponding the value of each geometrical deviation parameter p_i , as presented in section 4.1.2.1.2.

- Step 3. Simulate the performance of the product.

The deviated model created in the step 2 is used to simulate the performance of the product in order to determine the performance of the representative product. The result is appended into the response vector R , as described by equation 4.31.

$$R = \begin{Bmatrix} r_1 \\ r_2 \\ \vdots \\ r_k \end{Bmatrix} \quad (4.31)$$

- Step 4. Eliminate the drawn product in the set of M products. Repeat the step 1.

In this step, it is necessary to eliminate the product that has been drawn in step 1. The loop is repeated until the number of the drawn product is equal to N products.

Then the relationship between the performance of the product and the parameters of geometrical deviations p_i is obtained by using the linear or non-linear model

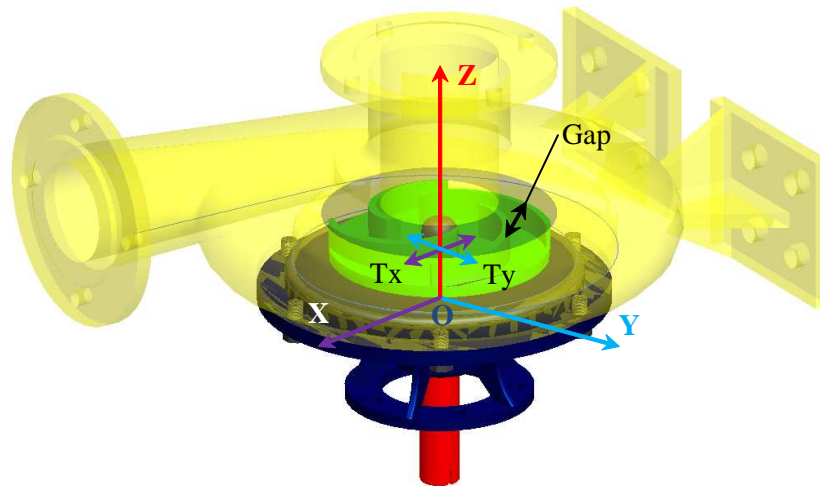


Figure 4.9: The selected factors of the pump

based on the design matrix P and the response vector R . The procedure has already been presented in subsection 4.1.2.2.

4.2 Case Studies

4.2.1 A centrifugal pump

As presented in subsection 4.1.1, the mathematical analysis approach can take the geometrical deviations of the pump into account in performance simulation. Hoshide et al. [HN72] only mention the influence of the gap $\Delta\lambda$ on the flowrate of the pump thus only the deviation of this gap is taken into account by mathematical analysis. In order to take into account more geometrical deviations, we use finite element method to simulate the flowrate of the pump and the design of experiment method (factorial design and Taguchi design) to establish the relationship between the flowrate and the geometrical deviation parameters.

4.2.1.1 Factorial design

First, it is necessary to define the factors and the level of each factor. The selected factors are, in this case, the geometrical and are chosen based on the experimental or expert knowledge according to their supposed influence. According to the experimental result of [EG01] and the study of [BKF00], the selected factors are the gap between the impeller and the casing of the pump, and the translation of the impeller along the two perpendicular axes X, Y of the global coordinate systems (see figure 4.9). The levels of each factor are then chosen from the results of the Monte-Carlo simulation according to the 6σ standard:

- High level at $\mu + 3\sigma$ (1)
- Medium level at μ (0) (average value of the parameter)
- Low level at $\mu - 3\sigma$ (-1)

	Gap (mm)	Tx (mm)	Ty (mm)
High level (1)	14.311	0.144	0.106
Medium level (0)	14.229	0	0
Low level (-1)	14.147	-0.144	-0.106

Table 4.2: The value of the selected parameters

In order to integrate these geometrical deviations into flowrate simulation, we use finite element method within CFD³ tool. From the selected factors and levels (see table 4.2), it is necessary to create 27 deviated models of the pump as shown table 4.3 with the selected deviations according to each level. These models are used to simulate the flowrate of the pump by CFDesign software. The working conditions of the pump are as follows:

- Temperature: 20°C
- Revolution speed: 2000 *RPM*

³Computational Fluid Dynamics

No.	Gap	Tx	Ty	Q(g/s)	No.	Gap	Tx	Ty	Q(g/s)
1	-1	-1	-1	62699.7	15	0	0	1	62960.5
2	-1	-1	0	63172.7	16	0	1	-1	55293.1
3	-1	-1	1	66700.6	17	0	1	0	63846.4
4	-1	0	-1	63782.8	18	0	1	1	63138.1
5	-1	0	0	63115.5	19	1	-1	-1	63432.4
6	-1	0	1	62976.7	20	1	-1	0	61907.2
7	-1	1	-1	63592.5	21	1	-1	1	61902.1
8	-1	1	0	63671.9	22	1	0	-1	61951.2
9	-1	1	1	63298.4	23	1	0	0	61909.1
10	0	-1	-1	62791	24	1	0	1	61990.3
11	0	-1	0	63527.1	25	1	1	-1	61979.7
12	0	-1	1	62980.2	26	1	1	0	62185
13	0	0	-1	63064.4	27	1	1	1	61907.2
14	0	0	0	63600.3					

Table 4.3: The results of the flowrate simulation

- Liquid: Water

The results are shown in table 4.3. The relationship between the performance of the pump and the selected parameters is determined by non-linear regression model. The mass flowrate Q of the pump as a function of the gap between the impeller and the casing of the pump (Gap) and the translation of the impeller relative to X, Y axes (Tx, Ty) is described by equation 4.32.

$$\begin{aligned}
Q = & -7.97795 \times 10^6 + 1.13956 \times 10^6 \text{Gap} - 40373.3 \text{Gap}^2 - 9.47196 \times 10^7 \text{Tx} \\
& + 1.33071 \times 10^7 \text{GapTx} - 467397. \text{Gap}^2 \text{Tx} + 6.1493 \times 10^8 \text{Tx}^2 - 8.64763 \times 10^7 \text{GapTx}^2 \\
& + 3.04026 \times 10^6 \text{Gap}^2 \text{Tx}^2 + 1.72515 \times 10^8 \text{Ty} - 2.42049 \times 10^7 \text{GapTy} + 849043. \text{Gap}^2 \text{Ty} \\
& + 26307. \text{TxTy} - 225203. \text{Tx}^2 \text{Ty} + 1.547 \times 10^9 \text{Ty}^2 - 2.1753 \times 10^8 \text{GapTy}^2 \\
& + 7.64703 \times 10^6 \text{Gap}^2 \text{Ty}^2 + 347389. \text{TxTy}^2 - 523800. \text{Tx}^2 \text{Ty}^2 (g/s)
\end{aligned}
\tag{4.32}$$

Figure 4.10 shows the associated response surfaces representing the dependence between the flowrate of the pump and the factors Gap, Tx (figure 4.10a), Gap, Ty (figure 4.10b) and Tx, Ty (figure 4.10c).

The product designer then calculates the flowrate of the 1 million pumps based on the values of the Gap, Tx and Ty found from Monte-Carlo simulation and equation

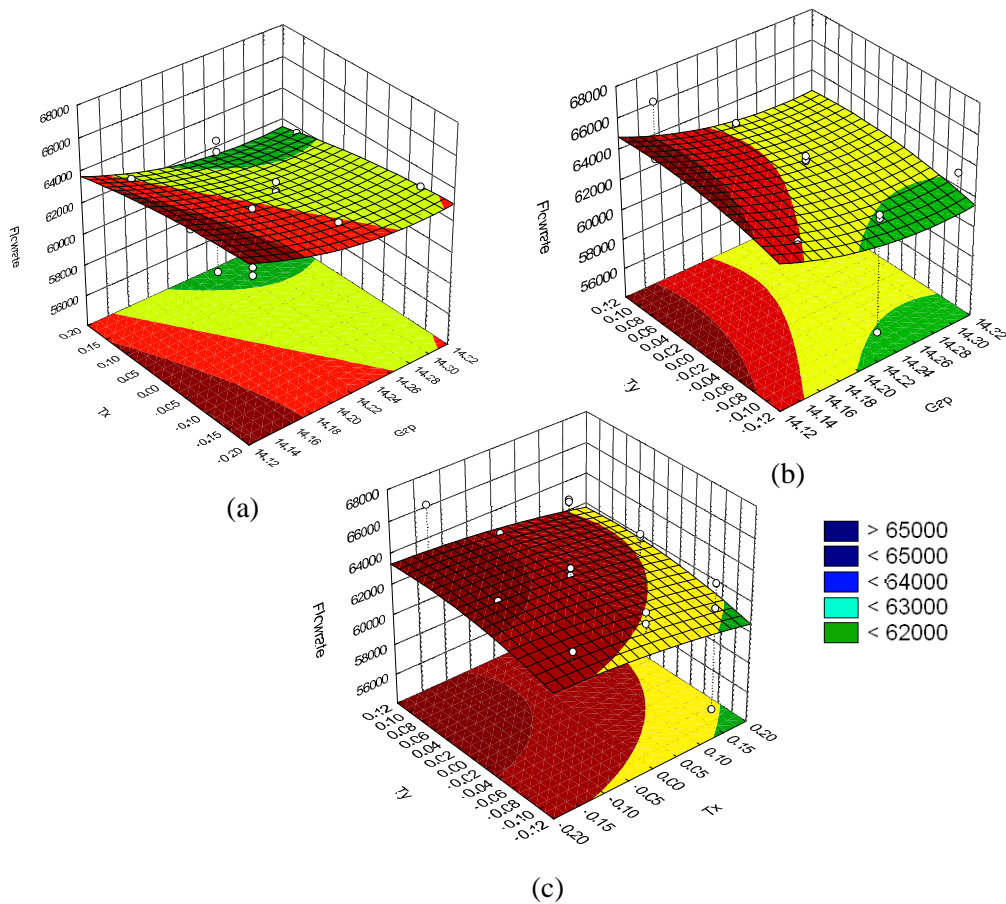


Figure 4.10: Response surfaces of the flowrate

4.32. The distribution for the 1 million of pumps is shown in figure 4.11. The mean and standard deviation of the flowrate of the pump are equal to 61.971kg/s and 0.530kg/s respectively. As a result, the product designer can verify that the real flowrate of the pump satisfies the requirements of the customers.

4.2.1.2 Taguchi design

Taguchi design method is used in case of increasing number of parameters taken into account in order to reduce the number of experimental runs. With the Taguchi design method, we only make 16 flowrate simulation to integrate 11 geometrical deviation parameters of the pump and two levels (see table 4.5). In comparison with the factorial design, it would be necessary to run $2^{11} = 2048$ simulations.

In order to integrate these deviations, we create 16 deviated models of the pump

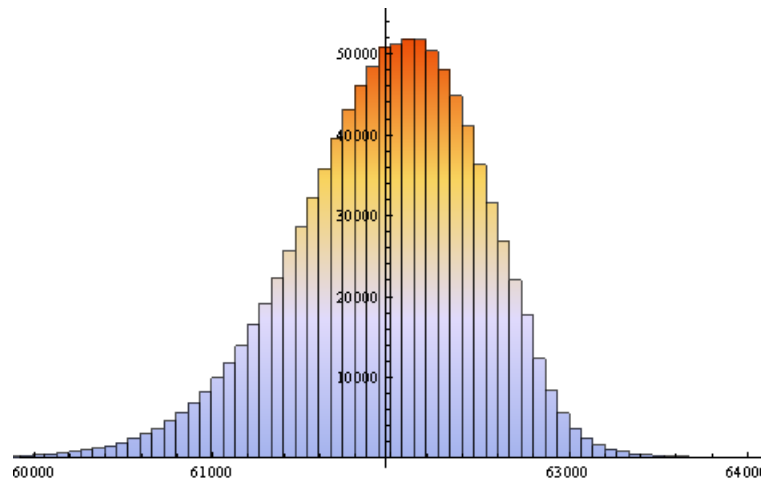


Figure 4.11: Distribution of the flowrate of one million pumps by factorial design in CAD software according to the value of each geometrical deviation parameter. These models are used to simulate the flowrate of the pump by CFDesign software. The results of 16 simulations on CFDesign are shown in table 4.5. The relationship between the flowrate and the geometrical deviation parameters is established by a linear regression model as presented in subsection 4.1.2.3. This relationship is expressed by equation 4.33.

$$Q = 128361. - 1657.08tx - 884.201Tx - 15766.7ty + 5441.39Ty + 7722.5tz - 4582.16Tz - 1133.32b_1 - 338.925b_2 + 1452.2b_3 + 42.7b_4 - 119.d_1 \quad (4.33)$$

The distribution for the 1 million of pumps is shown in figure 4.12. The mean and standard deviation of the flowrate of the pump are equal to 62.840 kg/s and 0.434 kg/s respectively.

4.2.2 A Spring System

As mentioned in subsection 4.1.2.1.2, there are difficulties to integrate all geometrical deviations of the pump in the CAD software, such as PTC ProEngineer, SolidWorks, Catia, etc. We could not automatically generate the deviated model of the pump by the random design approach. Thus, we propose, in this case, a simple case study as the spring system as represented in figure 4.13. This case study allows

Geometrical deviation parameters	High level (mm)	Low level (mm)	Geometrical deviation parameters	High level (mm)	Low level (mm)
Translation of conic surface of casing tx	0.03	-0.03	Fourth blade width of impeller b_4	0.05	-0.05
Translation of conic surface of casing ty	0.03	-0.03	Translation of impeller Tx	0.144	-0.144
Translation of conic surface of casing tz	0.04	-0.04	Translation of impeller Ty	0.106	-0.106
First blade width of impeller b_1	0.05	-0.05	Translation of impeller Tz	14.311	14.147
Second blade width of impeller b_2	0.05	-0.05	Outer diameter of impeller d_1	0.05	-0.05
Thirst blade width of impeller b_3	0.05	-0.05			

Table 4.4: List of the geometrical deviation parameters of the pump

us to compare the advantages and disadvantages among the proposed approaches (mathematical analysis, factorial design, Taguchi design and random design). The frequency of the spring system is the performance investigated in this case.

The frequency of the spring system is expressed by equation 4.34.

$$f = \frac{1}{2\pi} \sqrt{\frac{k}{m}} \quad (4.34)$$

Where m is a weight of the load. It depends on the density ρ and the volume V of the load. In other words, the deviation mass of the load depends on the geometrical deviations of the load. For example, the deviations of a cylinder and two planes including their rotation and translation effect on the mass m . It is calculated by equation 4.35.

$$m = \rho V \quad (4.35)$$

No.	tx	ty	tz	b_1	b_2	b_3	b_4	d_1	Tx	Ty	Tz	Q (g/s)
1	1	-1	1	1	-1	1	-1	-1	1	1	-1	63096.9
2	-1	1	1	1	1	-1	-1	1	-1	1	-1	60670.3
3	-1	-1	-1	1	1	1	1	-1	-1	-1	-1	63306.3
4	-1	1	1	-1	-1	1	1	1	-1	1	-1	64648
5	1	-1	1	1	-1	1	-1	1	-1	-1	1	65305.4
6	-1	-1	-1	1	1	1	1	1	1	1	1	63466.8
7	-1	1	1	1	1	-1	-1	-1	1	-1	1	62456.6
8	1	1	-1	-1	1	1	-1	-1	-1	1	1	63359.6
9	1	1	-1	1	-1	-1	1	-1	-1	1	1	63069.4
10	1	1	-1	1	-1	-1	1	1	1	-1	-1	59386.3
11	-1	-1	-1	-1	-1	-1	-1	-1	-1	-1	-1	63415.7
12	-1	-1	-1	-1	-1	-1	-1	1	1	1	1	63312.1
13	1	1	-1	-1	1	1	-1	1	1	-1	-1	63503.9
14	1	-1	1	-1	1	-1	1	1	-1	-1	1	64522.5
15	1	-1	1	-1	1	-1	1	-1	1	1	-1	62649.6
16	-1	1	1	-1	-1	1	1	-1	1	-1	1	64413.2

Table 4.5: The results of the flowrate simulation in CFDesign for Taguchi design

k is called spring constant or spring stiffness. It is calculated by equation 4.36.

$$k = \frac{Gd^4}{8nD^3} \quad (4.36)$$

Where:

G - Modulus of rigidity

d - Spring wire diameter.

D - Spring outer diameter.

n - Number of active windings.

From the expert knowledge as presented above, we can know that the frequency of the spring system depends on many parameters, especially the geometrical deviations such as deviations of the cylinder and plane shaping the load, spring wire diameter and spring outer diameter.

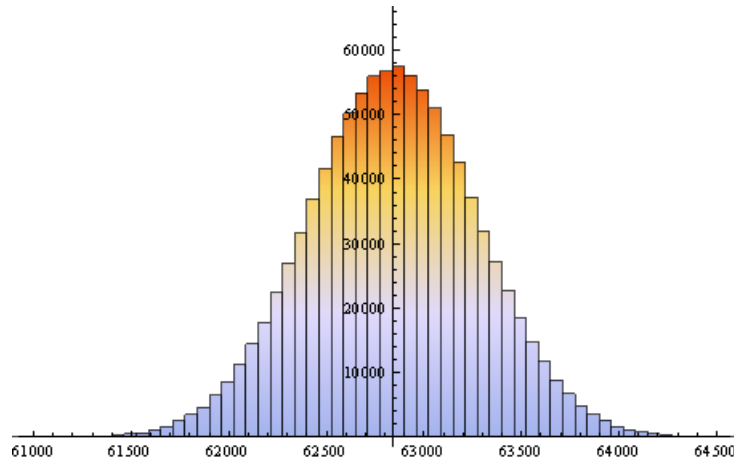


Figure 4.12: Distribution of the flowrate of one million pumps by Taguchi design

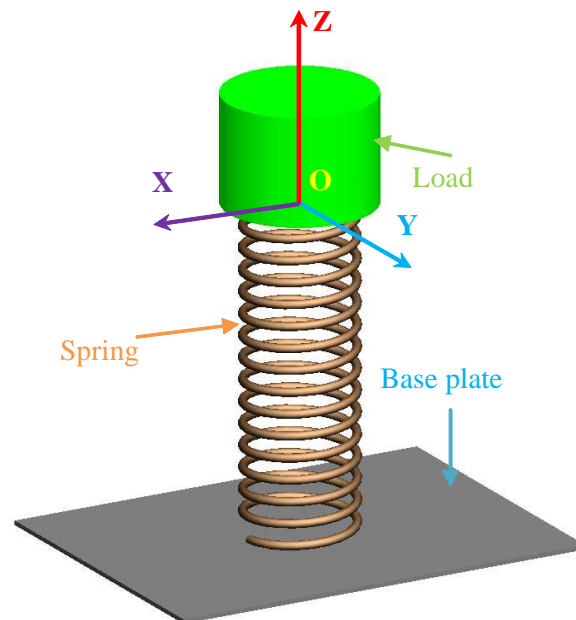


Figure 4.13: The parts of the spring system

4.2.2.1 Mathematical analysis approach

From the expert knowledge as presented above, the relationship between the frequency of the spring system and its geometrical deviations is expressed by equation 4.37.

$$f = \frac{1}{4\pi\sqrt{2}} \sqrt{\frac{G(d + \delta)^4}{n\rho(D + \Delta)^3 [-2h\pi R^2 + h\pi(dr + R)^2 + \pi R^2(h + Tz_1) + \pi R^2(h + Tz_3)]}} \quad (4.37)$$

Where:

Δ, δ – Dimensional deviation of the outer and wire diameter of the spring.

R, h – Radius and height of the cylinder of the load.

Tz_1, Tz_3 – Translational deviation of two planes of the load.

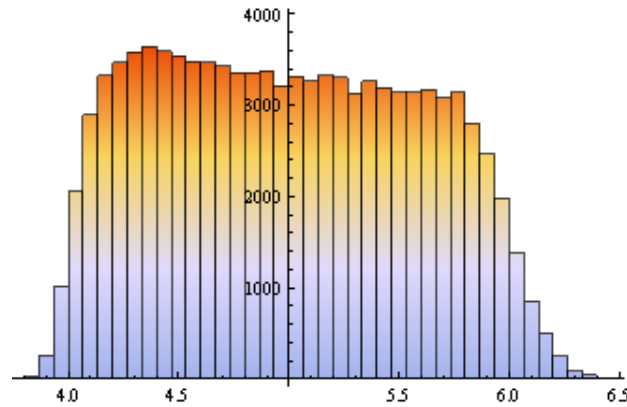


Figure 4.14: The distribution of frequency by mathematical analysis approach

The frequency of the system for 100000 products is calculated and the results are shown in figure 4.14. The results will be used for comparison with the 3 design of experiment methods and thus validation of these methods.

4.2.2.2 Factorial design

From expert knowledge, the geometrical deviations of the load and dimensional deviation of the spring are defined as factors that have the strongest influence on the frequency of the spring system. Thus, we can choose the following factors for the factorial design study:

- Tz_1, Tz_3 : translational deviation of the two planes of the load (P_1, P_3).
- Δ, δ : deviation of the spring outer and wire diameter.
- dr : deviation of the load cylinder radius.

The levels are calculated from the results of the Monte-Carlo simulation of the manufacturing stage. The number of levels is chosen as 2 and thus the number of

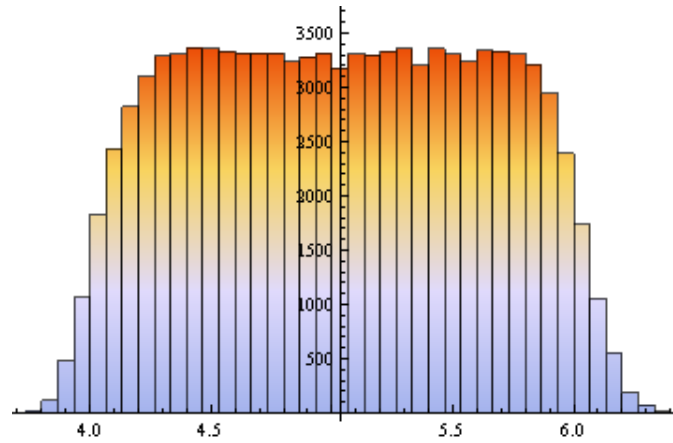


Figure 4.15: The distribution of frequency by factorial design

runs is 32. The low and high level are respectively selected at -3σ and $+3\sigma$ of the factor distribution. The relationship between the frequency and selected factors is established by using the linear regression model from the 32 runs results. This function is expressed by equation 4.38.

$$f = 4.82605 - 0.0560401Tz_1 - 0.16062dr - 0.0560471Tz_3 + 2.51307\delta - 0.152286\Delta \quad (4.38)$$

The population of the frequency is generated from the results of the simulation of the manufacturing stage. The distribution of the frequency is represented in figure 4.15.

4.2.2.3 Taguchi design

The selected factors include all the geometrical deviations parameters of the spring system. There are 15 parameters as follows:

- 6 parameters of the deviation torsor of two planes of the load.
- 4 parameters of the deviation torsor of the load's cylinder.
- 2 parameter of deviation of the spring's wire and outer diameter.
- 3 parameter of dimensional deviation of the base plate.

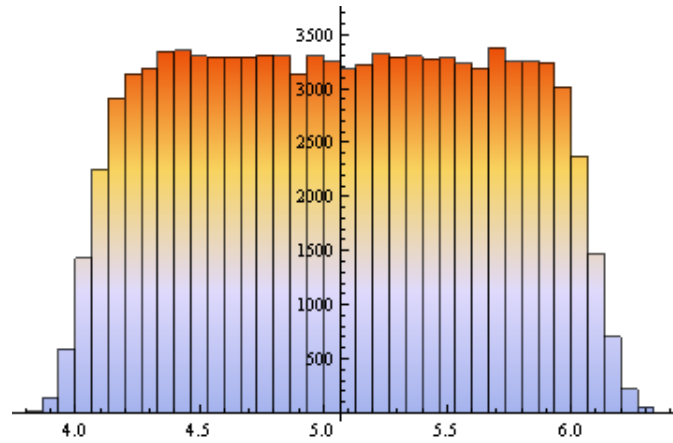


Figure 4.16: The distribution of frequency by Taguchi design

By using the table of Taguchi's orthogonal arrays with these 15 parameters and 2 levels, it is necessary to make 32 runs. The relationship between the frequency and selected factors is established by using linear regression model. This function is expressed by equation 4.39.

$$f = 4.91592 - 0.0387945Tz_1 - 0.201746dr - 0.0448108Tz_3 + 2.53885\delta - 0.1232\Delta \quad (4.39)$$

The population of the frequency is generated from the results of the simulation of the manufacturing stage. The distribution of the frequency is represented in figure 4.16.

4.2.2.4 Random design

This method is realized by the 4 steps as presented in section 4.1.2.5. 10 spring systems are randomly drawn from 10 thousands spring systems. The 10 frequencies are calculated by equation 4.37. Then the linear regression fit model is used to establish the relationship between the frequency and all parameters of geometrical deviations of the spring system. It is expressed by equation 4.40.

$$f = 4.82709 + 0.0226579Tz_1 - 0.184982dr - 0.117445Tz_3 + 2.61698\delta - 0.0989216\Delta \quad (4.40)$$

The population of the frequency is generated by the collected data in the Monte-

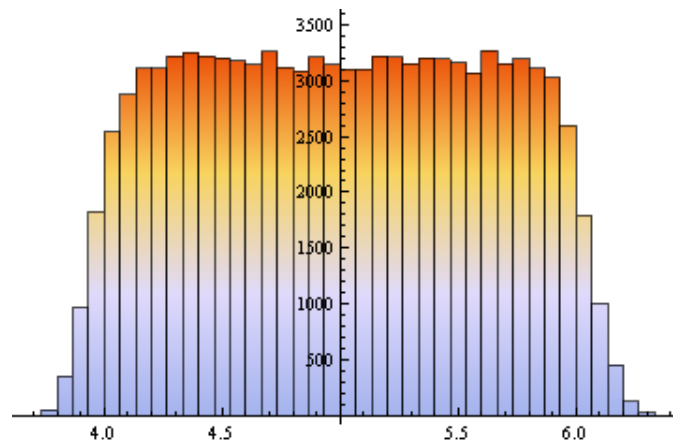


Figure 4.17: The distribution of frequency by random design

Carlo simulation stage. The distribution of the frequency is described in figure 4.17.

4.2.2.5 Comparison

In order to compare the proposed approaches in terms of accuracy, we calculate the error between the frequency of the three DOE methods and the mathematical analysis approach by equation 4.37. The distribution of the error for the three approaches (Factorial, Taguchi, Random design) is shown in figure 4.18. In the case of the spring system, the frequency is easily calculated by equation 4.34. Thus, the mathematical analysis approach can take into account all geometrical deviations of each part of the system. The accuracy of the approach, in this case, is obviously the most accurate in comparison with the DOE methods. The overview of the three proposed DOE approaches is shown in table 4.7. The relationship between the frequency and the geometrical deviation parameters of the spring system approximated by Factorial, Taguchi and Random design is given in equation 4.38, 4.39 and 4.40 respectively. However, the relationship can be established by using the linear regression model with the data of 100000 frequencies and parameters that

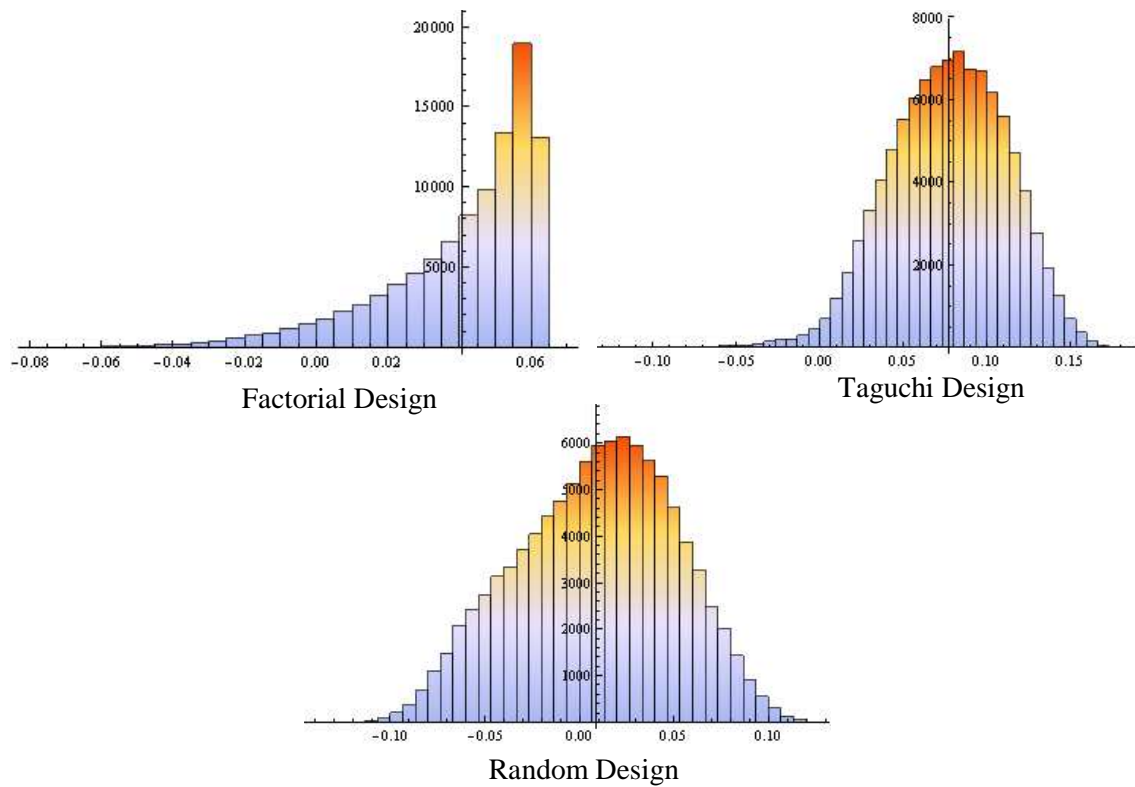


Figure 4.18: The distribution of frequency error

are generated in section 4.2.2.1. It is given in equation 4.41.

$$f = 4.79048 - 0.0547296Tz1 - 0.155346dr - 0.0545993Tz3 + 2.48972\delta - 0.149673\Delta \quad (4.41)$$

The coefficient of each geometrical deviations parameters are not too different for factorial, Taguchi and random design approach and real one, as given in table 4.6. However, it is necessary to realise 100000 runs to use the exact approach. In complex cases, the three DOE methods are obviously better than the real approach in terms of time and cost. Within the three DOE methods, the result from factorial design are more precise. However, for this approach, the number of experiments and the precision rely on expert knowledge.

In conclusion, the selection among the three methods to establish the relationship between the performance and the geometrical deviations of a product depends on the requirements concerning accuracy, time and cost. We can choose the factorial design when the expert knowledge is effective or the Taguchi method when the

Variables	Factorial design	Taguchi design	Random design	Exact model
Constant	4.82605	4.91592	4.82709	4.79048
Tz_1	-0.0560401	-0.0387945	0.0226579	-0.0547296
dr	-0.16062	-0.201746	-0.184982	-0.155346
Tz_3	-0.0560471	-0.0448108	-0.117445	-0.0545993
δ	2.51307	2.53885	2.61698	2.48972
Δ	-0.152286	-0.1232	-0.0989216	-0.149673

Table 4.6: Coefficient comparison among proposed approaches

number of factors is large. The random design is only chosen when it is difficult to determine the factors that have the strong influence on the performance of the product, or the number of the factors is considerably large.

	Factorial Design	Taguchi Design	Random Design	Exact Model
Mean of frequency	5.03582	5.0719	5.00409	4.99506
Standard deviation of frequency	0.594517	0.595919	0.614884	0.589002
Deviation parameters	5	All	All	All
Number of runs	32	32	10	100000

Table 4.7: Summary of the proposed approaches

4.3 Conclusion

In this chapter, we have proposed a method that allows to integrate geometrical deviations in product performance simulation and thus analyse the performance variation relative to the variation sources from the product life cycle. The relationship between the performance and the geometrical deviations of the product can be established by two approaches:

- The mathematical analysis approach establishes the relationship between the performance variation and geometrical parameters variation based on the mathematical model of the performance of the product.

- The design of experiment approaches establish the relationship between the performance and geometrical deviation parameters based on numerical simulation and regression model. This approach is used in the case of complex system where the mathematical relationship is not established or cannot take into account all geometrical deviations.

Chapter 5

INFLUENCE FACTOR ANALYSIS AND ROBUST DESIGN METHODOLOGY

THIS chapter proposes different approaches to determine the effect of the variation source parameters on the product performance. The aim is to minimize the variance of the product performance without eliminating the variation sources. In the first section, some approaches for identification and classification of the parameters are presented. Two approaches are presented in the second section to calculate the variance of the product performance relative to the variation sources parameters. Then a robust design solution can be found by finding design solution to minimize the variance of the product performance. In order to illustrate the proposed approaches, a case study is presented in the last section in this chapter.

5.1 Influence Factor Analysis

An image of the real performance of M products is given by using Monte-Carlo simulation as presented in chapter 4. The variation sources from product life cycle have an influence on the product performance. It is necessary to determine the effect of each parameter of the variation sources on the product performance. Thus,

we propose, in this section, two different approaches: mathematical approach and data mining approach, to classify their effect on the performance variability of the product.

5.1.1 Mathematical Approach

5.1.1.1 Global sensitivity analysis

The goal of sensitivity analysis is to determine how uncertainty in the output of a model depends upon the different sources of uncertainty in the model input [SRA⁺08]. In comparison with local sensitivity analysis which determines the variation of model output relative to input variables, global sensitivity analysis is able to identify the key parameters whose uncertainty most influences on the model output. Moreover, it can be used to classify the effect of the variables and determine unessential variables of the model input. Global sensitivity analysis has previously been applied for many purposes including design optimization [FDS09], design under uncertainty [WRA05], analysis of environmental issues [WCBA03], [FEB⁺03], food safety modelling [KTHZ07], thermal design [ND06].

Variance-based methods for sensitivity analysis were first employed by chemists in the early 1970s (Cukier et al. [CFS⁺73]). Cukier and colleagues not only proposed conditional variances for a sensitivity analysis based on first-order effects, but were already aware of the need to treat higher-order terms and of underlying variance decomposition theorems [CLS78]. Their method, known as FAST (Fourier Amplitude Sensitivity Test), although quite effective, enjoyed limiting success among practitioners, not least because of the difficulty in encoding it. The method did not allow the computation of higher-order indices, although this was much later made possible by extensions developed by other investigators (Saltelli et al. [STC99]). However, the FAST method is complicated to implement because of transforming multidimensional variable problems into frequency domain problems in contrast

with the Sobol's method, which can calculate the variances directly by integrating the multidimensional problems. Moreover, the model of geometrical deviations and the product performance function are complex in themselves. Thus, the global sensitivity indices proposed by Sobol [Sob90] will be used in this case due to the simple formulation and analysis procedure.

5.1.1.1.1 Sobol' global sensitivity indices Sobol's method [Sob90] is used to test the sensitivity indices of the input parameters $X = \{x_1, x_2, \dots, x_n\}$ relative to output function $f(X)$. Let's consider the integrable function $f(X)$ in the unit hypercube H^n ($0 \leq X \leq 1$) can be expanded in equation 5.1.

$$f(X) = f_0 + \sum_{i=1}^n f_i(x_i) + \sum_{i<j} f_{ij}(x_i, x_j) + \dots + f_{12..n}(x_1, x_2, \dots, x_n) \quad (5.1)$$

The total variance of the function $f(X)$ is calculated by equation 5.2.

$$V = \sum_{u=1}^n \sum_{i_1 < \dots < i_u} V_{i_1..i_u} \quad (5.2)$$

Where $V_{i_1..i_u} = \int_0^1 f_{i_1..i_u}^2(x_1, x_2, \dots, x_{i_u}) dx_1, \dots, x_{i_u}$ is called partial variances. It measures the joint effect of a set of input parameters $(x_1, x_2, \dots, x_{i_u})$ on the output function $f(X)$.

A global sensitivity index is defined as a partial variance contributed by an effect on the total variance V . It is expressed by equation 5.3.

$$S_{i_1..i_u} = \frac{V_{i_1..i_u}}{V} \quad (5.3)$$

Obviously,

$$S_{i_1..i_u} \geq 0; \sum_{u=1}^n \sum_{i_1 < \dots < i_u} S_{i_1..i_u} = 1 \quad (5.4)$$

For one-dimensional index $S_i = \frac{V_i}{V}$ shows the effect of the single factor x_i on the output $f(x)$. In order to estimate the total influence of the factor, it is necessary to determine the total partial variance. The input variables $X = \{x_1, x_2, \dots, x_n\}$ can consider two complementary subsets of variables Y and Z , as shown in equation 5.5.

$$X = (Y, Z) \quad (5.5)$$

Where $Y = \{x_{i_1}, \dots, x_{i_m}\}$, $1 \leq i_1 \leq \dots \leq i_m \leq n$, $Z = \{x_{i_1}, \dots, x_{i_m}\}$

The variance corresponding to a set y is defined by equation 5.6.

$$V_Y = \sum_{u=1}^n \sum_{(i_1 < \dots < i_u) \in K} V_{i_1 \dots i_u} \quad (5.6)$$

To quantify the total influence of each individual variable induced by both its main effect and interactions with other variables, the total variance corresponding to a set y is defined by equation 5.7.

$$V_Y^{tot} = V - V_Z \quad (5.7)$$

Finally, the corresponding total sensitivity index is expressed in equation 5.8.

$$S_Y^{tot} = \frac{V_Y^{tot}}{V} \quad (5.8)$$

5.1.1.1.2 Classification of design factors In order to apply the Sobol method for identification of the effect of design factors (geometrical deviation parameters) on the product performance, the function f representing the relationship between the performance and the geometrical deviation parameters must satisfy the conditions of the function defined section 5.1.1.1.1. Thus, it is necessary to transform all geometrical deviation parameters $\hat{P} = \{\hat{p}_j\}_{j=1..n}$ into the normed factors

$\{0 \leq \hat{p}_j \leq 1\}_{j=1..n}$. The performance function can then be expressed by equation 5.9.

$$f^N(\hat{P}) = f_0^N + \sum_{i=1}^n f_i^N(\hat{p}_i) + \sum_{i<j} f_{ij}^N(\hat{p}_i, \hat{p}_j) + \dots + f_{12..n}^N(\hat{p}_1, \hat{p}_2, \dots, \hat{p}_n) \quad (5.9)$$

According to the definition presented in paragraph 5.1.1.1.1, the main effect of each design parameter \hat{p}_i on the performance of the product are described by the global sensitivity index S_i . The total effect of the design parameter \hat{p}_i including the main effect and interaction with other parameters $\{\hat{p}_j\}_{j \neq i}$ is described by the total sensitivity indices S_i^{tot} . These sensitivity indices are calculated by equation 5.3 and 5.8. From the result of the global sensitivity analysis, the effect of design parameters $\hat{P} = \{\hat{p}_j\}_{j=1..n}$ on the performance of the product is given by the value of the global sensitivity indices. As a result, we can classify the design parameters according to their effect on the performance of the product.

5.1.2 Data Mining Approach

5.1.2.1 Covariance and correlation

The relationship between the performance of the product and the parameters of the manufacturing and assembly processes are established by the method presented in chapter 4. The function describing this relationship is not explicit and complex. Thus, it is not simple to use the global sensitivity analysis method for measuring and classifying the effect of parameters of the manufacturing and assembly processes on the product performance. We propose, in this section, to use multivariate analysis of covariance (MANCOVA) method presented by Raykov et al. [RM08] in order to identify the influence parameters on the product performance. This method allows to determine covariance and correlation between the performance of product $Y = \{Y_i\}$ and each parameter of the manufacturing and assembly processes $X = \{X_{ij}\}$. From the analysis result, we can use Pareto chart to represent

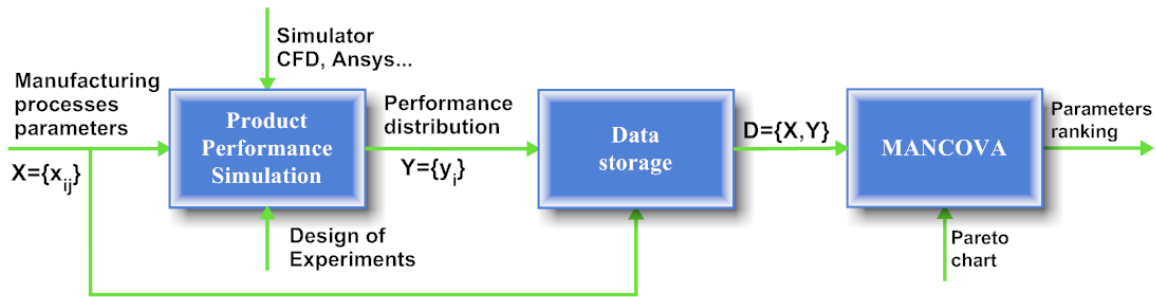


Figure 5.1: The overview of the covariance and correlation approach

the classification of the effect of the parameters. The overview of this method is shown in figure 5.1.

5.1.2.1.1 Covariance Covariance is a measure of dependency between random variables [WL07]. Covariance between two random variables X , Y is defined by equation 5.10.

$$\sigma_{XY} = Cov(X, Y) = E(XY) - E(X)E(Y) \quad (5.10)$$

Where $E(XY)$, $E(X)$ and $E(Y)$ are the expected value of XY , X and Y respectively. If the variable X is n -dimensional multivariate $X = \{X_1, X_2, \dots, X_n\}$, then covariances among all the components of X are matrix form, called covariance matrix, as shown in equation 5.11.

$$\Sigma = \begin{bmatrix} \sigma_{X_1X_1} & \cdots & \sigma_{X_1X_n} \\ \vdots & \ddots & \vdots \\ \sigma_{X_nX_1} & \cdots & \sigma_{X_nX_n} \end{bmatrix} \quad (5.11)$$

In general, the important property of covariance can be summarised as follows:

- If the value of covariance is high, the relationship between two variables X , Y is strong.
- If the covariance is zero, the relationship between two variables X , Y is non-linear or independent.
- If the value of covariance is negative, two variables X , Y vary inversely.

5.1.2.1.2 Correlation The correlation between two random variables X and Y is defined by equation 5.12.

$$\rho_{XY} = \frac{Cov(X, Y)}{\sigma_X \cdot \sigma_Y} \quad (5.12)$$

Where σ_X and σ_Y are standard deviation of the variables X and Y . In general, the important property of covariance is able to be summarised as follows:

- The value of correlation varies between -1 and +1.
- The sign of correlation indicates the direction of the relationship.
- The absolute value of correlation indicates the strength of the linear relationship between two variables. If the correlation is zero, there is no linear relationship between two variables.

The advantage of the correlation is that it is independent of the scale, i.e. changing the variables' scale of measurement does not change the value of the correlation. After determining the covariance and correlation between the performance of the product and the parameters of the manufacturing and assembly processes, we use the Pareto chart to classify the effect of parameters on the performance. Then we can compare the analysis result from the covariance and correlation. The purpose of the Pareto chart is to highlight the most influential in a set of factors.

5.1.2.2 Influence index approach

There are many variation sources that affect the performance of the product during its life cycle such as material properties, manufacturing operations, practical environment, etc. From the result of the performance simulation of the product based on the Monte-Carlo simulation method, we propose, in this chapter, a new method that allows to identify and classify the key variation sources parameters within the set of manufacturing defect parameters. This method is presented in figure 5.2.

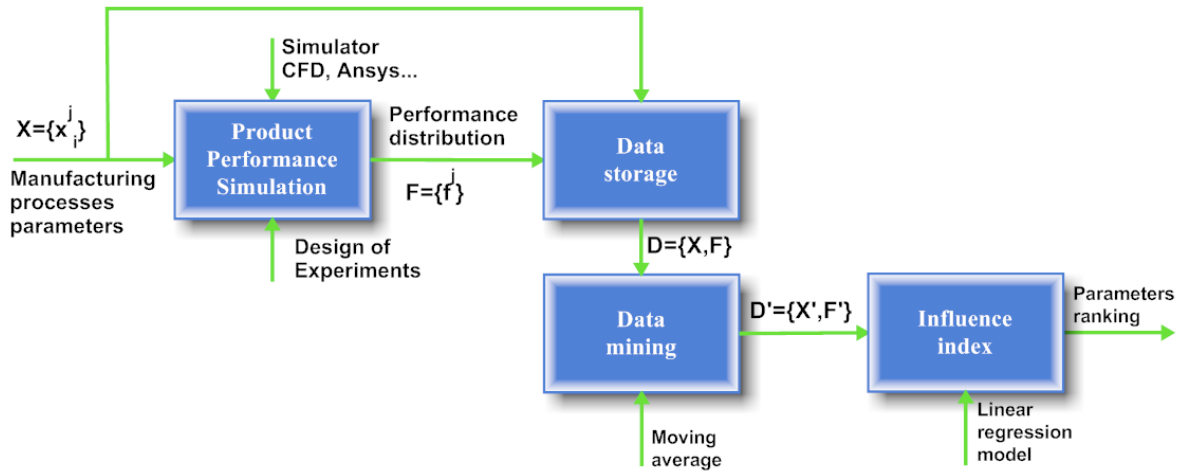


Figure 5.2: The overview of the influence index approach

The collected data consist in a set of defect parameters from manufacturing processes and the corresponding performance of the product obtain by the explained performance simulation method. The data can be described by the matrix $D = \{X, F\}$. Where $X = \{x_i^j\}_{i=1..n, j=1..M}$ is a data matrix, representing n values of manufacturing processes parameters for M products. $F = \{f^j\}_{j=1..M}$ is a data vector, representing the performance of the M products. The aim of this method is to evaluate the percentages of influence of each parameter X on the product performance F .

5.1.2.2.1 Data processing The function describing the relationship between the product performance and the manufacturing process parameters $X = \{x_i\}_{i=1..n}$ can be expressed by equation 5.13.

$$f(X) = g_i(x_i) + h_i(x_1, x_2, \dots, x_{i-1}, x_{i+1}, \dots, x_n) + q_i(x_i, x_j) \quad (5.13)$$

Where $g_i(x_i)$ is a function representing the trend and pattern of the relationship between product performance and the parameter x_i . $h_i(x_1, x_2, \dots, x_{i-1}, x_{i+1}, \dots, x_n)$ is a set of function representing the trend and pattern of the relationship between product performance and the manufacturing parameters $(x_1, x_2, \dots, x_{i-1}, x_{i+1}, \dots, x_n)$. $q_i(x_i, x_j)$ is a set of function representing interaction between the parameter x_i and

the rest of manufacturing parameters. As far as parameters $X = \{x_i\}_{i=1..n}$ have been created as independent variables, the function $h_i(x_1, x_2, \dots, x_{i-1}, x_{i+1}, \dots, x_n)$ and $q_i(x_i, x_j)$ can be considered as measurement noises that influence on the relationship between the product performance and the parameter x_i when studying the function. Thus, it is necessary to filter these noises.

Subsequently, data smoothing techniques, such as curve fitting, moving average, etc., is used to filter the data in order to evaluate the influence of each parameter x_i of the manufacturing processes on the performance of the product. We propose, in this case, to use the moving average method to filter the data. Moving average, a data smoothing method, aims at reducing noise and extracting the trends and patterns of the data set. The procedure to filter the data set D is described by two following steps:

- Sort data $D = \{x_i^j, f^j\}_{j=1..M}$ according to increasing value of x_i .

The data D_i include M instances of parameter x_i and M instances of product performance F .

- Filter data by moving average method.

The data $\hat{D}_i = \{\hat{x}_i^j, \hat{f}^j\}_{j=1..M-p}$ is a filtered data set of data D_i by moving average technique. The data \hat{D}_i is described by equation 5.14.

$$\begin{cases} \hat{x}_k = \frac{1}{p} \sum_{j=k}^{p+k} x_i^j \\ \hat{f}_k = \frac{1}{p} \sum_{j=k}^{p+k} f_i^j \end{cases} \quad (5.14)$$

Where p is a constant greater than zero defining the number of consecutive points to average. Higher values cause greater smoothing. The aim of this stage is to reduce the noises as presented above.

5.1.2.2.2 Definition of influence index The filtered data is then used to estimate the contribution of each parameter x_i to the variation of the product per-

formance based on the linear or second order regression model as presented in section 4.1.2. From the smoothed data, we can determine the relationship between the variation of the product performance and each parameter x_i of the manufacturing processes. In case of linear regression model, the coefficients $\frac{\partial f}{\partial x_i}$ in equation 2.25 and 2.26 can be estimated by the proposed analysis methods. It is, therefore, possible to implement a robust design technique for minimization of the variance of the performance of the product.

Another interesting indicator that can be subsequently calculated is the percentage $\Delta_i(\%)$ of the contribution of each parameter x_i to the variation of the product performance. In this case, linear or non-linear regression model is used to estimate the function $g_i(x)$ between each parameter x_i of the manufacturing processes and the product performance F based on the smoothed data $\hat{D}_i = \left\{ \hat{x}_i^j, \hat{f}^j \right\}_{j=1..M-p}$. The percentage $\Delta_i(\%)$ of influence of the parameter x_i is then defined by equation 5.15.

$$\Delta_i = \frac{\Delta g_i(x)}{\Delta F} = \frac{\max \{g_i(x)\} - \min \{g_i(x)\}}{\max \{F\} - \min \{F\}} \quad (5.15)$$

$$x \in \text{variation range of } x_i$$

The percentage $\Delta_i(\%)$ indicates how much the parameters x_i of the manufacturing processes contribute to the variation of the product performance F .

5.1.3 Case Study

5.1.3.1 A centrifugal pump

5.1.3.1.1 Global sensitivity analysis From the result of performance analysis presented in chapter 4, the relationship between performance and design factors is established by two different approaches. For example, by using factorial design method, the function of the flowrate Q of the pump relative to the gap between the impeller and the casing of the pump (Gap) and the translation (Tx, Ty) of the

impeller relative to two perpendicular axes OX , OY is expressed by equation 5.16.

$$Q = f_0 + f_1(Gap) + f_2(Tx) + f_3(Ty) + f_{12}(Gap, Tx) + f_{13}(Gap, Ty) + f_{23}(Tx, Ty) \quad (5.16)$$

Each geometrical deviation parameter Gap , Tx and Ty vary in an interval that is not the hypercube interval $H^n(0 \leq X \leq 1)$. Thus it is necessary to normalise the parameters Gap , Tx and Ty into the interval $[0, 1]$ by equation 5.17.

$$\begin{cases} Gap_N = \frac{Gap - \min\{Gap\}}{\max\{Gap\} - \min\{Gap\}} \\ Tx_N = \frac{Tx - \min\{Tx\}}{\max\{Tx\} - \min\{Tx\}} \\ Ty_N = \frac{Ty - \min\{Ty\}}{\max\{Ty\} - \min\{Ty\}} \end{cases} \quad (5.17)$$

The function of the flowrate of the pump Q can be rewritten by equation 5.18.

$$\begin{aligned} Q = & 62717.6 - 769.26Gap_N - 271.47Gap_N^2 - 566.71Tx_N + 74.34Tx_N^2 + 514.85Ty_N \\ & + 206.37Ty_N^2 + 70.03Gap_NTx_N - 452.56Gap_N^2Tx_N + 73.89Gap_NTx_N^2 + 423.9Gap_N^2Tx_N^2 \\ & - 372.03Gap_NTy_N + 605.15Gap_N^2Ty_N + 82.09Gap_NTy_N^2 + 577.74Gap_N^2Ty_N^2 \\ & + 401.55Tx_NTy_N - 495.Tx_N^2Ty_N + 562.07Tx_NTy_N^2 - 122.04Tx_N^2Ty_N^2 \end{aligned} \quad (5.18)$$

The global sensitivity indices for each parameter Gap , Tx , Ty is then calculated by equation 5.19.

$$\begin{cases} S_{Gap} = \int_0^1 (769.26Gap_N - 271.47Gap_N^2) dGap_N \\ S_{Tx} = \int_0^1 (-566.71Tx_N + 74.34Tx_N^2) dTx_N \\ S_{Ty} = \int_0^1 (514.85Ty_N + 206.37Ty_N^2) dTy_N \end{cases} \quad (5.19)$$

The result of global sensitivity analysis is expressed in table 5.1.

The global sensitivity indices of each parameter are also shown in figure 5.3. The global sensitivity index of the Gap is obviously the greatest. Thus the gap between the impeller and the casing of the pump is clearly the most significant parameter

Parameters	Global sensitivity indices	Total sensitivity indices	Interaction	Global sensitivity indices
Gap	0.5247	0.5758	GapTx	0.0013
Tx	0.1444	0.1767	GapTy	0.0497
Ty	0.2487	0.3295	TxTy	0.0309

Table 5.1: The result of global sensitivity analysis

that strongly effects on the flowrate of the pump. The effect of two parameters Tx and Ty on the flowrate of the pump is equal in this case. The effect of interaction between the Gap and Ty on the flowrate is stronger than others according to global sensitivity index. It agrees with the study of Wong et al. [WCH07] because the variation of Ty will affect the relative position between the impeller and the tongue of the volute casing of the pump.

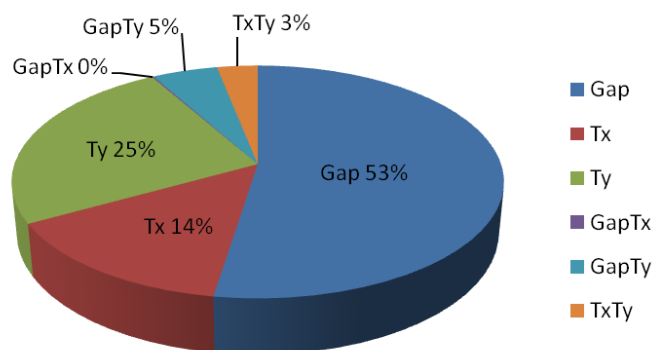


Figure 5.3: Global sensitivity indices of design parameters

5.1.3.1.2 Covariance and Correlation Analysis The relationship between the flowrate and the geometrical deviation parameters is established by two different approaches. For example, it is expressed by equation 4.32 according to the results of factorial design. The pump flowrate distribution is generated by using a Monte-Carlo method. The values of all parameters of the manufacturing and assembly processes and pump performance are collected and gathered in a matrix form table. Thus, we can calculate the covariance and correlation between the flowrate of the pump and each parameter of the manufacturing and assembly processes. A Pareto chart is, then, used to represent the importance of the parameters

of the manufacturing and assembly processes that linearly affect the flowrate of the pump. The result of analysis is shown in figure 5.4.

No.	Covariance Classification	Covariance value	Correlation Classification	Correlation value
1	$ty_{1,4S1}$	-0.360	$ty_{1,4S1}$	-0.137
2	$ty_{1,4}$	0.355	$ty_{1,4}$	0.135
3	$ty_{1,7}$	0.331	$ty_{1,7}$	0.126
4	$tx_{1,4S1}$	0.233	$tx_{1,4S1}$	0.088
5	$tz_{8,4}$	-0.215	$tz_{8,4}$	-0.082
6	$tz_{3,7}$	0.208	$tz_{3,7}$	0.079
7	$tx_{1,4}$	-0.205	$tx_{1,4}$	-0.079
8	$tz_{8,1}$	0.201	$tz_{8,1}$	0.077
9	$tz_{9,1}$	0.200	$tz_{9,1}$	0.076
10	$tz_{4,7}$	-0.197	$tz_{4,7}$	-0.075
...

Table 5.2: The classification of parameters

The order of the parameters of the manufacturing and assembly processes is classified by increasing value of covariance and correlation between the flowrate and these parameters. The classification of parameters by increasing correlation value is used to classify the linear influence of the parameters of the manufacturing and assembly processes on the performance of the pump, as shown in table 5.2. The covariance value is, however, used to study simultaneous variations between performance and each parameter from their respective averages.

From the analysis result, the arrangement of the parameters' effects on the performance of the pump is created. The designer, manufacturer and assembler can know what parameters have high influence on the performance. For example, set of parameters $ty_{1,4S1}$, $ty_{1,4}$, $ty_{1,7}$, $tx_{1,4S1}$, $tz_{8,4}$, $tz_{3,7}$, $tx_{1,4}$, $tz_{8,1}$, $tz_{9,1}$ and $tz_{4,7}$ are the first ten parameters of the manufacturing process that have the greatest influence on the performance of the pump.

5.1.3.1.3 Influence Index Analysis The set of values of manufacturing process values and pump flowrate are saved at the end of the performance simulation

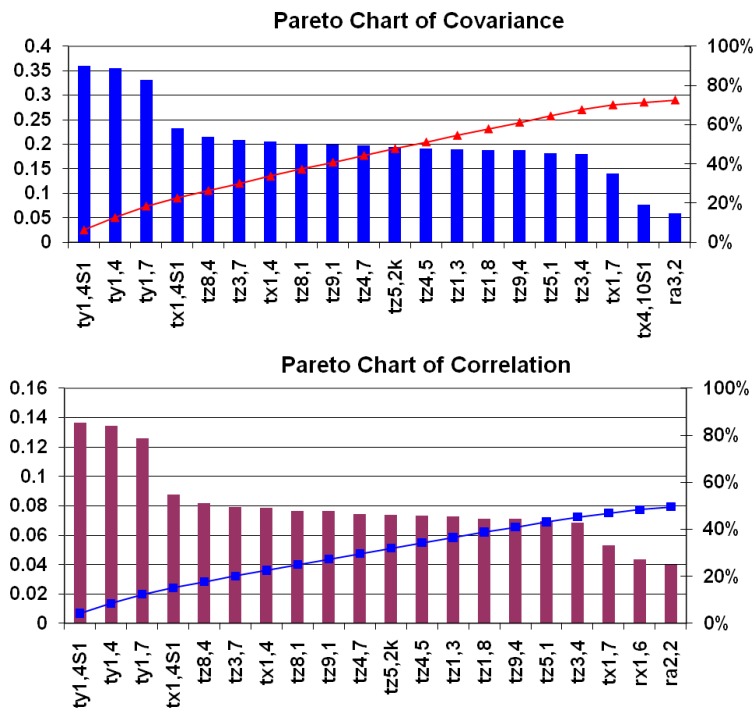


Figure 5.4: Pareto charts of covariance and correlation

stage. In order to identify the influence of each parameter of the manufacturing process on the flowrate of the pump, we use moving average data smoothing technique to reduce the random noise generated by the variation of the other manufacturing parameters. The filtered data are then fitted with a linear function as presented in figure 5.5 or non-linear function.

The influence index coefficient for each parameter is determined by equation 5.15. For example, the influence index of the parameter $rx_{1,9}$ as shown in figure 5.5 is calculated by equation 5.20.

$$\Delta_{rx_{1,9}} = \frac{y_{max} - y_{min}}{F_{max} - F_{min}} \quad (5.20)$$

Similarly, influence index of the other parameters is calculated. The result is shown in figure 5.6. We can see that the manufacturing process parameters, such as $ty_{1,4S1}$, $ty_{1,4}$, $ty_{1,7}$ and $tx_{1,4S1}$ from part 1 (revolute casing back) manufacturing are important contributors to flowrate variation of the pump.

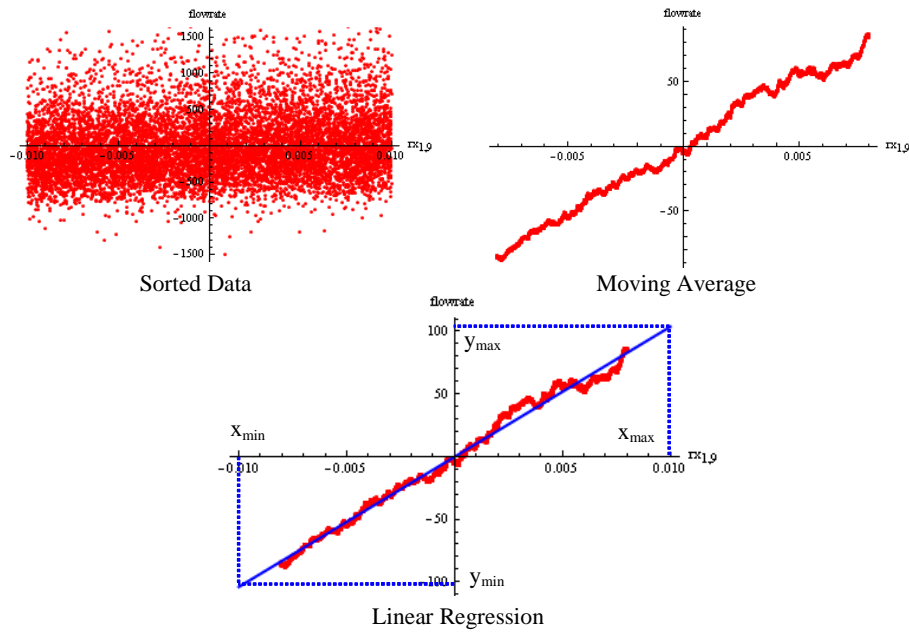


Figure 5.5: Data filtered by moving average technique

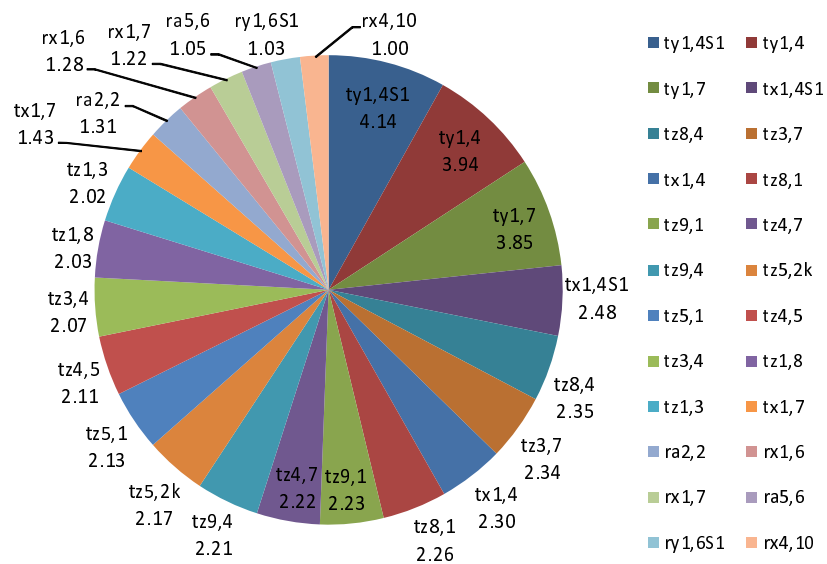


Figure 5.6: Influence index of manufacturing parameters

5.1.3.1.4 Conclusion From the result of global sensitivity analysis, covariance and correlation analysis and influence index, the design factors and the parameters of the manufacturing and assembly processes are classified according to their effects on the performance of the pump, as shown in table 5.3.

No.	Covariance approach	Correlation approach	Influence index approach	Global sensitivity
1	$ty_{1,4S1}$	$ty_{1,4S1}$	$ty_{1,4S1}$	Gap
2	$ty_{1,4}$	$ty_{1,4}$	$ty_{1,4}$	Ty
3	$ty_{1,7}$	$ty_{1,7}$	$ty_{1,7}$	Tx
4	$tx_{1,4S1}$	$tx_{1,4S1}$	$tx_{1,4S1}$	GapTy
5	$tz_{8,4}$	$tz_{8,4}$	$tz_{8,4}$	TxTy
6	$tz_{3,7}$	$tz_{3,7}$	$tz_{3,7}$	GapTx
7	$tx_{1,4}$	$tx_{1,4}$	$tx_{1,4}$	
8	$tz_{8,1}$	$tz_{8,1}$	$tz_{8,1}$	
9	$tz_{9,1}$	$tz_{9,1}$	$tz_{9,1}$	
10	$tz_{4,7}$	$tz_{4,7}$	$tz_{4,7}$	
...	

Table 5.3: The classification of parameters

In this case, the gap between the impeller and the casing of the pump is the design factor that has the greatest effect on the flowrate of the pump. If the flowrate of the pump does not satisfy the client, the designer has to manage the variation of the gap first, and the variation of Ty later. By the other methods, manufacturer and assembler can verify the influence of the parameters of the manufacturing and assembly processes. For example, the parameter $ty_{1,4S1}$ is a parameter of the manufacturing process that has the greatest effect on the flowrate of the pump. This is the quality of the part-holder surface in the set-up $S1$ to manufacture the casing back of the pump. Thus the manufacturer needs to manage this parameter variation if the mass flowrate does not satisfy the client. The manufacturer can change parameters of the manufacturing process based on the classification of parameters, capabilities of production means and the cost. The analysis result only proposes factors of the product life cycle to modify in order to adjust the performance of the product. The aim is to satisfy the client and make the design robust and reliable.

5.2 Robust Design within Product Life Cycle

Robustness of the performance of a product is a key factor in product design under uncertainty and variation sources during its life cycle, including material properties, manufacturing operations and practical environment. Actually, from designer's brain to users' hands, the product must overtake through many stages of its life cycle. The variability generated in each stage, as geometrical deviations, obviously have an influence on the performances of the product. It can make the designed product not to meet fully the requirements of the customers and the users. Moreover, it is difficult to determine the relationship between the performance variation and the variation of design variables, because the current modelling technology is not sufficient for taking the uncertainty and variation sources into account in the performance simulation. However, the method to integrate the geometrical deviations into performance simulation as presented in chapter 4 permits to overcome the limitation and approximate the real performance of the product taking into account the uncertainty and variation sources during its life cycle.

5.2.1 Mathematical approach

According to the definition of Chen et al. [CATM96], the fundamental principle in robust design is to improve the quality of a product by minimizing the effects of variation without eliminating its causes. In other words, the aim is to minimize the variations product performance caused by variation sources from product life cycle. Robust design methods as presented in section 2.3 only work for a model with established mathematical expression of the product performance. Thus it is necessary to know mathematical expression of the relationship between the performance and the parameters of the variation sources. The proposed methods as presented in chapter 4 allow to establish the relationship between the performance

variation and geometrical deviations of the product generated during its life cycle. It is expressed by equation 5.21.

$$\Delta Pr_i = f_i(\Delta \hat{p}_1, \Delta \hat{p}_2, \dots, \Delta \hat{p}_m) \quad (5.21)$$

Where $\{\hat{p}_i\}_{i=1..m}$ are geometrical parameters. The variance of the performance variation is calculated by equation 5.22.

$$Var(\Delta Pr_i) = E \{ [\Delta Pr_i - E(\Delta Pr_i)]^2 \} \quad (5.22)$$

According to Taylor series expansion principles, the variance of the performance variation can be rewritten by equation 5.23.

$$\begin{aligned} Var(\Delta Pr_i) = E \left\{ \left[\sum_{j=1}^m \frac{\partial F_i}{\partial \hat{p}_j} \Big|_{(\hat{\mu}_1, \dots, \hat{\mu}_m)} \cdot \Delta \hat{p}_j + \sum_{j=1}^m \sum_{k=1}^m \frac{\partial^2 F_i}{\partial \hat{p}_j \partial \hat{p}_k} \Big|_{(\hat{\mu}_1, \dots, \hat{\mu}_m)} \cdot \Delta \hat{p}_j \cdot \Delta \hat{p}_k \right. \right. \\ \left. \left. - E \left(\sum_{j=1}^m \frac{\partial F_i}{\partial \hat{p}_j} \Big|_{(\hat{\mu}_1, \dots, \hat{\mu}_m)} \cdot \Delta \hat{p}_j + \sum_{j=1}^m \sum_{k=1}^m \frac{\partial^2 F_i}{\partial \hat{p}_j \partial \hat{p}_k} \Big|_{(\hat{\mu}_1, \dots, \hat{\mu}_m)} \cdot \Delta \hat{p}_j \cdot \Delta \hat{p}_k \right) \right]^2 \right\} \end{aligned} \quad (5.23)$$

Then

$$\begin{aligned} Var(\Delta Pr_i) = \left(\sum_{j=1}^m \frac{\partial F_i}{\partial \hat{p}_j} \Big|_{(\hat{\mu}_1, \dots, \hat{\mu}_m)} \cdot \Delta \hat{p}_j \right)^2 E \{ [\Delta \hat{p}_j - E(\Delta \hat{p}_j)]^2 \} \\ + \left(\sum_{j=1}^m \sum_{k=1}^m \frac{\partial^2 F_i}{\partial \hat{p}_j \partial \hat{p}_k} \Big|_{(\hat{\mu}_1, \dots, \hat{\mu}_m)} \right)^2 E \{ [\Delta \hat{p}_j \cdot \Delta \hat{p}_k - E(\Delta \hat{p}_j \cdot \Delta \hat{p}_k)]^2 \} \end{aligned} \quad (5.24)$$

$$\sigma_{\Delta Pr_i}^2 = \sum_{j=1}^m \left(\frac{\partial F_i}{\partial \hat{p}_j} \Big|_{(\hat{\mu}_1, \dots, \hat{\mu}_m)} \right)^2 \cdot \sigma_{\Delta \hat{p}_j}^2 + \left(\sum_{j=1}^m \sum_{k=1}^m \frac{\partial^2 F_i}{\partial \hat{p}_j \partial \hat{p}_k} \Big|_{(\hat{\mu}_1, \dots, \hat{\mu}_m)} \right)^2 \sigma_{\Delta \hat{p}_j \cdot \Delta \hat{p}_k (i, j=1..m)}^2 \quad (5.25)$$

In order to obtain the robust solution, it is necessary to solve the problem, described by procedure 5.26.

$$\begin{aligned} \text{Minimize : } \sigma_{\Delta Pr_i}^2 \\ \text{Subject to : } a_j \leq \hat{p}_j \leq b_j; E(Pr_i) = P_i^N \end{aligned} \quad (5.26)$$

Where $E(Pr_i) = P_i^N$ is the expected performance (nominal performance) of the

product.

5.2.2 Data Mining Approach

The function describing the relationship between the performance of the product Pr_k and the parameters of variation sources $\Delta X = \{\Delta x_i\}_{i=1..n}$ can be expressed by equation 5.27.

$$Pr_k = f_k(\Delta X) = g_{ik}(\Delta x_i) + h_{ik}(\Delta x_j) + q_{ik}(\Delta x_i, \Delta x_j) \quad (j \neq i) \quad (5.27)$$

According to Taylor series expansion principles, the variance of the performance variation at first-order can be rewritten by equation 5.28.

$$\sigma_{\Delta Pr_k}^2 = \sum_{i=1}^n \left(\frac{\partial f_k}{\partial \Delta x_i} \Big|_{(\mu_{\Delta x_1}, \mu_{\Delta x_2}, \dots, \mu_{\Delta x_n})} \right)^2 \sigma_{\Delta x_i}^2 \quad (5.28)$$

Then

$$\sigma_{\Delta Pr_k}^2 = \sum_{i=1}^n \left(\frac{\partial g_{ik}(\Delta x_i)}{\partial \Delta x_i} \Big|_{(\mu_{\Delta x_1}, \mu_{\Delta x_2}, \dots, \mu_{\Delta x_n})} + \frac{\partial q_{ik}(\Delta x_i, \Delta x_j)}{\partial \Delta x_i} \Big|_{(\mu_{\Delta x_1}, \mu_{\Delta x_2}, \dots, \mu_{\Delta x_n})} \right)^2 \sigma_{\Delta x_i}^2 \quad (5.29)$$

If the variables $X = \{x_i\}_{i=1..n}$ are independent, the variance of the performance variation can be simplified by equation 5.30.

$$\sigma_{\Delta Pr_k}^2 = \sum_{i=1}^n \left(\frac{\partial g_{ik}(\Delta x_i)}{\partial \Delta x_i} \Big|_{(\mu_{\Delta x_1}, \mu_{\Delta x_2}, \dots, \mu_{\Delta x_n})} \right)^2 \sigma_{\Delta x_i}^2 = \sum_{i=1}^n C_i^2 \sigma_{\Delta x_i}^2 \quad (5.30)$$

Where $C_i = \frac{\partial g_{ik}(\Delta x_i)}{\partial \Delta x_i} \Big|_{(\mu_{\Delta x_1}, \mu_{\Delta x_2}, \dots, \mu_{\Delta x_n})}$ is a coefficient representing the effect of each parameter Δx_i on the performance variation of the product.

As presented in section 5.1.2.2.1, the function $g_{ik}(\Delta x_i)$ is estimated from the results of product performance simulation by using moving average data smoothing methods and linear or non linear regression model. Thus, the coefficient C_i is easily

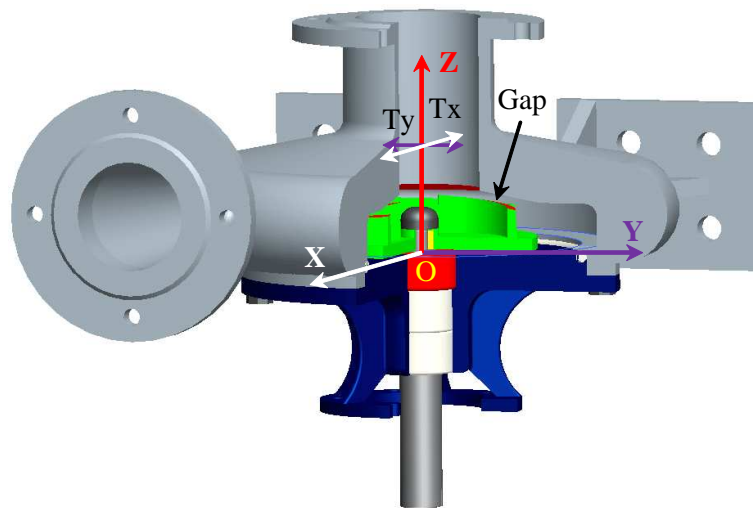


Figure 5.7: Pump flowrate and deviation parameters

determined by using equation 5.30. In order to determine the robust solution, it is necessary to minimize the variance of the performance variation, as described by procedure.

$$\text{Minimize : } \sigma_{\Delta Pr_k}^2$$

$$\text{Subject to : } a_i \leq x_i \leq b_i; E(Pr_k) = P_k^N$$

Where $E(Pr_k) = P_k^N$ is the expected performance (nominal performance) of the product.

5.2.3 A Case Study

5.2.3.1 A centrifugal pump

5.2.3.1.1 Mathematical approach The example of centrifugal pump as presented in chapter 3 and 4 is reused in this chapter in order illustrate this approach. The effect of variation source on pump flowrate variation is considered in this case. The relationship between the flowrate and the geometrical deviations parameters of the pump is established by one of the different approaches. According to factorial design approach as presented in section 4.2.1.1, the relationship between the

flowrate and the gap deviation and the translation deviations (T_x, T_y) (see figure 5.7) is expressed by equation 5.31.

$$\begin{aligned}
Q = & -7.97795 \times 10^6 + 1.13956 \times 10^6 \text{Gap} - 40373.3 \text{Gap}^2 - 9.47196 \times 10^7 \text{Tx} \\
& + 1.33071 \times 10^7 \text{GapTx} - 467397. \text{Gap}^2 \text{Tx} + 6.1493 \times 10^8 \text{Tx}^2 - 8.64763 \times 10^7 \text{GapTx}^2 \\
& + 3.04026 \times 10^6 \text{Gap}^2 \text{Tx}^2 + 1.72515 \times 10^8 \text{Ty} - 2.42049 \times 10^7 \text{GapTy} + 849043. \text{Gap}^2 \text{Ty} \\
& + 26307. \text{TxTy} - 225203. \text{Tx}^2 \text{Ty} + 1.547 \times 10^9 \text{Ty}^2 - 2.1753 \times 10^8 \text{GapTy}^2 \\
& + 7.64703 \times 10^6 \text{Gap}^2 \text{Ty}^2 + 347389. \text{TxTy}^2 - 523800. \text{Tx}^2 \text{Ty}^2 (g/s)
\end{aligned} \tag{5.31}$$

The variance of flowrate variation is calculated by using equation 5.32.

$$\begin{aligned}
\sigma_{Flowrate}^2 = & (1.13956 \times 10^6 - 80746.6 \mu_{\text{Gap}} + 1.33071 \times 10^7 \mu_{\text{Tx}} - 934794. \mu_{\text{Gap}} \mu_{\text{Tx}} \\
& - 8.64763 \times 10^7 \mu_{\text{Tx}}^2 + 6.08052 \times 10^6 \mu_{\text{Gap}} \mu_{\text{Tx}}^2 - 2.42049 \times 10^7 \mu_{\text{Ty}} + 1.69809 \times 10^6 \mu_{\text{Gap}} \mu_{\text{Ty}} \\
& - 2.1753 \times 10^8 \mu_{\text{Ty}}^2 + 1.52941 \times 10^7 \mu_{\text{Gap}} \mu_{\text{Ty}}^2)^2 \sigma_{\text{Gap}}^2 + (-9.47196 \times 10^7 + 1.33071 \times 10^7 \mu_{\text{Gap}} \\
& - 467397. \mu_{\text{Gap}}^2 + 1.22986 \times 10^9 \mu_{\text{Tx}} - 1.72953 \times 10^8 \mu_{\text{Gap}} \mu_{\text{Tx}} + 6.08052 \times 10^6 \mu_{\text{Gap}}^2 \mu_{\text{Tx}} \\
& + 26307. \mu_{\text{Ty}} - 450406. \mu_{\text{Tx}} \mu_{\text{Ty}} + 347389. \mu_{\text{Ty}}^2 - 1.0476 \times 10^6 \mu_{\text{Tx}} \mu_{\text{Ty}}^2)^2 \sigma_{\text{Tx}}^2 + (1.72515 \times 10^8 \\
& - 2.42049 \times 10^7 \mu_{\text{Gap}} + 849043. \mu_{\text{Gap}}^2 + 26307. \mu_{\text{Tx}} - 225203. \mu_{\text{Tx}}^2 + 3.09401 \times 10^9 \mu_{\text{Ty}} \\
& - 4.3506 \times 10^8 \mu_{\text{Gap}} \mu_{\text{Ty}} + 3.09401 \times 10^9 \mu_{\text{Ty}} - 4.3506 \times 10^8 \mu_{\text{Gap}} \mu_{\text{Ty}} + 1.52941 \times 10^7 \mu_{\text{Gap}}^2 \mu_{\text{Ty}} \\
& + 694778. \mu_{\text{Tx}} \mu_{\text{Ty}} - 1.0476 \times 10^6 \mu_{\text{Tx}}^2 \mu_{\text{Ty}})^2 \sigma_{\text{Ty}}^2 + (1.33071 \times 10^7 - 934794. \mu_{\text{Gap}} \\
& - 1.72953 \times 10^8 \mu_{\text{Tx}} + 1.2161 \times 10^7 \mu_{\text{Gap}} \mu_{\text{Tx}})^2 \sigma_{\text{GapTx}}^2 + (-2.42049 \times 10^7 \\
& + 1.69809 \times 10^6 \mu_{\text{Gap}} - 4.3506 \times 10^8 \mu_{\text{Ty}} + 3.05881 \times 10^7 \mu_{\text{Gap}} \mu_{\text{Ty}})^2 \sigma_{\text{GapTy}}^2 \\
& + (26307. - 450406. \mu_{\text{Tx}} + 694778. \mu_{\text{Ty}} - 2.0952 \times 10^6 \mu_{\text{Tx}} \mu_{\text{Ty}})^2 \sigma_{\text{TxTy}}^2 (g/s)
\end{aligned} \tag{5.32}$$

Where $\mu_{\text{Gap}}, \mu_{\text{Tx}}, \mu_{\text{Ty}}$ are respectively the nominal gap deviation between the impeller and the casing of the pump and the nominal translation deviation of the impeller relative to two perpendicular axes X, Y in the global coordinate systems of the pump. The robust optimization model of the flowrate of the pump is calcu-

lated as expressed in 5.33.

$$\begin{aligned}
 & \text{Minimize } \sigma_{Flowrate}^2 \\
 & \text{Subject to :} \\
 & E_{Flowrate} = \mu_{Flowrate} = 250(m^3/h) \simeq 69444g/s
 \end{aligned} \tag{5.33}$$

The solution is calculated by using a NMinimize function in Mathematica software and is given in 5.34.

$$\mu_{Gap} = 0.1659, \mu_{Tx} = 0.0770173, \mu_{Ty} = -0.0556371 \tag{5.34}$$

In conclusion, the designer should increase the nominal gap value to be $14.395mm$ and the nominal positioning of the impeller of the pump should be increased relative to the axis OX and decreased relative to the axis OY according to the global coordinate system $OXYZ$ of the pump.

5.2.3.1.2 Data mining approach In order to determine the variance of flowrate variation of the pump, it is necessary to calculate the coefficient C_i as in equation 5.30 by estimating the function $g_{ik}(x_i)$. This function is estimated by using moving average technique based on the result of flowrate simulation of the pump. The procedure to determine the function is presented in section 5.1.2.2 and 5.1.3.1.3. For example, the moving average is used to extract the trend of relationship between the flowrate and the parameter $tx_{1,4}$ of the manufacturing process is shown in figure 5.8 (see blue curve). Then the function representing this relationship can be determined by using linear or non linear regression model (see figure 5.8 in red and green colour respectively). It is expressed by equation 5.35.

$$\begin{aligned}
 g_1 &= 1.48948 - 251.287tx_{1,4} \\
 g_2 &= 6.437 - 258.298tx_{1,4} - 229682.tx_{1,4}^2
 \end{aligned} \tag{5.35}$$

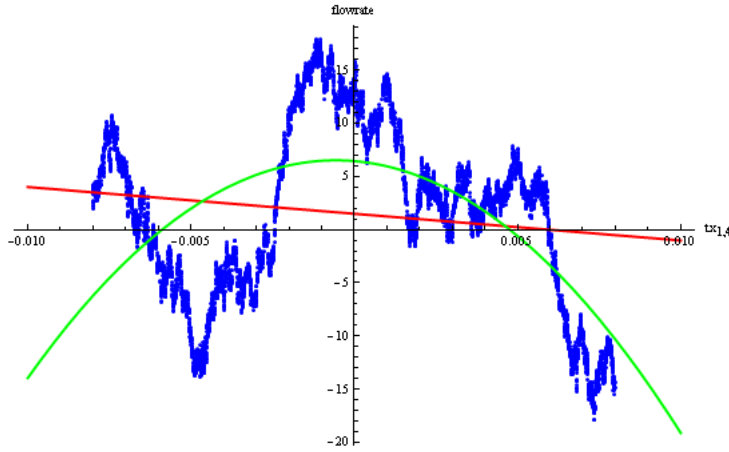


Figure 5.8: Linear and non linear regression

The coefficient C_i is easily calculated by equation 5.36 according to the function g_i .

$$\begin{aligned} C_1 &= 251.287 \\ C_2 &= -258.298 - 459365 \cdot \mu_{tx_{1,4}} \end{aligned} \quad (5.36)$$

Where $\mu_{tx_{1,4}}$ is the average value (nominal value) of the parameter $tx_{1,4}$ of the manufacturing process. Finally, the variance of the flowrate variation of the pump can be determined by a set of coefficients C_i relative to the manufacturing process parameters. For example, the variance of the pump flowrate relative to the ten first parameters of the manufacturing process is expressed by equation 5.37.

$$\begin{aligned} \sigma_{\Delta Flowrate}^2 &= (-1389.16 - 73275.3\mu_{rx_{1,2}})^2 \sigma_{rx_{1,2}}^2 + (-6030.19 + 293792 \cdot \mu_{rx_{1,3}})^2 \sigma_{rx_{1,3}}^2 \\ &+ (-3762.14 - 390749 \cdot \mu_{rx_{1,4}})^2 \sigma_{rx_{1,4}}^2 + (1013.89 + 28189.5\mu_{rx_{1,5}})^2 \sigma_{rx_{1,5}}^2 \\ &+ (10338.2 - 219712 \cdot \mu_{rx_{1,9}})^2 \sigma_{rx_{1,9}}^2 + (10046. - 856604 \cdot \mu_{rx_{1,10}})^2 \sigma_{rx_{1,10}}^2 \\ &+ (-5297.59 - 281869 \cdot \mu_{rx_{1,11}})^2 \sigma_{rx_{1,11}}^2 + (-811.732 + 272251 \cdot \mu_{rx_{1,12}})^2 \sigma_{rx_{1,12}}^2 \\ &+ (-186.959 + 511730 \cdot \mu_{rx_{1,11S1}})^2 \sigma_{rx_{1,11S1}}^2 + (5315.73 - 552909 \cdot \mu_{rx_{1,4S2}})^2 \sigma_{rx_{1,4S2}}^2 + \dots \end{aligned} \quad (5.37)$$

The robust design solution can be determined by minimizing the variance of the flowrate variation of the pump as in previous section.

5.3 Conclusion

In this chapter, we proposed two methods to give feedback to the product designers based on the result of the product performance simulation. The first one allows to identify and classify the effect of the parameters of the variation sources on the performance of the product during its life cycle. The determination is realized by two different approaches:

- **Mathematical approach:** The Sobol's indices, one of the global sensitivity analysis techniques, is used to determine the effect of the parameters on the product performance. The level of the effect of parameters is classified based on the value of the sensitivity indices. This approach is only used when the mathematical model describing the relationship between the product performance and the parameters is easily established.
- **Data mining approach:** The covariance-correlation analysis and influence factor are proposed to identify and classify the effect of the parameters on the product performance.

The second one allows to determine the variance of the product performance relative to the parameters of the variation sources and to find the robust solution. This method has two different approaches:

- **Mathematical approach:** When the mathematical model describing the relationship between the product performance and the parameters of the variation sources is easily established or available, the variance of the product performance variation relative to the parameters is calculated by Taylor expansion. Then the robust solution is found by minimizing the variance.
- **Data mining approach:** The variance of the product performance variation relative to the parameters of the variation sources is determined by using the moving average technique and linear or non linear regression model.

Chapter 6

CONCLUSION AND PERSPECTIVE

THE research work presented in this thesis contributes to develop a 3D Geometrical Deviation Model (GDM) for the product life cycle engineering. This GDM is based on the 3D Model of Manufactured Part (MMP) proposed by Villedeneuve and Vignat [VLL01, VV03, VV05b, Vig05] for modelling geometrical deviations (error stack-up) generated at manufacturing stage. The overview of the research work is given in figure 6.1. The geometrical deviation model includes the model of manufactured part for manufacturing stage and the model of assembled part (MAP) for assembly stage. It allows to model geometrical deviations generated during the manufacturing stage and to accumulate them on the final product at assembly stage. It is then used to integrate the geometrical deviations into the simulation of the product performance. An image of the real performance of the population of manufactured products is generated by using Monte-Carlo simulation method. The satisfaction of customer's requirements is then verified by comparison of the performance range with the customer requirements. The next step is to identify and classify the parameters of the variation sources according to their influence on the performance. Different approaches for influence factor analysis (IFA) are proposed. The results can then be used for the purpose of robust design, i.e. finding a design solution minimizing the effect of geometrical deviations on product performance.

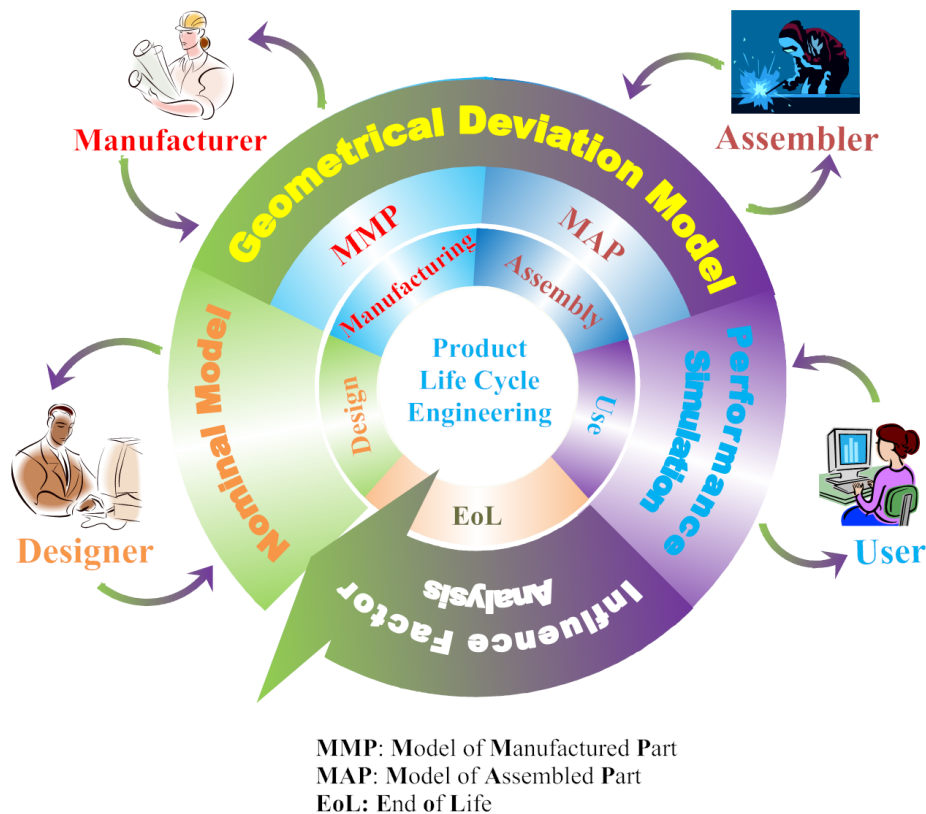


Figure 6.1: The overview of research works

The geometrical deviations of the product generated and accumulated during its life cycle are modelled by the GDM. This model allows to link the parameters of the manufacturing processes from the manufacturing stage to assembly stage. Thus, the first research question in the thesis is answered by this model.

- Manufacturing stage: The nominal model of the product created by designers must pass through the manufacturing stage where geometrical deviations are generated due to imperfection of materials, tools and machines. These deviations are modelled and collected by the model of manufactured part.
- Assembly stage: Each part making up the product is assembled during this stage. The deviations generated during manufacturing stage are accumulated on the subassembled part and then on the final product. The GDM is a total model of geometrical deviations generated during manufacturing stage and accumulated at assembly stage. Thus the GDM is able to take into ac-

count geometrical deviations of the surfaces of the parts and to link them with the parameters of the manufacturing process. Finally, the Monte-Carlo simulation method is used to produce an image of the manufactured products with geometrical deviations.

- Use stage: The deviations from the GDM are integrated in the simulation of the product performance. The relationship between the performance of the product and the parameters of variation sources is established by different approaches. The performance of the population of products from assembly stage is then calculated by using this relationship. An image of a population of the product performance is produced by using the Monte-Carlo simulation method. Finally, product designers can verify compliance of the performance of the designed product with the customers' requirements. As a result, the solution for second research issue in the thesis is found out.

The parameters of variation sources during the product life cycle obviously have an influence on the performance of the product. Thus two approaches proposed in chapter 5 allow to identify and classify their effect on the performance of the product. In addition, the variance of the performance variation of the product relative to the parameters of variation sources is constructed by mathematical and data mining approach. They are presented in detail in chapter 5. Then a robust design can be found by minimizing the variance of the performance variation. The research works presented in chapter 5 aim to give back useful information and results analysis to the actors of the product life cycle, such as product designer, producer and user (see figure 6.1).

MANY perspectives can be envisaged from the research works in the thesis. They are classified according to the following research axes:

- The geometrical deviation model developed in this thesis does not take into account the deformation. Thus a research axis is opened to integrate part deformations in product life cycle engineering and product performance simulation.
- In this thesis, the effect of geometrical deviations is only considered in the use stage to verify one performance of the product. However, there are many physical phenomena, such as thermal deformation, metal fatigue, metal wearing, etc. The second research axis should be to take the effect of the multi-physical phenomena into account in the simulation of the product multi-performances in the use stage.
- The Monte-Carlo simulation method is used to simulate the geometrical deviations of the part surfaces and later on the product performance. The input data including the variation range and distribution of defect parameters are supposed to be uniform and independent. The third research axis should consider to identifying the variation range and distribution of the defect parameters and establishing the correlation among them. Experimental measurements have been started by Tichadou and Kamli Nejad [TNVL07, TLH05] and currently continued by Bui-Minh et al [BMSVD10, SBMF⁺10].
- The relationship between the product performance and geometrical deviations parameters is established by the three approach as presented in the thesis. The deviated model of the product for the performance simulation is created in the CAD software by manual manipulation. In addition, the geometrical data of the product for building the GDM including dimensions, coordinate systems, etc., are also produced by hand. Therefore, the fourth research axis could be considered to develop an automatic interface in order

to collect useful data from CAD software and GDM and to generate automatically the deviated model of the product.

- Two different approach for determining the variance of the performance variation and implementing robust design are presented in this thesis. The algorithm for robust optimization is not mentioned in this thesis. Thus the fifth research axis could be developed to formulate the robust design problem, such as identification of the controllable and uncontrollable parameters of variation sources during the product life cycle. In addition, it is necessary to build the algorithm for robust multi-objective optimization in order to obtain a robust design solution taking into account multi-performance and multi-physical phenomena. The interval analysis method for finding out the robust domain has been done by Qureshi et al. [QDBB09, QDBB10a, QDBB10b]. This is a good idea to apply in this case for finding the robust domain considering multi-physical phenomena within the product life cycle.

Bibliography

- [AS64] ABRAMOWITZ, Milton ; STEGUN, Irene A.: *Handbook of Mathematical Functions with Formulas, Graphs, and Mathematical Tables*. ninth Dover printing, tenth GPO printing. New York : Dover, 1964
- [AWA05] AL-WIDYAN, Khalid ; ANGELES, Jorge: A Model-Based Formulation of Robust Design. In: *Journal of Mechanical Design* 127 (2005), Nr. 3, S. 388–396
- [BB95] BOURDET, Pierre ; BALLOT, Eric: Geometrical Behavior Laws for Computer Aided Tolerancing. In: *Proceedings of the 4th CIRP Seminar on Computer Aided Tolerancing, University of Tokyo, 1995*
- [BB97] BALLOT, Eric ; BOURDET, Pierre: Détermination mathématique des spécifications à partir d'un modèle formel de chaînes 3D de défauts. In: *Colloque national PRIMECA, 1997, S. 163–170*
- [BB98] BALLOT, E. ; BOURDET, P.: A computation method for the consequences of geometric errors in mechanisms. In: *5th CIRP Seminar on Computer-Aided Tolerancing, Toronto, Canada., 1998*
- [BB00] BALLOT, Eric ; BOURDET, Pierre: A mathematical model of geometric errors in the case of specification and 3D control of mechanical parts. In: *Advances in Mathematics for applied Sciences, Advanced Mathematical & Computational Tools in Metrology IV* Vol. 53 (2000), S. 11–20

BIBLIOGRAPHY

- [BKF00] BAUN, Daniel O. ; KÖSTNER, Lutz ; FLACK, Ronald D.: Effect of Relative Impeller-to-Volute Position on Hydraulic Efficiency and Static Radial Force Distribution in a Circular Volute Centrifugal Pump. In: *Journal of Fluids Engineering* Vol.122, No. 3 (2000), S. 598–605
- [BMLB96] BOURDET, P. ; MATHIEU, L. ; LARTIGUE, C. ; BALLU, A.: The concept of the small displacement tosor in metrology. In: *Advanced Mathematical Tools in Metrology II, Edited by World Scientific Publishing Company, Series Advances in Mathematics for Applied Sciences* Vol. 40 (1996), S. 110–122
- [BMSVD10] BUI-MINH, H. ; SERGENT, A. ; VILLENEUVE, F. ; DURET, D.: Assessment of the impact of calculation methodologies on defect determinations in manufacturing. In: *Proceedings of IDMMME - Virtual Concept, Bordeaux, France, 2010*
- [Bou87] BOURDET, Pierre: *Contribution à la mesure tridimensionnelle : Modèle d'identification des surfaces, Métrologie fonctionnelle des pièces mécaniques, Correction géométrique des machines à mesurer tridimensionnelle*, Nancy I - LURPA ENS CACHAN, Diss., 1987
- [BT01] BRISSAUD, D. ; TICHKIEWITCH, S.: Product Models for Life-Cycle. In: *CIRP Annals - Manufacturing Technology* Vol. 50, No. 1 (2001), S. 105–108
- [CATM96] CHEN, Wei ; ALLEN, J. K. ; TSUI, Kwok-Leung ; MISTREE, F.: A Procedure for Robust Design: Minimizing Variations Caused by Noise Factors and Control Factors. In: *Journal of Mechanical Design* 118 (1996), Nr. 4, S. 478–485
- [CBW05] CARO, Stephane ; BENNIS, Fouad ; WENGER, Philippe: Tolerance Synthesis of Mechanisms: A Robust Design Approach. In: *Journal of Mechanical Design* 127 (2005), Nr. 1, S. 86–94

BIBLIOGRAPHY

- [CFS⁺73] CUKIER, R. I. ; FORTUIN, C. M. ; SCHULER, K. E. ; PETSCHKEK, A. G. ; SCHAIBLY, J. H.: Study of the sensitivity of coupled reaction systems to uncertainties in rate coefficients. i theory. In: *The Journal of Chemical Physics* 59 (1973), S. 3873–3878
- [CHC03] CAMELIO, Jaime ; HU, S. J. ; CEGLAREK, Dariusz: Modeling Variation Propagation of Multi-Station Assembly Systems With Compliant Parts. In: *Journal of Mechanical Design* Vol. 125 (2003), S. 673–681
- [CLS78] CUKIER, R. ; LEVINE, H. ; SHULER, K.: Nonlinear sensitivity analysis of multiparameter model systems. In: *Journal of Computational Physics* 26 (1978), S. 1–42
- [CRT94] CLÉMENT, A. ; RIVIÈRE, A. ; TEMMERMAN, M.: *Cotation tridimensionnelle des systèmes mécaniques: théorie et pratique*. PYC Editions, 1994
- [CS95] CEGLAREK, Dariusz ; SHI, Jianjun: Dimensional Variation Reduction for Automotive Body Assembly. In: *Manufacturing Review* Vol. 8, No. 2 (1995), S. 139 – 154
- [DC00] DU, Xiaoping ; CHEN, Wei: Towards a Better Understanding of Modeling Feasibility Robustness in Engineering Design. In: *Journal of Mechanical Design* 122 (2000), Nr. 4, S. 385–394
- [DN03] DJURDJANOVIC, Dragan ; NI, Jun: Dimensional Errors of Fixtures, Locating and Measurement Datum Features in the Stream of Variation Modeling in Machining. In: *Journal of Manufacturing Science and Engineering* Vol. 125 (2003), S. 716–730
- [EG01] ENGIN, Tahsin ; GUR, Mesut: Performance Characteristics of a Centrifugal Pump Impeller With Running Tip Clearance Pumping Solid-Liquid Mixtures. In: *Journal of Fluids Engineering* 123 (2001), Nr. 3, S. 532–538

BIBLIOGRAPHY

- [FDS09] FESANGHARY, M. ; DAMANGIR, E. ; SOLEIMANI, I.: Design optimization of shell and tube heat exchangers using global sensitivity analysis and harmony search algorithm. In: *Applied Thermal Engineering* 29 (2009), Nr. 5-6, S. 1026–1031
- [FEB+03] FRANCO, A. ; ELORZA, F. J. ; BOURAOU, F. ; BIDOGLIO, G. ; GALBIATI, L.: Sensitivity analysis of distributed environmental simulation models: understanding the model behaviour in hydrological studies at the catchment scale. In: *Reliability Engineering & System Safety* 79 (2003), Nr. 2, S. 205 – 218. – ISSN 0951–8320
- [GDTA92] GIORDANO, M. ; DURET, D. ; TICHADOU, S. ; ARRIEUX, R.: Clearance Space in Volumic Dimensioning. In: *CIRP Annals - Manufacturing Technology* 41 (1992), Nr. 1, S. 565 – 568. – ISSN 0007–8506
- [GJ92] GEP, Box ; JONES, S: Designing products that are robust to the environment. In: *Total Quality Management* 3 (1992), S. 265–286
- [GLS04] GU, P. ; LU, B. ; SPIEWAK, S.: A New Approach for Robust Design of Mechanical Systems. In: *CIRP Annals - Manufacturing Technology* 53 (2004), Nr. 1, S. 129 – 133. – ISSN 0007–8506
- [GPS99] GIORDANO, M. ; PAIREL, E. ; SAMPER, S.: Mathematical representation of tolerance zones. In: v., Houten F. (Hrsg.) ; H., Kals (Hrsg.): *6th CIRP International Seminar on Computer-Aided Tolerancing*, Un Enschede, The Netherlands., 1999
- [GYX07] GHASEMPOOR, A. ; YANG, Y. ; XI, F.: A geometric method for three-dimensional modelling of surface finish in grinding. In: *IJMR* 2 (2007), Nr. 4, S. 389–402
- [HC02] HONG, Y. S. ; CHANG, T. C.: A comprehensive review of tolerancing research. In: *International Journal of Production Research* Vol. 40, No. 11 (2002), S. 2425–2459

BIBLIOGRAPHY

- [HLB⁺07] HUANG, Wenzhen ; LIN, Jijun ; BEZDECNY, Michelle ; KONG, Zhenyu ; CEGLAREK, Dariusz: Stream-of-Variation Modeling-Part I: A Generic Three-Dimensional Variation Model for Rigid-Body Assembly in Single Station Assembly Processes. In: *Journal of Manufacturing Science and Engineering* Vol. 129 (2007), S. 821–831
- [HLKC07] HUANG, Wenzhen ; LIN, Jijun ; KONG, Zhenyu ; CEGLAREK, Dariusz: Stream-of-Variation (SOVA) Modeling-Part II: A Generic 3D Variation Model for Rigid Body Assembly in Multistation Assembly Processes. In: *Journal of Manufacturing Science and Engineering* Vol. 129 (2007), S. 832–842
- [HN72] HOSHIDE, R. K. ; NIELSON, C. E.: Study of blade clearance effects on centrifugal pumps / Report of NASA center. 1972. – Forschungsbericht
- [HS04] HUANG, Qiang ; SHI, Jianjun: Stream of Variation Modeling and Analysis of Serial-Parallel Multistage Manufacturing Systems. In: *Journal of Manufacturing Science and Engineering* Vol. 126 (2004), S. 611–618
- [HSY03] HUANG, Qiang ; SHI, Jianjun ; YUAN, Jingxia: Part Dimensional Error and Its Propagation Modeling in Multi-Operational Machining Processes. In: *Journal of Manufacturing Science and Engineering* Vol. 125 (2003), S. 256–262
- [JS99] JIN, Jionghua ; SHI, Jianjun: State Space Modeling of Sheet Metal Assembly for Dimensional Control. In: *Journal of Manufacturing Science and Engineering* 121 (1999), Nr. 4, S. 756–762
- [Kac85] KACKAR, R. N.: Off-line quality control, parameter design, and the Taguchi method. In: *Journal of Quality Technology* 17 (1985), S. 176–188

BIBLIOGRAPHY

- [KHL01] KALSI, Monu ; HACKER, Kurt ; LEWIS, Kemper: A Comprehensive Robust Design Approach for Decision Trade-Offs in Complex Systems Design. In: *Journal of Mechanical Design* 123 (2001), Nr. 1, S. 1–10
- [Kim07] KIMURA, F.: Modeling, Evaluation and Design of Product Quality under Disturbances throughout the Total Product Life Cycle. In: *The Future of Product Development*, Heidelberg, Springer Berlin, 2007, S. 675–684
- [KTHZ07] KING, J. ; TITCHENER-HOOKER, N. ; ZHOU, Y.: Ranking bioprocess variables using global sensitivity analysis: a case study in centrifugation. In: *Bioprocess and Biosystems Engineering* 30 (2007), S. 123–134. – 10.1007/s00449-006-0109-5. – ISSN 1615–7591
- [LAB06] LI, Mian ; AZARM, Shapour ; BOYARS, Art: A New Deterministic Approach Using Sensitivity Region Measures for Multi-Objective Robust and Feasibility Robust Design Optimization. In: *Journal of Mechanical Design* 128 (2006), Nr. 4, S. 874–883
- [LJ09] LIU, D. ; JIANG, P.: Modelling of machining error flow based on form features for multistage processes. In: *International Journal of Computer Integrated Manufacturing* 22 (2009), Nr. 9, S. 857 – 876
- [LL09] LU, XinJiang ; LI, Han-Xiong: Perturbation Theory Based Robust Design Under Model Uncertainty. In: *Journal of Mechanical Design* 131 (2009), Nr. 11, S. 111006–9
- [LR92] LOBANOFF, Val S. ; ROSS, Robert R.: *Centrifugal Pumps: Design and Application*. Bd. 2th Edition. Gulf Professional Publishing, 1992
- [LVB99] LEGOFF, O. ; VILLENEUVE, F. ; BOURDET, P.: Geometrical tolerancing in process planning: a tridimensional approach. In: *Proceedings of the Institution of Mechanical Engineers, Part B: Journal of Engineering Manufacture* 213 (1999), Nr. 6, S. 635–640

BIBLIOGRAPHY

- [LZC07] LOOSE, Jean-Philippe ; ZHOU, Shiyu ; CEGLAREK, Darek: Kinematic Analysis of Dimensional Variation Propagation for Multistage Machining Processes With General Fixture Layouts. In: *IEEE Transactions on Automation Science And Engineering* Vol. 4, No. 2 (2007), S. 141–152
- [LZZC10] LOOSE, Jean-Philippe ; ZHOU, Qiang ; ZHOU, Shiyu ; CEGLAREK, Darek: Integrating GD&T into dimensional variation models for multistage machining processes. In: *International Journal of Production Research* 48 (2010), Nr. 11, S. 3129 – 3149
- [Mar93] MARTINSEN, Kristian: Vectorial tolerancing for all types of surfaces. In: *American Society of Mechanical Engineers, Design Engineering Division* Vol. 2 (1993), S. 187–198
- [MSA08] MOHANASUNDARARAJU, N. ; SIVASUBRAMANIAN, R. ; ALAGUMURTHI, N.: Optimisation of work roll grinding using Response Surface Methodology and evolutionary algorithm. In: *IJMR* 3 (2008), Nr. 2, S. 236–251
- [MW99] MANTRIPRAGADA, R. ; WHITNEY, Daniel E.: Modeling and Controlling Variation Propagation in Mechanical Assemblies. In: *IEEE Transactions on Robotics and Automation* Vol.15, No. 1 (1999), S. 124–140
- [ND06] NJOMO, Donatien ; DAGUENET, Michel: Sensitivity analysis of thermal performances of flat plate solar air heaters. In: *Heat and Mass Transfer* 42 (2006), S. 1065–1081. – 10.1007/s00231-005-0063-9. – ISSN 0947–7411
- [NVV09] NEJAD, M. K. ; VIGNAT, F. ; VILLENEUVE, F.: Simulation of the geometrical defects of manufacturing. In: *The International Journal of Advanced Manufacturing Technology* Vol. 45 (2009), S. 631–648

BIBLIOGRAPHY

- [Par95] PARKINSON, A.: Robust Mechanical Design Using Engineering Models. In: *Journal of Mechanical Design* 117 (1995), Nr. B, S. 48–54
- [Pha89] PHADKE, M. S.: *Quality Engineering Using Robust Design*. Prentice Hall, 1989
- [QDBB09] QURESHI, Ahmed J. ; DANTAN, Jean-Yves ; BRUYERE, Jérôme ; BIGOT, Régis: Parametric and robust design using the quantifier notion. In: *Proceedings of the International Conference on Computers & Industrial Engineering*, 2009, S. 1359 –1366
- [QDBB10a] QURESHI, Ahmed J. ; DANTAN, Jean-Yves ; BRUYERE, Jérôme ; BIGOT, Régis: Set based robust design of mechanical systems using the quantifier constraint satisfaction algorithm. In: *Engineering Applications of Artificial Intelligence* 23 (2010), Nr. 7, S. 1173 – 1186. – ISSN 0952–1976
- [QDBB10b] QURESHI, Ahmed J. ; DANTAN, Jean-Yves ; BRUYERE, Jérôme ; BIGOT, Régis: Set Based Robust Design of Systems - Application to Flange Coupling. In: *Proceedings of the 20th CIRP International Conference on Design, France*, 2010
- [RM08] RAYKOV, Tenko ; MARCOULIDES., George A.: *An Introduction to Applied Multivariate Analysis*. Taylor & Francis Inc, 2008
- [RMP00a] RAMESH, R. ; MANNAN, M. A. ; POO, A. N.: Error compensation in machine tools – a review: Part I: geometric, cutting-force induced and fixture-dependent errors. In: *International Journal of Machine Tools and Manufacture* 40 (2000), Nr. 9, S. 1235–1256
- [RMP00b] RAMESH, R. ; MANNAN, M. A. ; POO, A. N.: Error compensation in machine tools – a review: Part II: thermal errors. In: *International Journal of Machine Tools and Manufacture* 40 (2000), Nr. 9, S. 1257–1284

BIBLIOGRAPHY

- [RT95] RAO, C.R ; TOUTENBURG, H.: *Linear Models: Least squares and Alternatives*. Springer, New York., 1995
- [SBMF⁺10] SERGENT, A. ; BUI-MINH, H. ; FAVRELIERE, H. ; DURET, D. ; SAMPER, S. ; VILLENEUVE, F.: Identification of machining defects by Small Displacement Torsor and form parameterization method. In: *Proceedings of IDMME - Virtual Concept, Bordeaux, France, 2010*
- [SBR08] SAHOO, P. ; BARMAN, T. K. ; ROUTARA, B. C.: Fractal dimension modelling of surface profile and optimisation in CNC end milling using Response Surface Method. In: *IJMR* 3 (2008), Nr. 3, S. 360–377
- [SCS96] SHIU, B.W. ; CEGLAREK, D. ; SHI, J.: Multi-stations Sheet Metal Assembly Modeling and Diagnostics. In: *Transactions of NAMRI/SME* Vol. XXIV (1996), S. 199–204
- [Sob90] SOBOL', I. M.: On sensitivity estimation for nonlinear mathematical models. In: *Matem. Mod.* Vol 2 (1990), Nr. No.1, S. 112–118
- [SRA⁺08] SALTELLI, Andrea ; RATTO, Marco ; ANDRES, Terry ; CAMPO-LONGO, Francesca ; CARIBONI, Jessica ; GATELLI, Debora ; SAISANA, Michaela ; TARANTOLA, Stefano: *Global Sensitivity Analysis: The Primer*. John Wiley & Sons, 2008
- [STC99] SALTELLI, A. ; TARANTOLA, S. ; CHAN, K.: Quantitative model-independent method for global sensitivity analysis of model output. In: *Technometrics* 41 (1999), S. 39–56
- [Suh01] SUH, N. P.: *Axiomatic Design-Advances and Applications*. Oxford University Press, 2001
- [Tag86] TAGUCHI, G.: *Introduction to Quality Engineering-Designing Quality into Products and Processes*. Asian Productivity Organization: Tokyo, 1986

BIBLIOGRAPHY

- [TB99] TICHKIEWITCH, S. ; BRISSAUD, D.: Diverse Aspects of Tolerancing on an Integrated Design Context. In: *CIRP Annals - Manufacturing Technology* 48 (1999), Nr. 1, S. 107 – 110. – ISSN 0007–8506
- [TB00] TICHKIEWITCH, S. ; BRISSAUD, D.: Co-Ordination Between Product and Process Definitions in a Concurrent Engineering Environment. In: *CIRP Annals - Manufacturing Technology* 49 (2000), Nr. 1, S. 75 – 78. – ISSN 0007–8506
- [TCG96] TEISSANDIER, Denis ; COUETARD, Yves ; GERARD, Alain: Three-dimensional functional tolerancing with proportioned assemblies clearance volume. In: *Proceedings of the Engineering Systems Design and Analysis Conference*, 1996
- [TCG98] TEISSANDIER, Denis ; COUETARD, Yves ; GERARD, Alain: Three-dimensional functional tolerancing with proportioned assemblies clearance volume. In: *Proceedings of the 5th CIRP Seminar on Computer-Aided Tolerancing*, 1998
- [TCG99] TEISSANDIER, Denis ; COUETARD, Yves ; GERARD, Alain: A computer aided tolerancing model: proportioned assembly clearance volume. In: *Computer-Aided Design* 31 (1999), Nr. 13, S. 805–817
- [Thi01] THIEBAUT, François: *Contribution à la définition d'un moyen unifié de gestion de la géométrie réaliste basée sur le calcul des lois de comportement des mécanismes.*, ENS de Cachan, Diss., 2001
- [Tic05] TICHADOU, Stephane: *Modélisation et quantification tridimensionnelles des écarts de fabrication pour la simulation d'usinage*, L'École Centrale de Nantes, Diss., 2005
- [TL96] TING, Kwun-Lon ; LONG, Yufeng: Performance Quality and Tolerance Sensitivity of Mechanisms. In: *Journal of Mechanical Design* 118 (1996), Nr. 1, S. 144–150

BIBLIOGRAPHY

- [TLH05] TICHADOU, Stéphane ; LEGOFF, Olivier ; HASCOET, Jean-Yves: 3D Geometrical Manufacturing Simulation: Compared approaches between integrated CAD/CAM systems and small displacement torsor models. In: A. BRAMLEY, D. C. (Hrsg.) ; MCMAHON, C. (Hrsg.): *Advances in Integrated Design and Manufacturing in Mechanical Engineering*. Springer Netherlands, 2005, S. 201–214
- [TNVL07] TICHADOU, S. ; NEJAD, M. K. ; VIGNAT, F. ; LEGOFF, O.: 3-D manufacturing dispersions: two experimental applications. In: *Proceedings of the 10th CIRP International Seminar on Computer Aided Tolerancing, France (2007)*, 2007
- [TS08] THANGAVEL, P. ; SELLADURAI, V.: An experimental investigation on the effect of turning parameters on surface roughness. In: *IJMR* 3 (2008), Nr. 3, S. 285–300
- [TV97] TICHKIEWITCH, S. ; VÉRON, M.: Methodology and Product Model for Integrated Design Using a Multiview System. In: *CIRP Annals - Manufacturing Technology* 46 (1997), Nr. 1, S. 81 – 84. – ISSN 0007–8506
- [Vig05] VIGNAT, Frédéric: *Contribution à l'élaboration d'un modèle 3D de simulation de fabrication pour l'analyse et la synthèse des tolérances, le modèle MMP*, INPG, Diss., 2005
- [VKDS03] VLAHINOS, Andreas ; KELLY, Kenneth ; D'ALEO, Jim ; STATHOPOULOS, Jim: Effect of material and manufacturing variations on membrane electrode assembly pressure distribution. In: *Proceedings of The First International Conference on Fuel Cell Science, Engineering and Technology April 21-23, 2003, Rochester, New York, USA*, 2003

BIBLIOGRAPHY

- [VLL01] VILLENEUVE, F. ; LEGOFF, O. ; LANDON, Y.: Tolerancing for manufacturing: a three-dimensional model. In: *International Journal of Production Research* Vol. 39, No. 8 (2001), S. 1625 – 1648
- [VV03] VIGNAT, Frédéric ; VILLENEUVE, François: 3D Transfer of Tolerances Using a SDT Approach: Application to Turning Process. In: *Journal of Computing and Information Science in Engineering* Vol. 3 (2003), S. 45–53
- [VV05a] VIGNAT, Frédéric ; VILLENEUVE, François: Simulation of the manufacturing process (2) Analysis of its consequences on a functional tolerance. In: *Proceedings of the 9th CIRP International Seminar on Computer Aided Tolerancing, 2005*
- [VV05b] VILLENEUVE, François ; VIGNAT, Frédéric: Simulation of the manufacturing process (1) Generic resolution of the positioning problem. In: *Proceedings of the 9th CIRP International Seminar on Computer Aided Tolerancing, 2005*
- [VV07] VIGNAT, Frédéric ; VILLENEUVE, François: Simulation of the Manufacturing Process, Generation of a Model of the Manufactured Parts. In: US, Springer (Hrsg.): *Digital Enterprise Technology, 2007*, S. 545–552
- [WCBA03] WHITCOMBE, J. M. ; CROPP, R. A. ; BRADDOCK, R. D. ; AGRANOVSKI, I. E.: Application of sensitivity analysis to oil refinery emissions. In: *Reliability Engineering & System Safety* 79 (2003), Nr. 2, S. 219 – 224. – ISSN 0951–8320
- [WCH07] WONG, Yew-Wah ; CHAN, Weng-Kong ; HU, Wei: Effects of Tongue Position and Base Circle Diameter on the Performance of a Centrifugal Blood Pump. In: *Artificial Organs* Vol. 31, No. 8 (2007), S. 639–645

BIBLIOGRAPHY

- [Whi68] WHITNEY, Daniel E.: *State space models of remote manipulation tasks*, Massachusetts Institute of Technology, Diss., 1968
- [WHK05] WANG, Hui ; HUANG, Qiang ; KATZ, Reuven: Multi-Operational Machining Processes Modeling for Sequential Root Cause Identification and Measurement Reduction. In: *Journal of Manufacturing Science and Engineering* Vol. 127 (2005), S. 512–521
- [Wik10] WIKIPEDIA. *Constructive solid geometry*. 2010
- [WL07] WOLFGANG, Härdle ; LEOPOLD, Simar: *Applied Multivariate Statistical Analysis*. Softcover, 2007
- [Wol83] WOLFRAM, Stephen: Statistical mechanics of cellular automata. In: *Rev. Mod. Phys.* 55 (1983), Jul, Nr. 3, S. 601–644
- [WRA05] WEI, Chen ; RUICHEN, Jin ; AGUS, Sudjianto: Analytical Variance-Based Global Sensitivity Analysis in Simulation-Based Design Under Uncertainty. In: *Journal of Mechanical Design* Vol. 127 (2005), Nr. No. 5, S. 875–886
- [ZBZG09] ZHANG, Jian ; BAO, Nengsheng ; ZHANG, Guojun ; GU, Peihua: Analytical approach to robust design of nonlinear mechanical systems. In: *Frontiers of Mechanical Engineering in China* 4 (2009), Nr. 2, S. 203–214
- [ZHS03] ZHOU, Shiyu ; HUANG, Qiang ; SHI, Jianjun: State Space Modeling of Dimensional Variation Propagation in Multistage Machining Process Using Differential Motion Vectors. In: *IEEE Transactions on Robotics and Automation* Vol. 19, No.2 (2003), S. 296–309
- [ZLB⁺10] ZHANG, J. ; LI, S.P. ; BAO, N.S. ; ZHANG, G.J. ; XUE, D.Y. ; GU, P.H.: A robust design approach to determination of tolerances of mechanical products. In: *CIRP Annals - Manufacturing Technology* 59 (2010), Nr. 1, S. 195 – 198. – ISSN 0007–8506

BIBLIOGRAPHY

- [ZT01] ZHU, Jianmin ; TING, Kwun-Lon: Performance Distribution Analysis and Robust Design. In: *Journal of Mechanical Design* 123 (2001), Nr. 1, S. 11–17

RÉSUMÉ DE THÈSE

INTRODUCTION

AUJOURD'HUI, les exigences des clients concernant les produits qu'ils acquièrent sont de plus en plus élevées. La satisfaction de ces exigences telles que la qualité, la fiabilité, la robustesse, l'innovation et le coût joue un rôle important dans le contexte d'économie globale et de concurrence. Grâce au développement des technologies de l'information, les ordinateurs sont devenus un outil incontournable d'assistance des activités d'ingénierie de conception du produit et du processus de fabrication. Les concepteurs travaillent principalement sur le modèle numérique du produit dans un environnement CAO¹, ce modèle est ensuite utilisé pour simuler la performance du produit. Le modèle créé dans l'environnement CAO est une représentation nominale du produit, et il ne peut donc prendre en compte les variations générées durant le cycle de vie du produit.

En fait, le produit doit passer à travers plusieurs étapes de son cycle de vie avant d'arriver dans les mains du client. Chaque pièce composant le produit est fabriquée à partir de matière brute au cours des opérations successives du processus de fabrication (forgeage, usinage, affilage, etc.). Des déviations géométriques sont générées à chaque opération (phase) du processus de fabrication et accumulées tout au long des étapes de fabrication. Ces déviations sont le résultat des imperfections de la matière, de l'outillage et des machines. La pièce fabriquée et ses déviations sont

1. Concepteur Assisté par l'Ordinateur

assemblées dans l'étape d'assemblage pour construire le produit. Les déviations des surfaces de la pièce impactent l'assemblabilité du produit et sont accumulées sur le produit final. La géométrie réelle du produit est donc différente de sa géométrie nominale à la fin de l'étape de fabrication et d'assemblage, et la performance du produit est certainement donc certainement différente. Finalement, le produit réel est différent du produit prévu par le concepteur et promis au client au début de la conception du produit et il y a donc un risque de ne pas satisfaire le client. Il est donc important de se demander comment on peut gérer la variation de performance du produit afin de la réduire et tout au moins de s'assurer qu'elle est compatible avec la satisfaction du client.

La technologie actuelle de modélisation du produit n'est pas capable de prendre en compte les déviations géométriques. La plupart des simulations pour prédire le comportement du produit (cinématique, dynamique, écoulement de fluides, etc.) et évaluer sa performance sont réalisées en s'appuyant sur le modèle nominal du produit. Le résultat de la simulation de performance du produit peut donc être considéré comme la performance nominale et donc différer de la performance réelle. Le risque est alors que le produit conçu ne répond pas totalement aux exigences des clients et des utilisateurs. La principale problématique pour le concepteur est alors : « Est-ce que le produit réel satisfait aux exigences des clients du point de vue de sa performance ? ». La gestion des variations géométriques durant le cycle de vie du produit est donc une question importante dans la conception du produit-process il faut donc considérer les question suivante :

- Comment modéliser les déviations géométriques générées tout au long du cycle de vie du produit ?
- Comment intégrer les déviations géométriques à la simulation de performance du produit ?
- Comment gérer leurs causes et conséquences dans la phase de la conception et identifier les sources de variation qui influence la performance du produit ?

Les travaux de recherche que j'ai mené ont été réalisés au sein du laboratoire G-

SCOP². La thèse contribue au développement d'un modèle unifié pour la modélisation des déviations géométriques générées et accumulées au cours de l'étape de fabrication et d'assemblage du cycle de vie du produit. Ce modèle est basé sur les travaux de recherche du pôle Conception Intégrée en combinant le modèle de pièce fabriquée MMP³ proposé par Villeneuve et Vignat [VLL01, VV05a, VV05b, VV07], et le modèle du produit pour le cycle de vie développé par Brissaud et Tichkiewitch [TV97, TB99, TB00, BT01]. La méthodologie de recherche appliquée dans ce travail s'appuie sur des études de cas, surtout sur la conception d'une pompe centrifuge. On a proposé et testé des méthodes et des outils pour modéliser les déviations tout au long du cycle de vie et intégrer celles-ci à la simulation de la performance du produit et l'identification des paramètres de variation influents. L'étape suivante a été de généraliser les méthodes et les outils proposés afin de définir la méthodologie globale pour l'intégration des déviations géométriques issues de l'étape de fabrication et d'assemblage dans la simulation de performance du produit et l'identification des paramètres de variation influents. La dernière étape a consisté en l'application de certaines parties de la méthode globale afin de les tester sur un exemple simple et de comparer les résultats obtenus avec les résultats théoriques afin de vérifier la validité de la méthode proposée.

De nombreuses recherches pour modéliser les déviations géométriques générées et accumulées durant le processus de fabrication et d'assemblage ont déjà été conduites. Elles seront présentées dans le chapitre 2. Toutefois, aucun modèle ne couvre toutes les étapes du cycle de vie du produit. Le travail présenté dans ce mémoire se concentre donc sur la proposition d'une méthode qui permet de modéliser les déviations géométriques générées tout au long du cycle de vie du produit et l'intégration de celles-ci à la simulation de performance du produit.

La vue d'ensemble de la méthode proposée est décrite figure 1. La méthode est divisée en deux branches. La première consiste en la génération du modèle de dévia-

2. Laboratoire des Science pour la Conception, l'Optimisation et la Production de Grenoble

3. Model of Manufactured Part

tions géométriques par la simulation du processus de fabrication et d'assemblage. Ce modèle est basé sur le concept de torseur des petits déplacements proposé par Bourdet [Bou87]. Il se compose du modèle MMP proposé par Vignat et al pour modéliser les déviations géométriques générées par le processus de fabrication et du modèle MAP⁴ qui s'appuie sur le modèle proposé par Ballot et al et Thiébaud. Les une population de produits avec déviations géométriques est ensuite créée biais d'une méthode stochastique de type Monte-Carlo. La génération et la simulation des déviations géométriques du produit sont présentées chapitre 3.

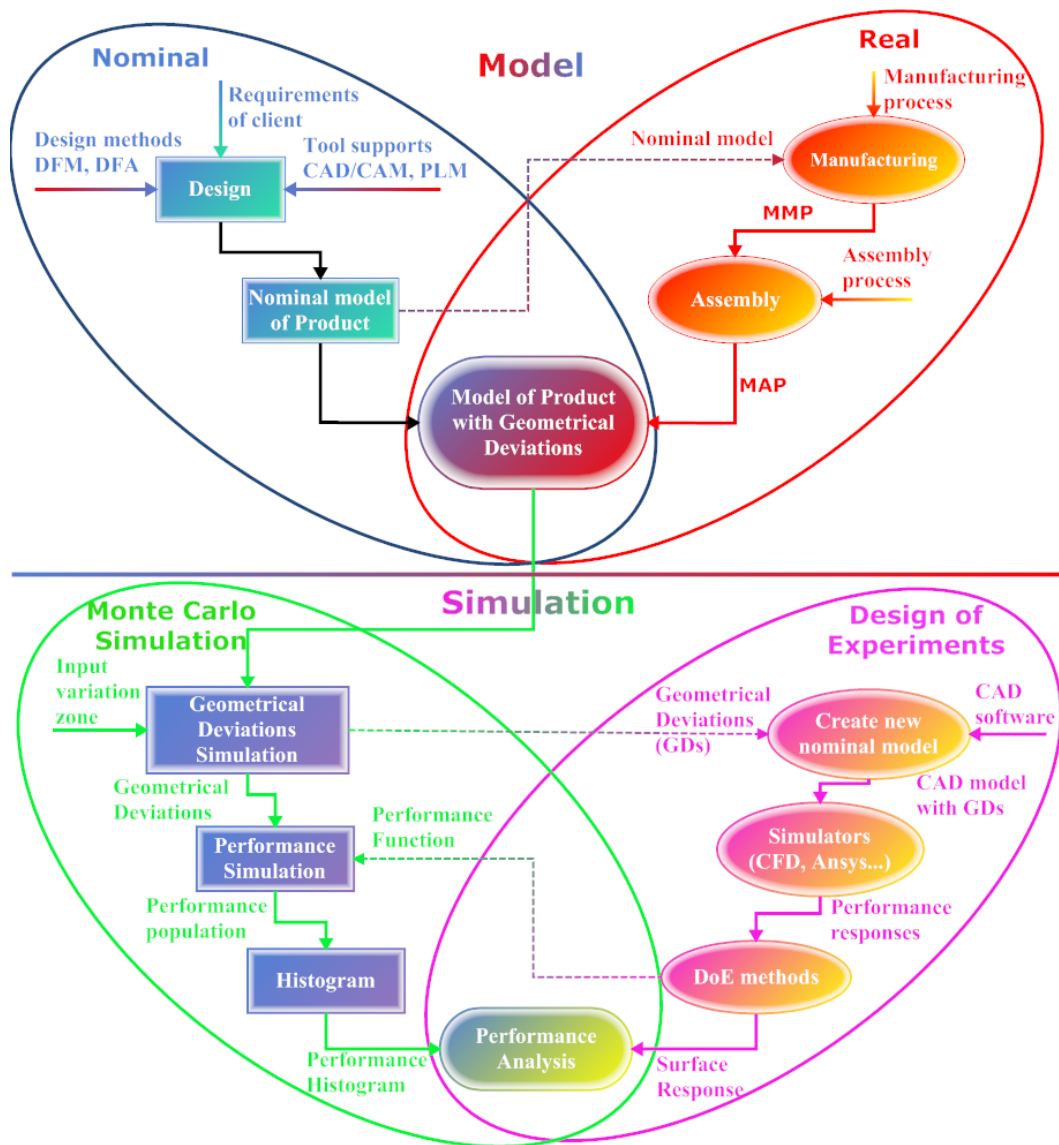


FIGURE 1 – La vue d'ensemble de la méthode

La seconde partie est une méthode qui permet d'intégrer les déviations géométriques dans la simulation de performance du produit. La relation entre la performance et les paramètres de déviations géométriques est d'abord établie. La performance de la population du produit est ensuite déterminée à partir des résultats de la simulation Monte-Carlo. Le calcul de cette population permet de vérifier la conformité du produit conçu aux exigences du client. Cette méthode va être présentée chapitre 4. Le chapitre 5 présente une méthode qui permet d'identifier et de classer l'influence des paramètres de déviation géométrique sur la performance du produit. Cette méthode permet aussi de déterminer la variance de la performance du produit relativement à chacun des paramètres. La solution robuste de conception peut être trouvée à partir des résultats précédents par minimisation de la variance de la performance du produit. Conclusion et perspective sont ensuite présentés chapitre 6.

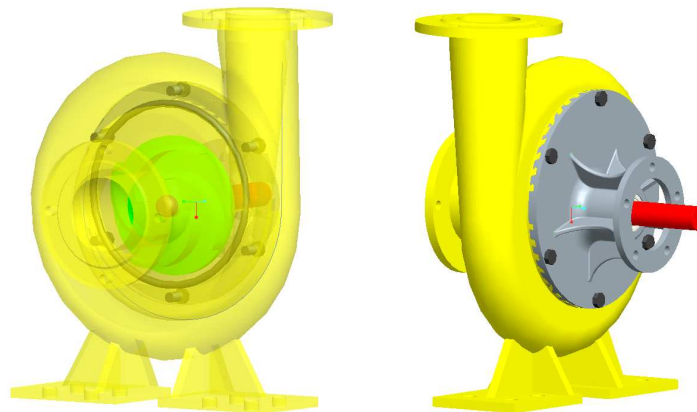


FIGURE 2 – Le model nominal de la pompe centrifuge

Afin d'illustrer les méthodes présentées dans ce mémoire de thèse, une étude de cas est proposée tout au long du mémoire. L'exemple choisit consiste en la conception d'une pompe centrifuge (voir la figure 2) avec les spécifications suivantes :

- Débit : $250m^3/h$
- Hauteur manométrique totale : $100m$
- Moteur : $2000RPM$
- Fluide : Eau
- Température : $20^{\circ}C$

PROBLÉMATIQUE SCIENTIFIQUE

QUELQUES travaux de recherche existent dans la recherche académique couvrant chacune un étape du cycle de vie du produit. Plusieurs modèles pour modéliser les déviations géométriques générées au cours des étapes de fabrication et d'assemblage ont été développés en utilisant des approches différentes. Le résumé des modèles sont présentés dans le tableau 1 pour les déviations géométriques générées à l'étape de fabrication et le tableau 2 pour l'étape d'assemblage.

	State space approach			Small displacement torsor	
	Zhou et al. (2003)	Huang et al. (2003)	Wang et al. (2005)	Villeneuve et al. (2001)	Vignat et al. (2005)
Fixture errors	Yes	Yes	Yes	Yes	Yes
Machining tool errors	Yes	Yes	Yes	Yes	Yes
Multioperation	Yes	Yes	Yes	Yes	Yes
2D/3D	3D	3D	3D	3D	2D and 3D

Table 1: The geometrical deviation models in manufacturing stage.

Le principe des modèles proposés par Mantripragada et Whitney [MW99], Jin et Shi [JS99], Huang et al. [HLKC07], Thiebaut [Thi01] est de modéliser les variations géométriques des pièces assemblées à chaque phase du processus d'assemblage. Ils prennent en compte des déviations géométriques des surfaces des pièces, mais celles-ci ne proviennent pas d'une simulation du processus de fabrication et ne sont donc liées à aucuns modèle de déviations géométriques de fabrication proposés par Zhou et al. [ZHS03], Huang et al [HSY03], Wang et al. [WHK05], Villeneuve et al. [VLL01], Vignat et al. [Vig05]. De plus, toutes les méthodologies de conception robuste ont besoin pour fonctionner d'un modèle précis qui décrit la relation entre la performance du produit et les sources de variation. Ce modèle est difficile à obtenir du fait de la complexité des processus de fabrication et d'assemblage. Pour ces

	State transition approach	State space approach			Small displacement torsor	
	Mantripragada and Whitney (1999)	Jin and Shi (1999)	Camelio et al., (2003)	Huang et al., (2007)	Ballot et al., (1997)	Thiebaut (2001)
Fixture errors	No	Yes	Yes	Yes	Yes	Yes
Part deviation	Yes	No	Yes	Yes	Yes	Yes
Machining tool errors	N/A	N/A	N/A	N/A	N/A	N/A
Multistation	No	Yes	Yes	Yes	N/A	Yes
2D/3D	N/A	2D	3D	3D	3D	3D

Table 2: The geometrical deviation models in assembly stage

raisons, on a besoin de définir une réponse complète aux questions scientifiques suivantes :

- Comment modéliser les déviations géométriques du produit tout en couvrant toutes les étapes de son cycle de vie ?
- Comment intégrer les déviations géométriques à la simulation de performance du produit ?
- Comment gérer les causes et conséquences dès la phase de la conception et identifier les sources de variation qui influence la performance du produit ?

MODÈLE DES DÉVIATIONS GÉOMÉTRIQUES

LE modèle des déviations géométriques développé dans ce travail de thèse permet de modéliser toutes les déviations géométriques générées au cours de l'étape de fabrication et l'étape d'assemblage. Ce modèle est basé sur le modèle de pièce fabriquée proposé par Vignat et al [VV07], et celui de comportement des mécanismes proposé par Thiébaud [Thi01].

Modèle de pièce fabriquée (MMP)

Les déviations géométriques générées à l'étape de fabrication sont modélisées par le modèle MMP. Elles résultent de deux phénomènes indépendants :

- La mise en position qui génère les défauts de positionnement de la pièce par rapport à sa position nominale dans le porte-pièce de la machine. Ces défauts dans la phase S_j sont modélisés par un torseur de petits déplacements 1.

$$T_{S_j, P^i} = -T_{P^i, P_m^i} + T_{S_j, H_i S_j} + T_{H_i S_j, P_m^i} \quad (1)$$

T_{P^i, P_m^i} : torseur d'écart de la surface m de la pièce i réalisée dans la phase précédente.

$T_{S_j, H_i S_j}$: torseur d'écart de la surface H_i du porte-pièce dans la phase S_j

$T_{H_i S_j, P_m^i}$: torseur lien décrivant l'interface entre la surface m de la pièce et la surface H_i du porte-pièce dans la phase S_j .

- L'usinage qui génère des défauts géométriques sur les surfaces réalisées dans la phase S_j par rapport à la machine. Ces défauts de la surface i dans la phase S_j sont modélisés par le torseur T_{S_j, P_j^i} comme présenté équation 2 pour une surface cylindrique.

$$T_{S_j, P_j^i} = \left\{ \begin{array}{cc} rx_{i, j S_j} & tx_{i, j S_j} \\ ry_{i, j S_j} & ty_{i, j S_j} \\ 0 & 0 \end{array} \right\}_{(O, XYZ)} \quad (2)$$

Les déviations géométriques de la surface usinée j dans la phase S_j par rapport à la pièce nominale sont donc exprimées par un torseur T_{P^i, P_m^i} comme présenté équation 3.

$$T_{P^i, P_j^i} = -T_{S_j, P^i} + T_{S_j, P_j^i} \quad (3)$$

Modèle de la pièce assemblée (MAP)

Les pièces fabriquées lors de l'étape de fabrication sont assemblées en suivant un processus d'assemblage définit. Les déviations géométriques générées par le processus de fabrication vont s'accumuler lors de l'assemblage. Les déviations de la surface k de la pièce i dans la phase j par rapport à sa position nominale dans la coordonnée globale du produit sont exprimées par un torseur T_{P^i, P_k^i} , comme décrit équation 4.

$$T_{P^i, P_k^i} = T_{P, P^i} + T_{P^i, P_k^i} \quad (4)$$

T_{P^i, P_k^i} est un torseur décrivant les déviations géométriques de la surface k de la pièce i par rapport à sa position nominale dans le repère globale du produit. Il est calculé à partir du modèle MMP i .

T_{P, P^i} est un torseur exprimant le défaut de positionnement de la pièce i par rapport à sa position nominale dans l'assemblage. Ce torseur est calculé à partir des liaisons élémentaires entre la pièce i et les autres.

Simulation des déviations géométriques du produit

Un ensemble des M produits assemblés est généré par l'utilisation de la simulation Monte-Carlo et du modèle GDM. Les variables entrées sont les paramètres des torseurs du modèle GDM, comme les paramètres du torseur décrivant la qualité des surfaces du porte-pièce et les défauts d'usinage. On suppose que toutes les variables sont indépendantes dans ce cas et que leur distribution est uniforme. Les données de celles-ci peuvent être basées des résultats de mesures expérimentales.

A partir de ces résultats, le concepteur peut vérifier les exigences géométriques du produit. De plus, il peut utiliser ces résultats pour intégrer les déviations géométriques du produit dans la simulation de performance.

L'image des déviations géométriques de la population du produit est générée par la méthode de Monte-Carlo, comme suit :

- Etape 1. Définir la probabilité de distribution et la zone de variation des variables entrées.

Les variables entrées sont des paramètres du torseur représentant la qualité du porte-pièce et la capabilité de la machine. Ce sont les paramètres des déviations géométriques des surfaces du porte-pièce et des défauts d'usinage. La détermination de leur distribution est basée sur des résultats de mesures expérimentales [TNVL07]. La stratégie pour limiter les zones de variation des variables entrées est présentée par Kamali Nejad [NVV09].

- Etape 2. Générer par tirage aléatoire des valeurs des variables entrées en respectant la distribution et la zone de variation déterminées.

Dans notre cas, les valeurs des variables d'entrées est générée par un algorithme de type cellular automata défini par Wolfram.

- Etape 3. Calculer les déviations géométriques des surfaces de la pièce fabriquée en s'appuyant sur le modèle MMP.

On détermine d'abord les paramètres du torseur lien du modèle MMP. Ils sont déterminés par les contraintes de non-pénétration et la fonction de positionnement. Cette procédure est expliqué en détail par [NVV09].

Etape 4. Assembler les pièces fabriquées en s'appuyant sur la vérification des contraintes d'assemblage.

- Etape 5. Calculer les déviations géométriques des surfaces du produit final par rapport au repère globale en s'appuyant sur le modèle GDM.

INTÉGRATION DES DÉVIATIONS GÉOMÉTRIQUES DANS LA SIMULATION DE PERFORMANCE

LES déviations géométriques générées de l'étape de fabrication à l'étape d'assemblage vont évidemment influencer la performance du produit. Pourtant, la technologie actuelle de modélisation des produits ne peut pas prendre en compte ces déviations. La plupart des simulations pour prédire le comportement du produit telles que simulations cinématique, dynamiques, de résistance, fluide, etc. sont réalisées en s'appuyant sur le modèle nominal. La performance prédite par ces simulation est donc différente de la performance du produit réel. Le risque est que le produit conçu ne satisfasse pas aux exigences du client. Il est donc nécessaire d'intégrer les déviations géométriques à la simulation de performance du produit.

On propose dans ce mémoire de thèse deux approches afin de répondre à ce problème. La première approche est utilisée dans le cas que l'on connaît bien la relation mathématique entre la performance et les paramètres des déviations géométriques du produit. La variation de performance du produit est déterminée par l'équation 5.

$$\Delta Pr_i = f_i(\Delta \hat{p}_1, \Delta \hat{p}_2, \dots, \Delta \hat{p}_m) = \sum_{j=1}^m \left. \frac{\partial F_i}{\partial \hat{p}_j} \right|_{(\hat{\mu}_1, \dots, \hat{\mu}_m)} \cdot \Delta \hat{p}_j + \sum_{j=1}^m \sum_{k=1}^m \left. \frac{\partial^2 F_i}{\partial \hat{p}_j \partial \hat{p}_k} \right|_{(\hat{\mu}_1, \dots, \hat{\mu}_m)} \cdot \Delta \hat{p}_j \cdot \Delta \hat{p}_k \quad (5)$$

$\{\Delta \hat{p}_i\}_{i=1..m}$ sont les paramètres des déviations géométriques et ΔPr_i est la variation de performance du produit. A partir de cette relation, on peut générer une image de la performance du produit en s'appuyant sur les résultats de la simulation Monte-Carlo effectuée à l'étape précédente.

La deuxième approche est basée sur la méthode des plans d'expérience et l'expertise des concepteurs. Elle est utilisée dans le cas où la relation entre la performance et les paramètres des déviations géométriques n'est pas disponible ou difficile à obtenir mathématiquement. On propose alors trois méthodes différentes que nous

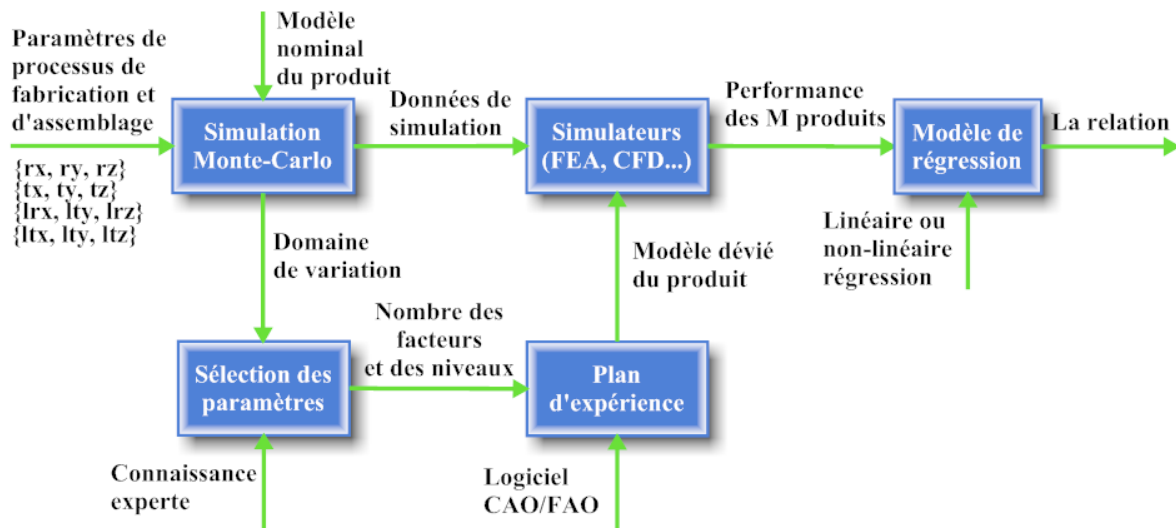


FIGURE 3 – Simulation de performance du produit avec les déviations géométriques

nommons factorial, Taguchi et random design pour déterminer une version approchée de cette relation. Dans ce cas, on peut utiliser la méthode des éléments finis afin de calculer la performance en s'appuyant sur des modèles déviés du produit. Les modèles dévié sont créés dans des logiciels CAO a partir des résultats, en terme de déviations géométriques, de la simulation Monte-Carlo effectuée à l'étape précédente. La relation entre la performance et les paramètres des déviations géométriques est déterminée par un modèle de régression linéaire ou non-linéaire en s'appuyant sur la méthode des plans d'expérience a partir de plusieurs résultats de simulation réparti dans la zone de variation des deviation en utilisant des modèles factoriel, Taguchi ou aléatoire. La vue d'ensemble de la méthode est présentée figure3. Finalement, une image de la performance des produits fabriqués (réels) est générée par l'utilisation des résultats de la simulation Monte-Carlo effectuée à l'étape précédente et la relation ainsi déterminée.

ANALYSE DES FACTEURS D'INFLUENCE

UNE image des produits réels a été générée par l'utilisation d'une simulation Monte-Carlo présentée dans le chapitre ci-dessus. Les sources de variation influence de manière certaine la performance du produit. Il faut donc développer une méthode qui permet d'identifier et classier les paramètres des sources de variation ayant une influence sur la performance du produit. On a présenté deux approches dans ce mémoire de thèse en s'appuyant sur l'analyse de sensibilité globale et l'analyse des données qui permette d'identifier et classier le niveau d'influence des paramètres des sources de variation.

Analyse de sensibilité globale

La première approche est basée sur la définition des indices de sensibilité globale proposée par Sobol [Sob90]. Ces indices permettent de mesurer le niveau d'influence de chaque paramètre de déviation géométrique sur la performance du produit. Elles sont définies en divisant par la variance de chaque paramètre par rapport à la variance de la performance présenté équation 6.

$$S_{i_1..i_u} = \frac{V_{i_1..i_u}}{V} \quad (6)$$

$V_{i_1..i_u}$ est la variance partielle qui mesure l'effet de l'ensemble des paramètres d'entrée sur le paramètre de sortie tel que la performance du produit. Elle est calculée en s'appuyant sur la relation f entre les paramètres de déviations géométriques et la performance. Elle est décrite par l'équation 7.

$$V_{i_1..i_u} = \int_0^1 f_{i_1..i_u}^2(x_1, x_2, \dots, x_{i_u}) dx_1, \dots, x_{i_u} \quad (7)$$

Le coefficient d'influence de chaque paramètre est calculé par cette équation. Les paramètres sont classifiés par rapport à la valeur du coefficient d'influence calculé.

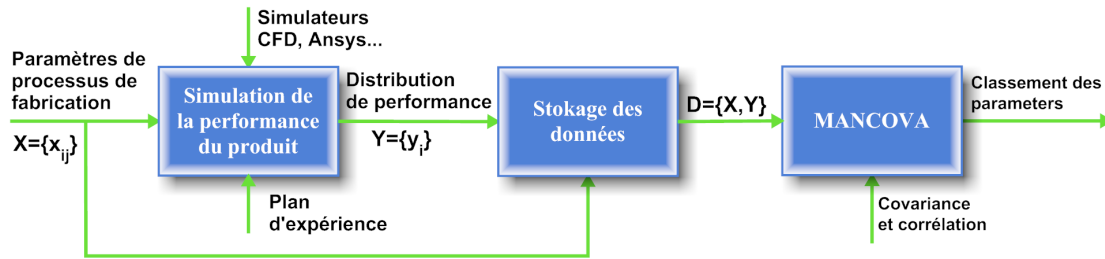


FIGURE 4 – L'ensemble de l'approche de la covariance et de la corrélation

Approche d'analyse de donnés

L'approche d'analyse de sensibilité globale est utilisée pour identifier et classer les paramètres des déviations géométriques générées par les sources de variation durant le cycle de vie du produit. Toutefois, si la relation entre celles-ci et les paramètres des sources de variation n'est pas explicite Cette approche ne peut pas être utilisée. On va donc proposer une autre approche pour identifier les source de variation qui influencent le plus la performance du produit.

Covariance et Corrélation

Les résultats de la simulation de performance par l'utilisation de la méthode Monte-Carlo sont utilisées pour calculer la covariance et la corrélation entre la performance et chaque paramètre de source de variation. Ce coefficient permet de mesurer le niveau d'influence linéaire de chaque paramètre. Il est calculé par l'équation 8.

$$\sigma_{XY} = Cov(X, Y) = E(XY) - E(X)E(Y) \quad (8)$$

$$\rho_{XY} = \frac{Cov(X,Y)}{\sigma_X \cdot \sigma_Y}$$

A partir des résultats de l'analyse de covariance et de corrélation, on peut classer les paramètres par rapport au niveau d'influence des paramètres sur la performance du produit. La vue d'ensemble de la méthode est résumée dans la figure 4.

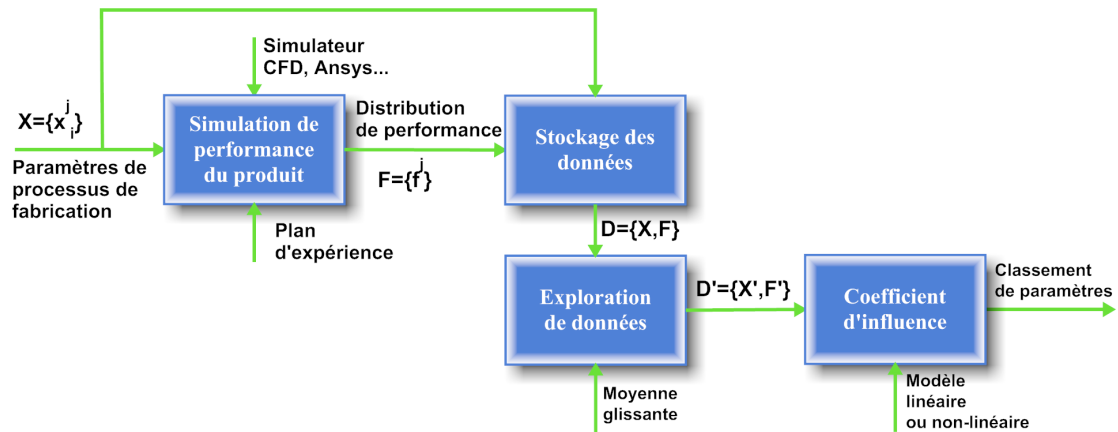


FIGURE 5 – L'ensemble de l'approche

Coefficient d'influence

On définit un coefficient qui permet de mesurer le pourcentage d'influence de chaque paramètre sur la performance du produit, comme présenté dans l'équation 9.

$$\Delta_i = \frac{\Delta g_i(x)}{\Delta F} = \frac{\max \{g_i(x)\} - \min \{g_i(x)\}}{\max \{F\} - \min \{F\}} \quad (9)$$

La fonction $g_i(x)$ est estimée par régression linéaire ou non-linéaire en s'appuyant sur des données filtrées par la méthode de la moyenne glissante. Donc, l'avantage de cette approche par rapport à l'approche de covariance et corrélation est la possibilité de prise en compte de relation non-linéaire entre la performance du produit et les paramètres des sources de variation. La méthode pour déterminer le coefficient est exposée dans la figure 5.

MÉTHODOLOGIE DE LA CONCEPTION ROBUSTE

LA d'une solution robuste de conception permet de minimiser la variation de performance du produit par rapport aux incertitudes et aux sources de variation. Nous avons proposé, dans ce travail de thèse, deux approches qui permettent de déterminer la variance de la variation de la performance du produit par rapport à la variation des paramètres des déviations géométriques ou des sources de variation durant son cycle de vie. A partir de ces résultats, la solution de la conception robuste peut être trouvée par minimisation de la variance.

Approche mathématique

A partir de la relation entre la performance du produit Pr_i et les paramètres des déviations géométriques \hat{p}_j , la variance de la variation de la performance peut être calculée par l'utilisation de la série de Taylor. Elle est exprimée par l'équation 10.

$$\sigma_{\Delta Pr_i}^2 = \sum_{j=1}^m \left(\frac{\partial f_i}{\partial \hat{p}_j} \Big|_{(\hat{\mu}_1, \dots, \hat{\mu}_m)} \right)^2 \cdot \sigma_{\Delta \hat{p}_j}^2 + \left(\sum_{j=1}^m \sum_{k=1}^m \frac{\partial^2 F_i}{\partial \hat{p}_j \partial \hat{p}_k} \Big|_{(\hat{\mu}_1, \dots, \hat{\mu}_m)} \right)^2 \sigma_{\Delta \hat{p}_j, \Delta \hat{p}_k}^2 (i, j=1..m) \quad (10)$$

Afin d'obtenir la solution robuste, il est nécessaire de résoudre le problème en suivant la procédure suivante 11.

$$\begin{aligned} & \text{Minimize : } \sigma_{\Delta Pr_i}^2 \\ & \text{Subject to : } a_j \leq \hat{p}_j \leq b_j; E(Pr_i) = P_i^N \end{aligned} \quad (11)$$

$E(Pr_i) = P_i^N$ est la performance nominale du produit conçu.

Approche d'analyse des données

La variance de la variation de la performance peut être calculée par l'équation 12.

$$\sigma_{\Delta Pr_k}^2 = \sum_{i=1}^n \left(\frac{\partial g_{ik}(\Delta x_i)}{\partial \Delta x_i} \Big|_{(\mu_{\Delta x_1}, \mu_{\Delta x_2}, \dots, \mu_{\Delta x_n})} \right)^2 \sigma_{\Delta x_i}^2 = \sum_{i=1}^n C_i^2 \sigma_{\Delta x_i}^2 \quad (12)$$

La fonction g_{ik} est estimée dans le chapitre ci-dessus à partir des données traitées par la méthode de la moyenne glissante. La solution de la conception robuste peut être trouvée par la procédure suivante 13.

$$\begin{aligned} & \text{Minimize : } \sigma_{\Delta Pr_k}^2 \\ & \text{Subject to : } a_i \leq x_i \leq b_i; E(Pr_k) = P_k^N \end{aligned} \quad (13)$$

$E(Pr_k) = P_k^N$ est la performance nominale du produit conçu.

CONCLUSION ET PERSPECTIVE

LES travaux de recherche présentés dans le mémoire de thèse contribuent à développer un modèle de déviations géométriques (GDM⁵) en 3D couvrant le cycle de vie du produit. Ce modèle est basé sur le modèle de la pièce fabriquée (MMP⁶) proposé par Villeneuve et Vignat [VLL01, VV03, VV05b, Vig05] pour modéliser les déviations géométriques générées lors de l'étape de fabrication. La vue d'ensemble des travaux de recherche est montrée figure 6. Le modèle de déviations géométriques est composé du modèle MMP pour l'étape de fabrication et du modèle de pièce assemblée (MAP⁷) pour l'étape d'assemblage. Celui-ci permet de modéliser tous les déviations géométriques générées dans l'étape de fabrication et accumulées sur le produit final lors de l'étape d'assemblage. Ce modèle est ensuite utilisé pour intégrer les déviations géométriques à la simulation de performance du produit. Une image de la performance réelle de la population de produits fabriqués est calculée par l'utilisation d'une simulation Monte-Carlo. La satisfaction des exigences du client est vérifiée par comparaison de la performance "réelle" aux exigences. L'étape suivante est d'identifier et de classifier les paramètres des sources de variation par rapport à leur effet sur la performance du produit. Des approches différentes pour analyser les coefficients d'influence (IFA) sont proposées dans le mémoire de thèse. Ses résultats permettent de trouver une solution robuste par minimisation des effets des déviations géométriques sur la performance du produit.

Les déviations géométriques du produit générées et accumulées durant son cycle de vie sont modélisées par le modèle GDM. Ce modèle permet de lier les paramètres des processus de fabrication de l'étape de fabrication et les résultats en termes de déviation de l'étape d'assemblage. La réponse à la première question scientifique est ainsi donnée par ce modèle.

5. Geometrical Deviation Model

6. Model of Manufactured Part

7. Model of Assembled Part

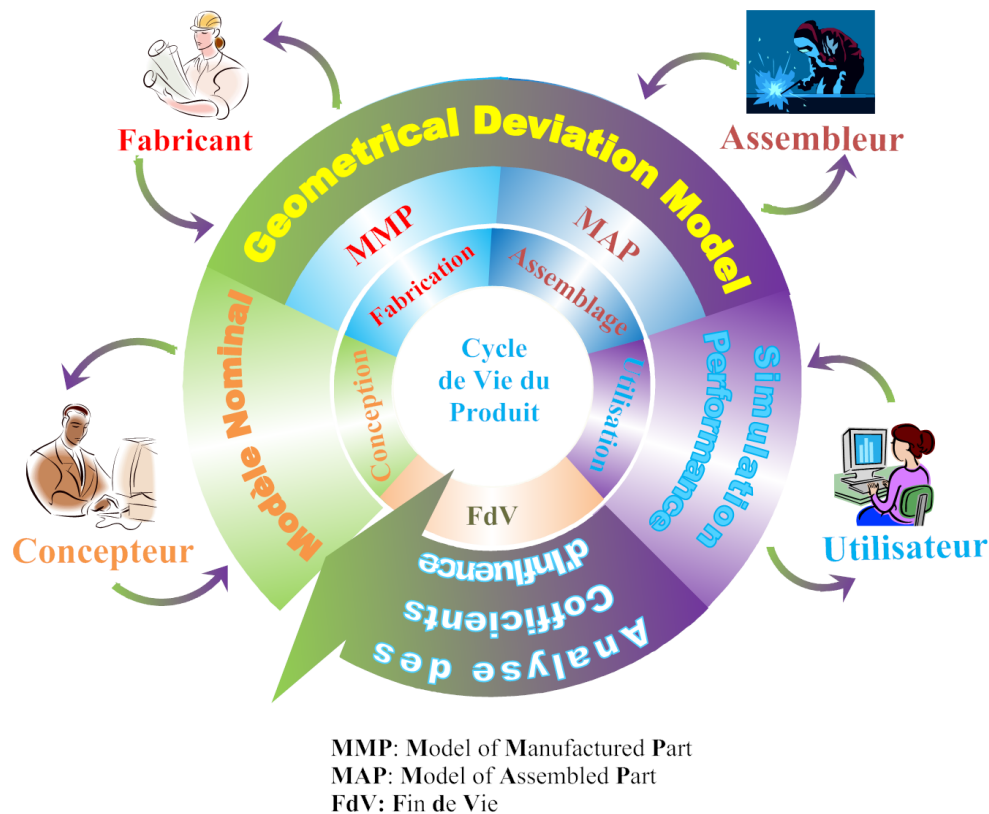


FIGURE 6 – La vue d'ensemble des travaux de recherche

- Etape de fabrication : Le modèle nominal du produit créé par le concepteur doit passer par cette étape et des déviations géométriques sont générées du fait des imperfections de la matière, de l'outillage et des machines. Celles-ci sont modélisées et collectées par le modèle de pièce fabriquée.
- Etape d'assemblage : Chaque pièce composant le produit est assemblée au cours de cette étape. Les déviations générées lors de l'étape de fabrication sont accumulées sur l'assemblage et donc sur le produit final. Le modèle de déviations géométrique GDM est un modèle total qui modélise toutes les déviations géométriques de l'étape de fabrication à l'étape d'assemblage. Ce modèle est donc capable de prendre en compte des déviations géométriques des surfaces des pièces du produit et de les lier avec des paramètres du processus de fabrication. Enfin, la méthode Monte-Carlo est utilisée pour créer une image des produits fabriqués avec déviations géométriques.
- Etape d'usage : Les déviations modélisées par le modèle GDM sont intégrées

dans la simulation de la performance du produit. La relation entre la performance du produit et les paramètres des sources de variation est établie par des approches différentes. Les performances de la population des produits sont calculée en s'appuyant sur cette relation et les résultats de la simulation Monte-Carlo. Finalement, le concepteur peut vérifier la conformité de la performance du produit conçu par rapport aux exigences du client. La réponse à la deuxième question de recherche est donc donnée.

Deux approches, proposées dans le chapitre 5, permettent d'identifier et de classer les effets sur la performance du produit des paramètres des sources de variation. De plus, la variance de la variation de performance par rapport aux paramètres des sources de variation est construite par deux approches l'une analytique et l'autre basée sur l'analyse de données. Elles sont présentées en détail dans le chapitre 5. Une solution robuste de conception peut être ensuite trouvée par minimisation la variance de la performance du produit. Les informations utiles peuvent ensuite être transmises aux acteurs du cycle de vie du produit tel que les concepteurs, fabricants et utilisateurs (voir la figure 6).

PLUSIEURS perspectives de poursuites de nos travaux sont envisageables. Elles sont classifiées selon les pistes de recherche suivante :

- Le modèle des déviations géométriques développées dans le mémoire de thèse ne prend pas en compte la déformation de la pièce. Un axe de recherche est ouvert pour intégrer aussi la déformation de la pièce à la simulation de performance du produit.
- L’effet des déviations géométriques est seulement considéré dans l’étape de l’utilisation pour vérifier une performance du produit. Pourtant, il y a plusieurs phénomènes physiques comme la déformation thermique, la fatigue des métaux, l’usure, etc. La deuxième piste de recherche est de prendre l’effet de phénomène multi-physique en compte dans la simulation multi-performance du produit.
- La méthode Monte-Carlo est utilisée pour simuler les déviations géométriques des surfaces et ensuite la performance du produit. Les données entrées y compris le domaine de variation et la distribution des paramètres sont supposées être uniformes et indépendantes. La troisième piste de recherche considère les domaines de variation et la distribution des paramètres ainsi que la corrélation. Des mesures ont été réalisées par Tichadou et al. [TNVL07, TLH05] et sont actuellement continuées par Bui-Minh [BMSVD10, SBMF⁺10].
- La relation entre la performance du produit et les paramètres des déviations géométriques est établie par les trois approches présentées dans ce mémoire. Le modèle dévié du produit pour la simulation de performance est créé dans un environnement CAO par manipulation manuelle. La quatrième piste de recherche est ouverte pour développer une interface qui permet de collecter les résultats des simulations en terme de déviation géométrique et de générer automatiquement le modèle dévié correspondant.
- Deux approches différentes pour déterminer la variance de la performance du produit et chercher la conception robuste sont présentées dans ce mémoire de thèse. La cinquième piste de recherche consiste à formuler le problème de conception robuste comme l’identification des paramètres contrôlable et incontrôlable

des sources de variation durant le cycle de vie du produit. De plus, il a nécessaire de construire un algorithme pour l'optimisation robuste multi-objectif afin de trouver une conception robuste prenant en compte les phénomènes multi-physiques. La méthode d'analyse intervalle pour chercher le domaine robuste a été réalisée par Qureshi et al. [QDBB09, QDBB10a, QDBB10b]. Celle-ci peut être appliquée à nos problèmes de conception robuste au sein du cycle de vie du produit.

LISTE DES PUBLICATIONS ET COMMUNICATIONS REALISEES

Revue Internationale

1. Nguyen, D. S., Vignat, F., Brissaud, D. (2010) 'Geometrical deviation model of product throughout its life cycle', *International Journal of Manufacturing Research*, (Accepted)
2. Nguyen, D. S., Vignat, F., Brissaud, D. (2010) 'Taking into account geometrical variation effect on product performance', *International Journal of Product Lifecycle Management*, (Accepted)

Congrès Internationaux avec actes :

1. Dinh Son Nguyen, Frédéric Vignat, Daniel Brissaud, "Geometrical Deviations Model for Product Life Cycle Engineering". *Proceedings of the 5th International Conference on Digital Enterprise Technology. Nantes, France, 2008*, pp 57-74.
2. Dinh Son Nguyen, Frédéric Vignat, Daniel Brissaud, "Applying Monte-Carlo Methods to Geometric Deviations Simulation within Product Life Cycle". *Proceedings of the 11th CIRP International Conference on Computer-Aided Tolerancing, Annecy, France, 2009*, pp 10.
3. Dinh Son Nguyen, Frédéric Vignat, Daniel Brissaud, "Product Performance Simulation with Geometric Deviations throughout Its Life Cycle". *Proceedings of the 6th International Conference on Digital Enterprise Technology. Hongkong, 2009*, pp 79-95.
4. Dinh Son Nguyen, Frédéric Vignat, Daniel Brissaud, "Integration of multiphysical phenomena in robust design methodology". *Proceedings of the 20th International Conference on Design, Nantes, France, 2010*, pp 10.
5. Dinh Son Nguyen, Frédéric Vignat, Daniel Brissaud, "Integration of geometrical deviations throughout product lifecycle into performance simulation". *The 10th Global Congress on Manufacturing and Management, Bangkok, Thailand, 2010*, pp.11.

The Impact of Geometrical Deviations on Product Life Cycle

Abstract:

The research work presented in my thesis aims to manage geometrical variability throughout product life cycle and its consequence on the product performance. The geometrical variations generated from the manufacturing to assembly stage are modeled by the geometrical deviation model. Monte-Carlo simulation method is then used to generate an image of the real manufactured product. As a result, the geometrical deviations are integrated into simulation of product performance in order to establish the relationship between the performance and the parameters of geometrical deviations or variation sources. An image of real performance of the manufactured product is then generated. From this result, the parameters of variation sources influencing the product performance are identified and classified according to their impact level. The variance of the product performance variation is also established by the relation between the performance and the parameters of geometrical deviations or variation sources. Finally, the robust design solution can be found by minimization of the variance of the product performance variation.

Keywords: Life-cycle Engineering, Geometrical Deviation Model, Performance simulation, Manufacturing simulation, Geometrical variability management.

Résumé:

Le travail de recherche présenté dans ce mémoire de thèse est de gérer la variabilité géométrique durant le cycle de vie du produit et ses conséquences sur la performance du produit. Le modèle des déviations géométriques du produit exposé dans ce mémoire permet de modéliser les déviations géométriques générées de l'étape de fabrication à l'étape d'assemblage de son cycle de vie. La méthode de simulation Monte-Carlo est utilisée pour générer une image des produits fabriqués. A partir de ces résultats, les déviations géométriques sont intégrées dans la simulation de la performance du produit afin d'établir la relation entre la performance et les paramètres des sources de variation. Une image de la performance réelle du produit fabriqué est générée par l'utilisation de résultat de simulation des déviations géométriques. Les paramètres de sources de variation influençant la performance du produit sont ensuite identifiés et classifiés par rapport au leur niveau d'impact. La variance de la variation de la performance est établie s'en appuyant sur cette relation. Finalement, la solution de la conception robuste est trouvée par la minimisation de la variance de la performance du produit.

Mots clés : Cycle de vie du produit, Modèle des déviations géométriques, Simulation de performance, Simulation de fabrication, Gestion de variabilité géométrique.